NBS

Technical Note No. 15

Boulder Laboratories

PREDICTION OF THE CUMULATIVE DISTRIBUTION WITH TIME OF GROUND WAVE AND TROPOSPHERIC WAVE TRANSMISSION LOSS

PART I - THE PREDICTION FORMULA

BY P. L. RICE , A. G. LONGLEY , AND K. A. NORTON

U. S. DEPARTMENT OF COMMERCE
NATIONAL BUREAU OF STANDARDS

NATIONAL BUREAU OF STANDARDS

Technical Note

15

July, 1959

Prediction of the Cumulative Distribution with Time of Ground Wave and Tropospheric Wave Transmission Loss

Part 1 - The Prediction Formula

by

P. L. Rice, A. G. Longley and K. A. Norton

DISTRIBUTED BY

UNITED STATES DEPARTMENT OF COMMERCE

OFFICE OF TECHNICAL SERVICES

WASHINGTON 25, D. C.

Price $1.50

This Technical Note was originally given limited distribution as NBS Report No. 5582, dated June 30, 1958. There have been some minor corrections and additions, including more graphs of some functions in order to simplify the calculations. Also added here is a figure showing deviations of all of the currently available forward scatter data from predicted values; the theory itself was used to eliminate, insofar as this is feasible, those long-term median values influenced by diffraction.

The following reports which depend upon the prediction methods described in this Technical Note are now being prepared for publication:

(1) A. P. Barsis, K. A. Norton, and P. L. Rice, "Predicting the Performance of Long Distance Tropospheric Communication Circuits."

(2) A. P. Barsis, P. L. Rice, and K. A. Norton, "The Use of Measurements in Predicting the Performance of Tropospheric Communication Circuits."

The recent report* of the Television Allocations Study Organization to the Federal Communications Commission, "Engineering Aspects of Television Allocations," includes smooth earth curves of field strength versus distance calculated using the methods of this Technical Note, as well as comparisons with data obtained over land at VHF and UHF. This TASO report also includes estimates of long-term variability as a function of distance, antenna height, and frequency, rather than angular distance. For angular distances less than 10 milliradians and for line-of-sight distances, the estimates prepared for TASO are better than those given in this Note.

Within a year it is hoped to submit for publication in the NBS Journal of Research, Part D, a detailed explanation of the prediction methods of this Technical Note, greatly simplified without loss of accuracy, and including a discussion of the theory. At that time, improved estimates of long-term variability will also be made available, with an explanation of how they were obtained from the data.

NBS Technical Note No. 12, "Transmission Loss in Radio Propagation - II", by K. A. Norton and the paper "System Loss in Radio Propagation," by K. A. Norton, J. Research, NBS, 63D, pp. 53-73, July - August, 1959, both contain examples of the use of the methods of calculation given in this Technical Note.

---

* This report may be obtained from Dr. G. R. Town, Ames, Iowa at a cost of $10.00.

Prediction of the Cumulative Distribution with Time of Ground Wave and Tropospheric Wave Transmission Loss

Part I - The Prediction Formula

by

P. L. Rice, A. G. Longley, K. A. Norton

This report describes a method for predicting the cumulative distribution with time of transmission loss at frequencies above 10 megacycles per second over paths of arbitrary length. The method makes use of available information about terrain profiles and surface meteorological data, and is based on the CRPL radio standard atmospheres, in which the radio refractive index decreases linearly with height for the first kilometer above ground, and then decreases exponentially with height [1/]. Discussion of the theoretical basis for this formula and a demonstration of its accuracy by comparison with experimental data are reserved for later parts of this report.

1. Introduction

Terrain irregularities, climate, and weather play principal roles in determining the strength and fading properties of a tropospheric signal. Estimates of transmission loss [2/] and its long-term and short-term variability are essential to the design and allocation of military and commercial communication links and broadcasting and navigational facilities.

Until fairly recently, distances much beyond the horizon of a radio transmitting antenna were considered too great for useful communication links at frequencies above 100 megacycles per second. This particular range of distance, the extra-diffraction region out to about 1,000 miles, is important in the application of tropospheric forward scatter techniques, and our prediction formula is especially reliable in this range. For propagation paths longer than 1,000 miles, only the ionosphere will support measurable scatter signals. For distances well beyond the horizon in the frequency range above 100 Mc, observed scatter signals are tropospheric. The present usefulness of the

ionospheric scatter mechanism ceases at about 60 Mc [3], while tropospheric propagation promises to be useful for communication purposes for frequencies between 40 Mc and about 10,000 Mc [4].

At these frequencies and out to distances just beyond the radio horizon of a transmitter, the dominant propagation mechanism is diffraction. An earlier report by Norton, Rice, and Vogler [5] gives a formula for calculating transmission loss due to diffraction over rough terrain profiles.

At greater distances, the dominant propagation mechanism is usually forward scatter [6], especially during winter afternoon hours when strong ducts or elevated layers are rare. During these hours, observed transmission losses are in excellent agreement with forward scatter theory.

Often, for other times of day and seasons of the year, the scatter phenomenon may more properly be called reflection, and sometimes no distinction can be made between "forward scatter" from a turbulent atmosphere [6] and the addition of "incoherent reflections" from patchy elevated layers [7]. The examination of transmission loss variations over a particular path during some period for which detailed information about layer heights and intensities is available can be very illuminating [8]. The prediction method described here gives good estimates of results to be expected over such paths when only surface meteorological data are available. Median diffraction and scatter fields estimated for winter afternoons are combined and then converted empirically to estimates for other periods of time.

2. Definition of Transmission Loss

Transmission loss, L, is defined as the ratio expressed in decibels of the power, p_r, radiated from a transmitting antenna to the power, p_a, available from the receiving antenna:

$$L = 10 \log_{10} (p_r/p_a) \qquad (2.1)$$

It is convenient to express the results of propagation measurements and theoretical calculations in terms of the "basic transmission loss" expected if isotropic transmitting and receiving antennas were used. This basic transmission loss, L_b, may be determined from the measured transmission loss, L, by adding the path antenna gain G_p:

$$L_b = L + G_p \tag{2.2}$$

When G_p is not known, an estimate of L_b may be made for short paths by assuming that the free space gains of the transmitting and receiving antennas are realized, i.e., that $G_p = G_t + G_r$. The corresponding value of basic transmission loss will be a little too large. For larger distances, see Section 11 and Reference 9 for methods of estimating G_p.

Basic transmission loss L_b is related to field strength, E, expressed in decibels above one microvolt per meter for one kilowatt of effective power radiated from a half-wave dipole:

$$L_b = 139.367 + 20 \log_{10} f_{mc} - E - G_L \tag{2.3}$$

where

$$G_L = G_t + G_r - G_p \,. \tag{2.4}$$

In determining E from measured data it is implicitly assumed that the free space antenna gains are realized; i.e., that $G_L = 0$. The appendix contains a brief summary of useful relationships between such quantities as transmission loss, field strength, attenuation relative to free space, and the voltage or power available at receiver terminals, including relationships useful for the solution of some systems design problems.

3. Cumulative Distribution of Transmission Loss

This paper considers cumulative distributions of hourly median values of transmission loss. All subsequent discussion and the distributions shown in Figs. 2 - 12, are concerned with hourly medians of basic transmission loss and their diurnal and seasonal variability. This paper is not concerned with estimating short-term (within-the-hour) variability.

Basic transmission loss L_{bd} expected for the diffraction mode of propagation during winter afternoons is calculated according to the formulas in Reference 5, as modified for high antennas in Section 7. For winter afternoons, the median basic transmission loss, L_{bms}, due to forward scatter, is given by the following:

$$L_{bms} = G(\eta) + 30 \log_{10} f_{mc} - 20 \log_{10} d_{mi}$$

$$+ H_o - F_o - F_s - F(h_{cg}, N_s) + A_a \tag{3.1}$$

The radio wave frequency, f_{mc}, is in megacycles per second, and the great circle propagation path distance, d, is in statute miles. Other terms are explained in later sections.

Reference 4 gives a less complex formula for calculating L_{bms}, but (3.1) is more reliable for propagation paths with unusual profiles or climatology, for very high antennas, and for the lower frequencies.

Given L_{bd} and L_{bms}, corresponding to diffraction and forward scatter, the resultant median basic transmission loss is

$$L_{bm} = L_{bd} - R\,(0.5), \qquad (3.2)$$

R (0.5) is given graphically as a function of (L_{bd} - L_{bms}) on Fig. 1, as determined from a paper by Norton, Vogler, Mansfield and Short [10]. Within one-tenth of a decibel, $L_{bm} = L_{bd}$ when (L_{bd} - L_{bms}) is less than -18.1 db, and $L_{bm} = L_{bms}$ when L_{bd} - L_{bms} is greater than 17.9 db.

The analysis of transmission loss data was concentrated mainly on times of day, 1 p.m. to 6 p.m., when great departures of refractive index profiles from a linear gradient are least likely, in order to avoid the frequent occurrence of ducting and layer conditions. Field strengths are higher in summer than in winter on an average, and diurnal trends are usually most pronounced between May and October in the northern hemisphere, with minimum fields occurring in the afternoon. To allow for such effects, data were grouped into eight "Time Blocks", defined in the following table:

Table I

Time Blocks

1.	Nov. - Apr.	6 A.M. - 1 P.M.
2.	Nov. - Apr.	1 P.M. - 6 P.M.
3.	Nov. - Apr.	6 P.M. - 12 Mn.
4.	May - Oct.	6 A.M. - 1 P.M.
5.	May - Oct.	1 P.M. - 6 P.M.
6.	May - Oct.	6 P.M. - 12 Mn.
7.	May - Oct.	12 Mn. - 6 A.M.
8.	Nov. - Apr.	12 Mn. - 6 A.M.

Hourly median distributions for winter (Time Blocks 1, 2, 3, 8) and summer (Time Blocks 4, 5, 6, 7) are shown as Figs. 12a and 12b.

THE MEDIAN, $R_{0.5}$, FROM THE CUMULATIVE DISTRIBUTION OF THE RESULTANT AMPLITUDE OF A CONSTANT DIFFRACTED FIELD PLUS A RAYLEIGH DISTRIBUTED SCATTERED FIELD

$$L_{bm} = L_{bd} - R(0.5)$$

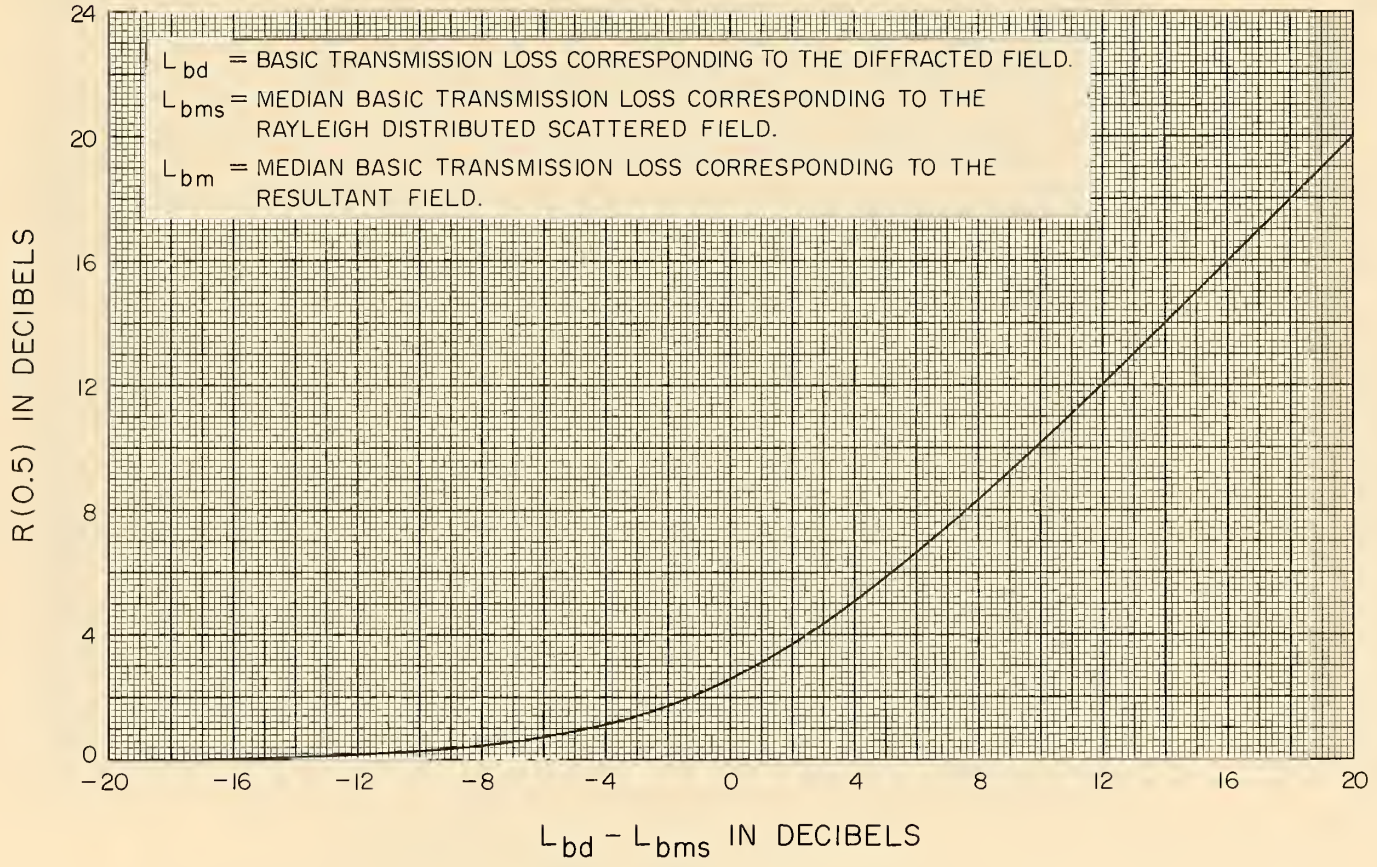

Figure 1

EXPECTED SIGNAL LEVEL, $V(p,\theta)$, EXCEEDED BY p PERCENT OF ALL HOURLY MEDIANS IN TIME BLOCK NO. 1
NOVEMBER - APRIL, 6 A.M. - 1 P.M.
$L_b(p) = L_{bm} - V(p,\theta)$

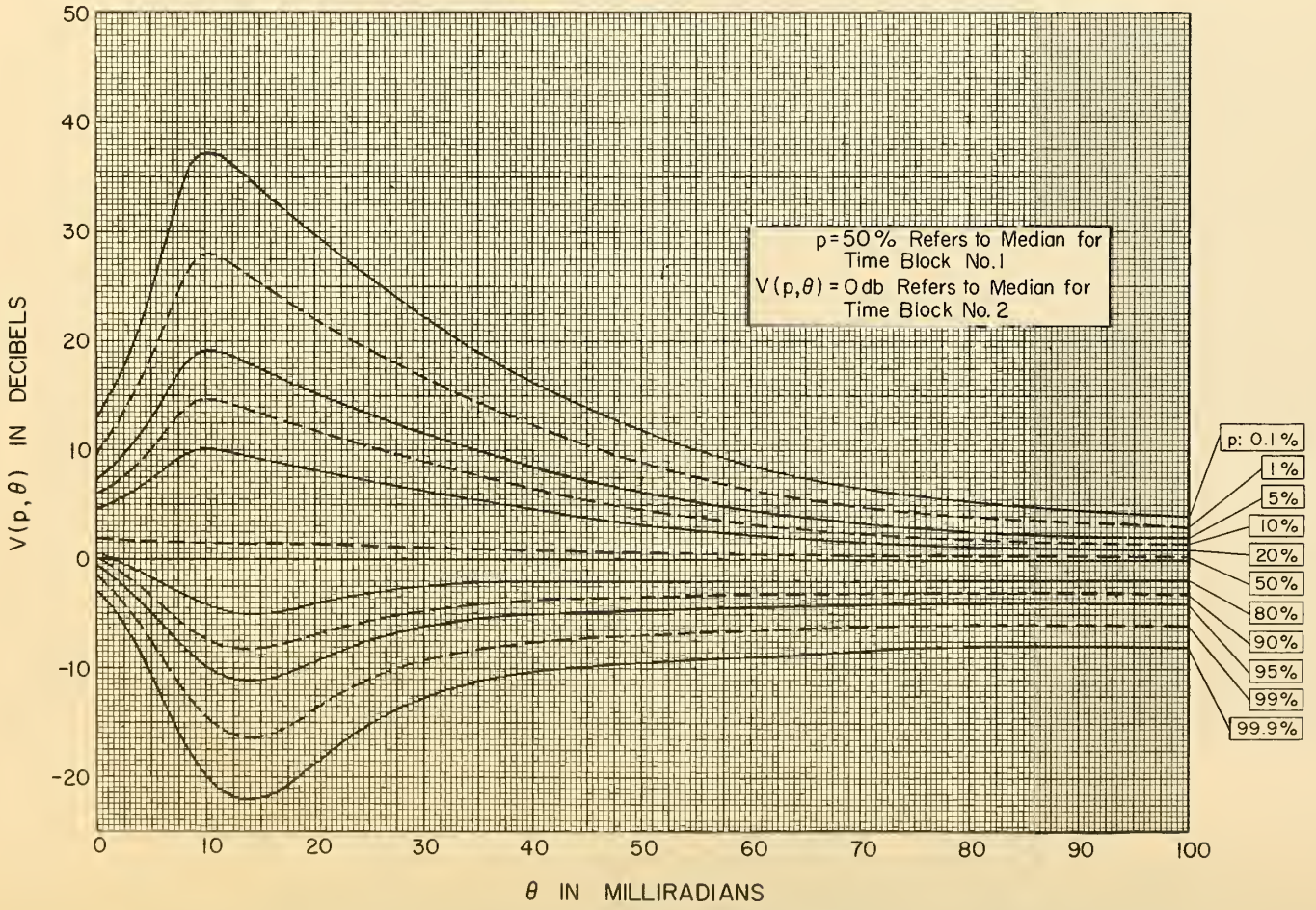

Figure 2

EXPECTED SIGNAL LEVEL, $V(p, \theta)$, EXCEEDED BY p PERCENT OF ALL HOURLY MEDIANS IN TIME BLOCK NO. 2
NOVEMBER-APRIL, 1 P.M.-6 P.M.
$L_b(p) = L_{bm} - V(p, \theta)$

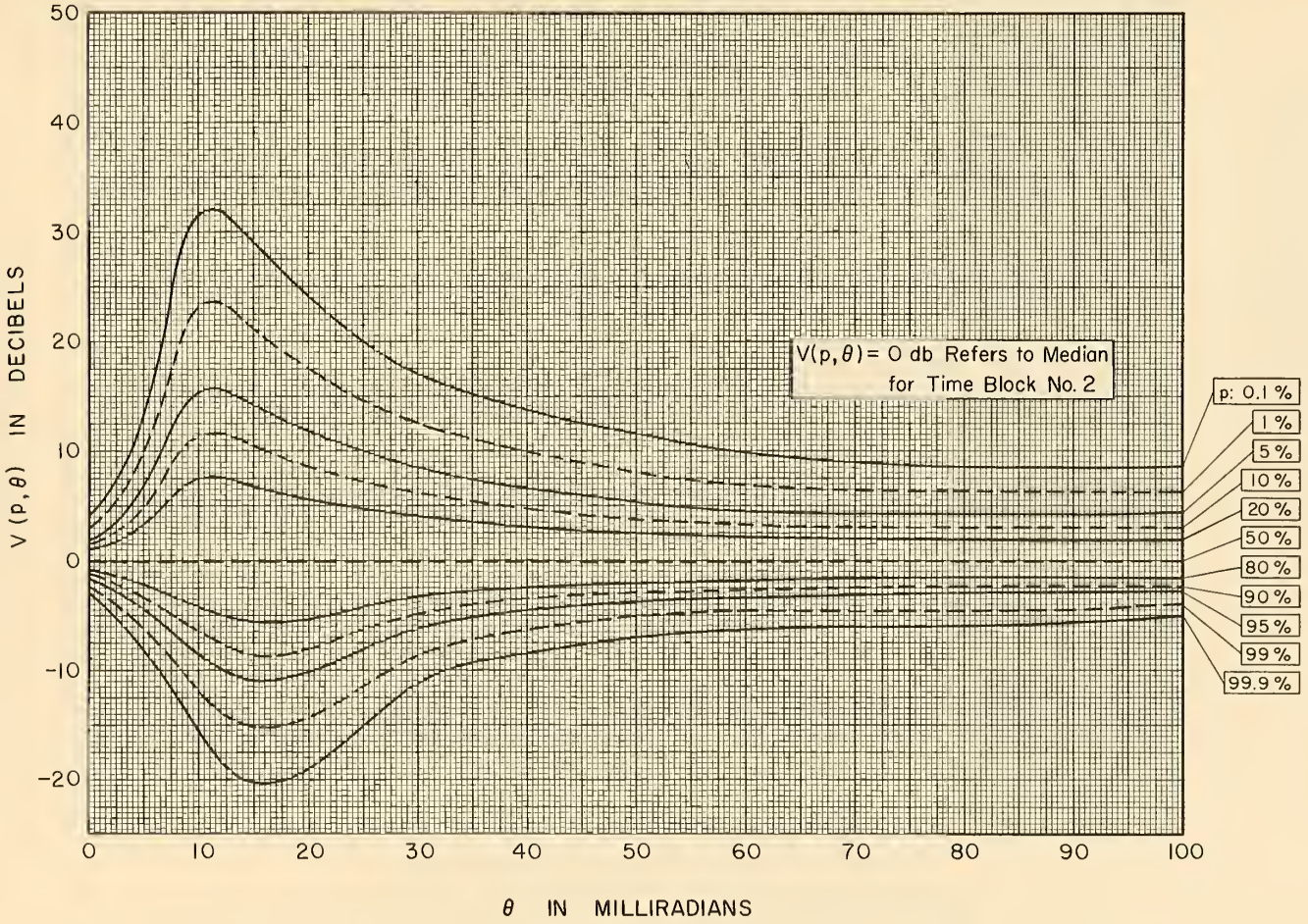

Figure 3

EXPECTED SIGNAL LEVEL, $V(p,\theta)$, EXCEEDED BY p PERCENT OF ALL HOURLY MEDIANS IN TIME BLOCK NO. 3 NOVEMBER-APRIL, 6P.M-12 MIDNIGHT

$L_b(p) = L_{bm} - V(p,\theta)$

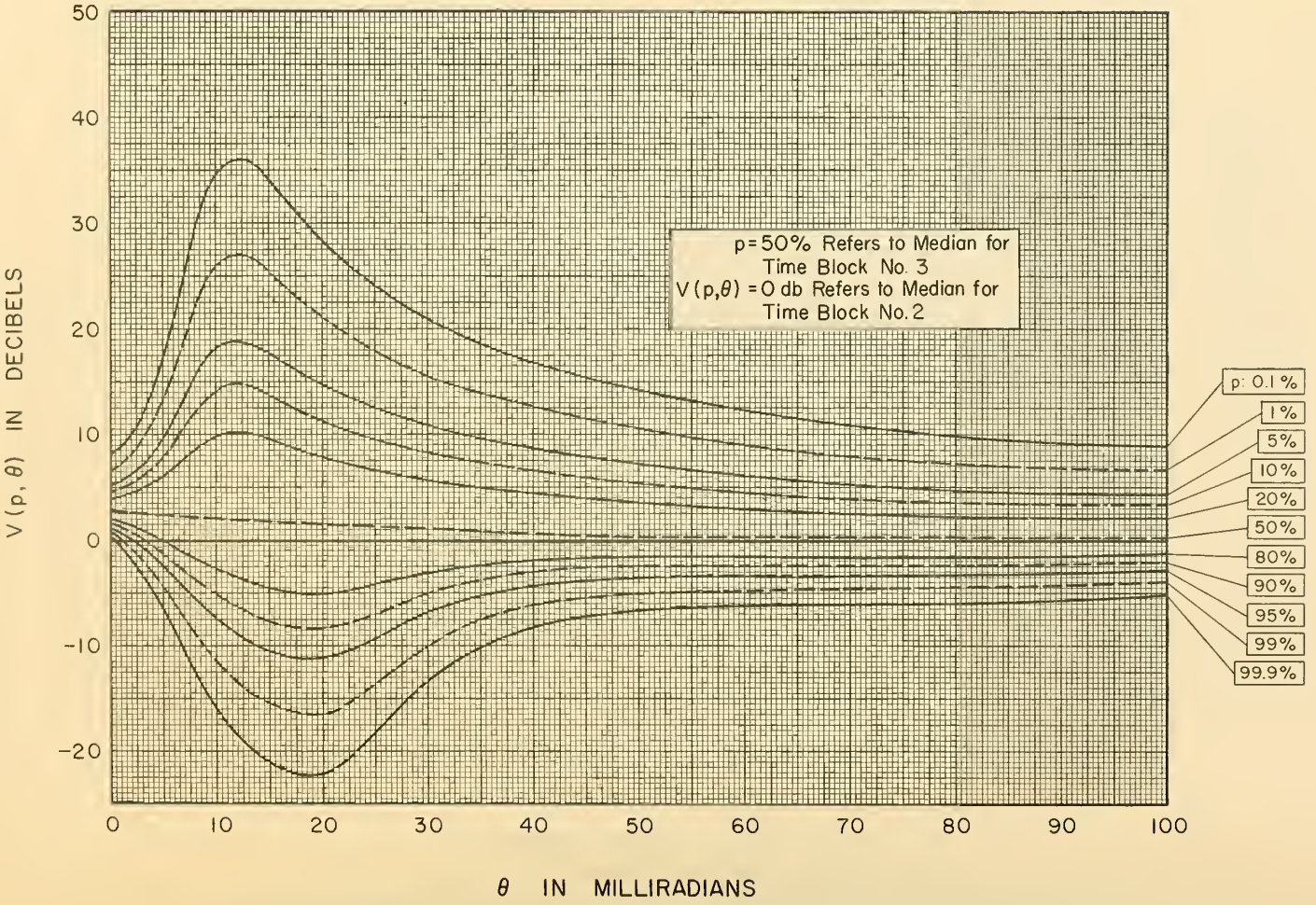

Figure 4

EXPECTED SIGNAL LEVEL, $V(p,\theta)$, EXCEEDED BY p PERCENT OF ALL HOURLY MEDIANS IN TIME BLOCK NO. 4
MAY-OCTOBER, 6A.M.-1P.M.
$L_b(p) = L_{bm} - V(p,\theta)$

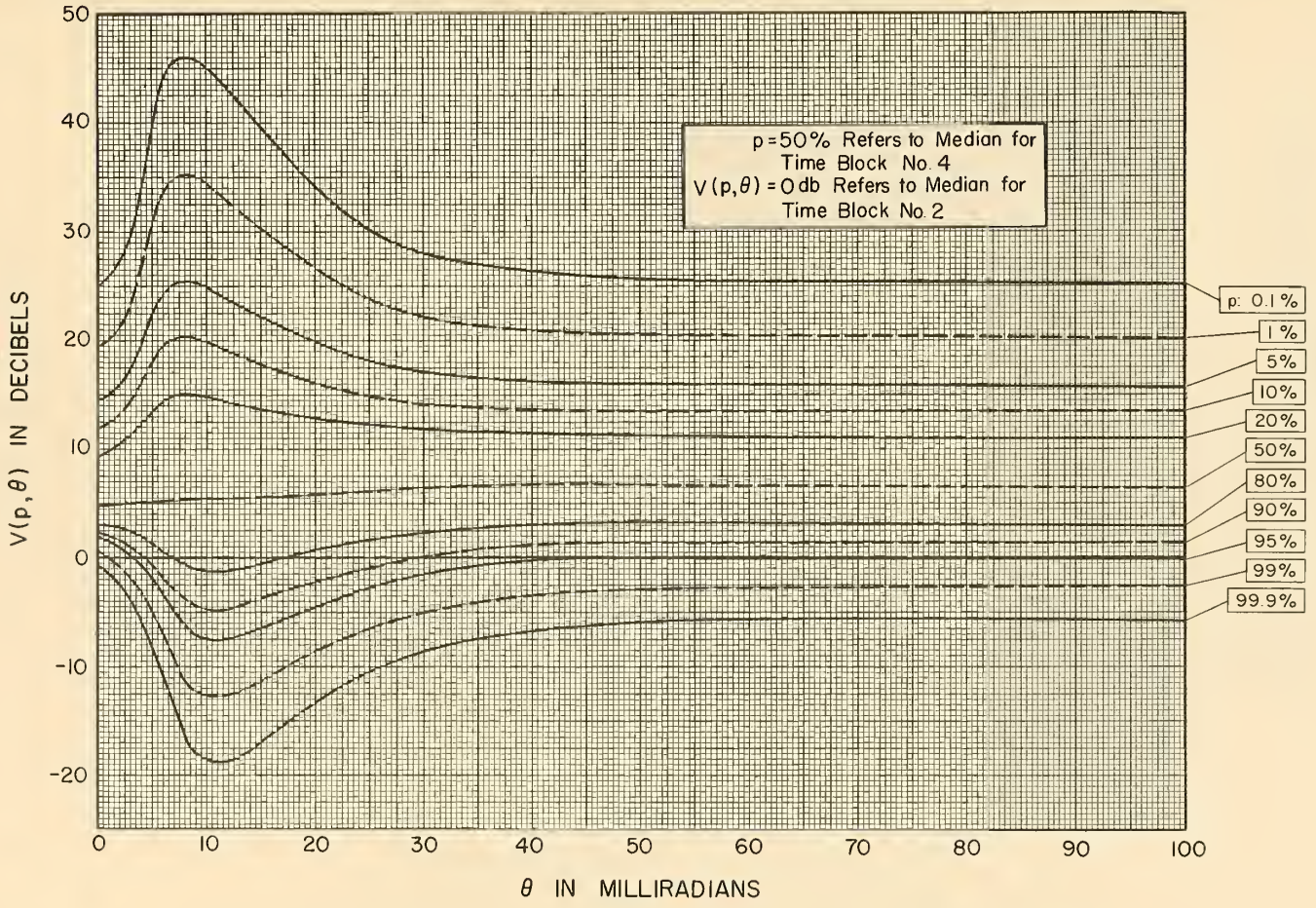

Figure 5

EXPECTED SIGNAL LEVEL, $V(p,\theta)$, EXCEEDED BY p PERCENT OF ALL HOURLY MEDIANS IN TIME BLOCK NO. 5
MAY-OCTOBER, 1 P.M. - 6 P.M.
$L_b(p) = L_{bm} - V(p,\theta)$

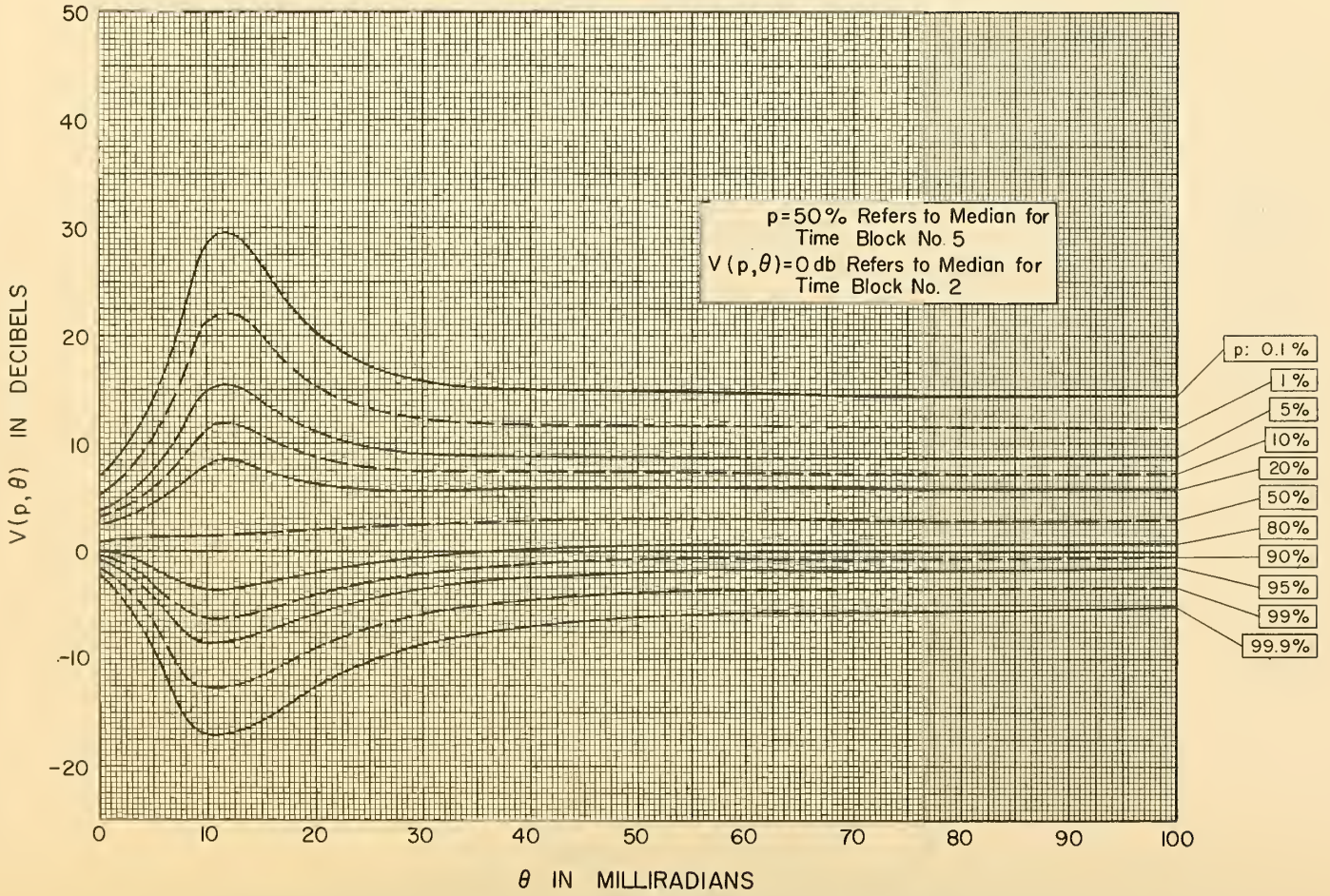

Figure 6

EXPECTED SIGNAL LEVEL, $V(p,\theta)$, EXCEEDED BY p PERCENT OF ALL HOURLY MEDIANS IN TIME BLOCK NO. 6
MAY - OCTOBER, 6 P.M. - 12 MIDNIGHT

$L_b(p) = L_{bm} - V(p,\theta)$

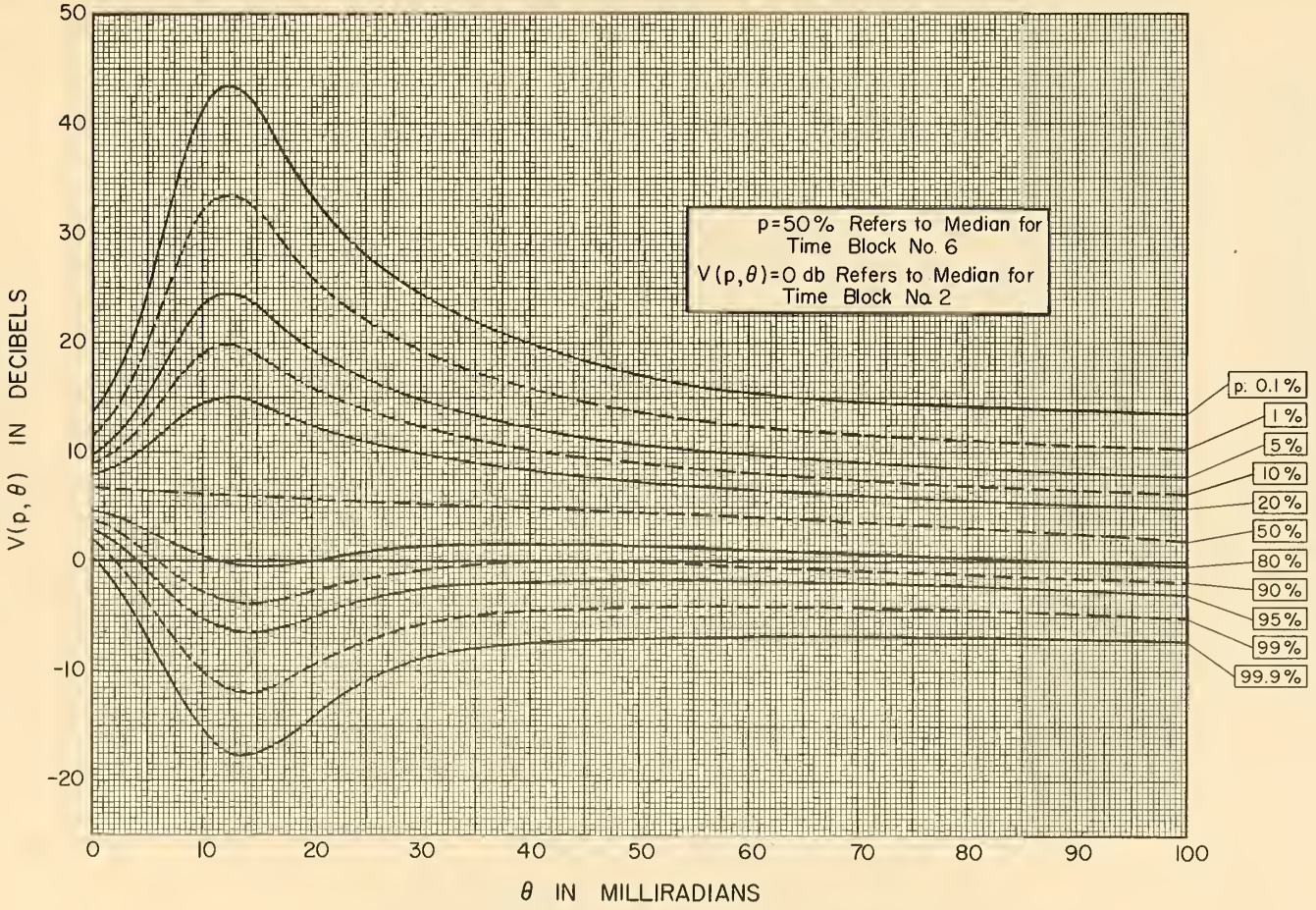

Figure 7

EXPECTED SIGNAL LEVEL, $V(p, \theta)$, EXCEEDED BY p PERCENT OF ALL HOURLY MEDIANS IN TIME BLOCK NO. 7
MAY–OCTOBER, 12 MIDNIGHT–6 A.M.
$L_b(p) = L_{bm} - V(p, \theta)$

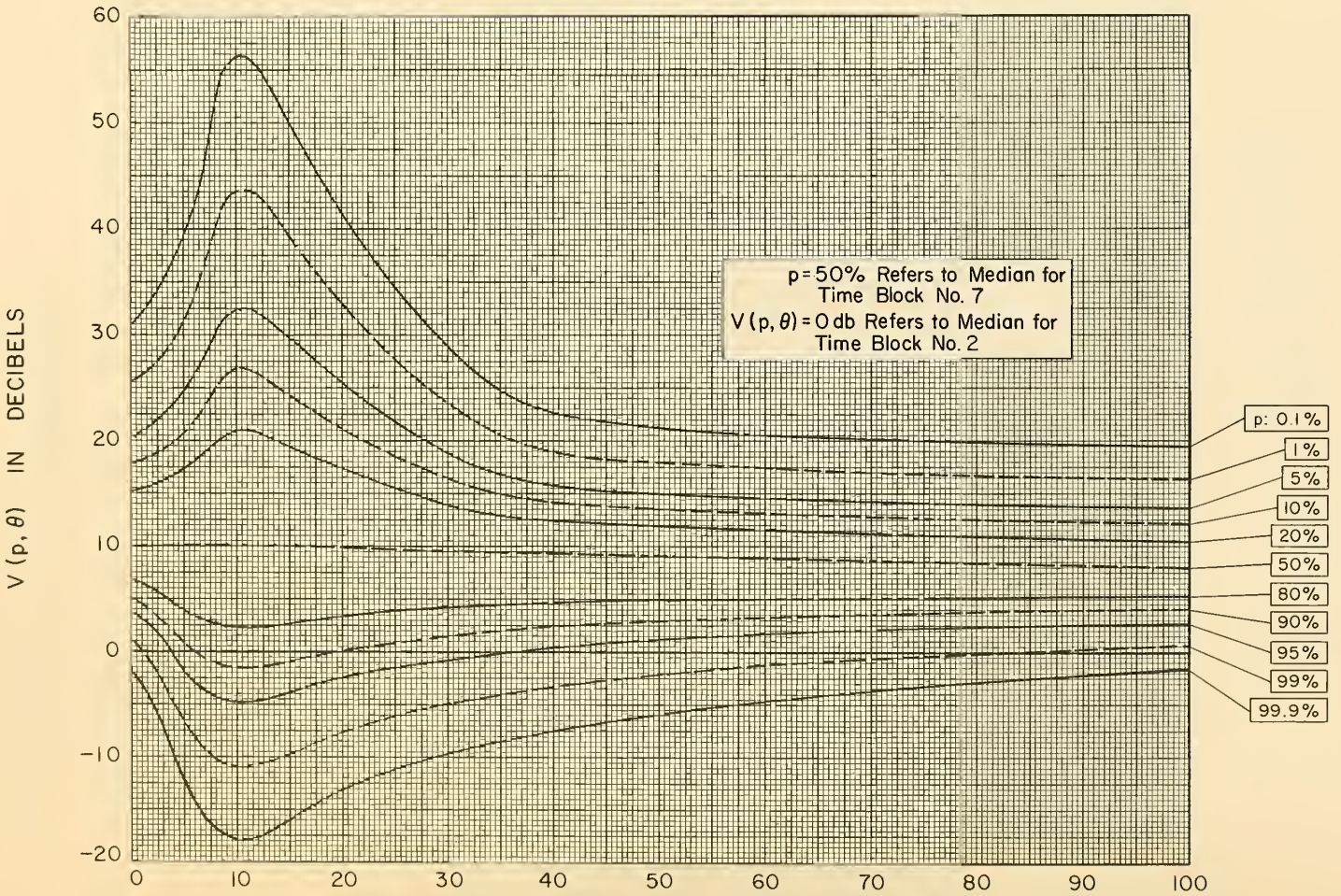

Figure 8

EXPECTED SIGNAL LEVEL, $V(p,\theta)$, EXCEEDED BY p PERCENT OF ALL HOURLY MEDIANS IN TIME BLOCK NO. 8
NOVEMBER-APRIL, 12 MIDNIGHT 6 A.M.
$L_b(p) = L_{bm} - V(p,\theta)$

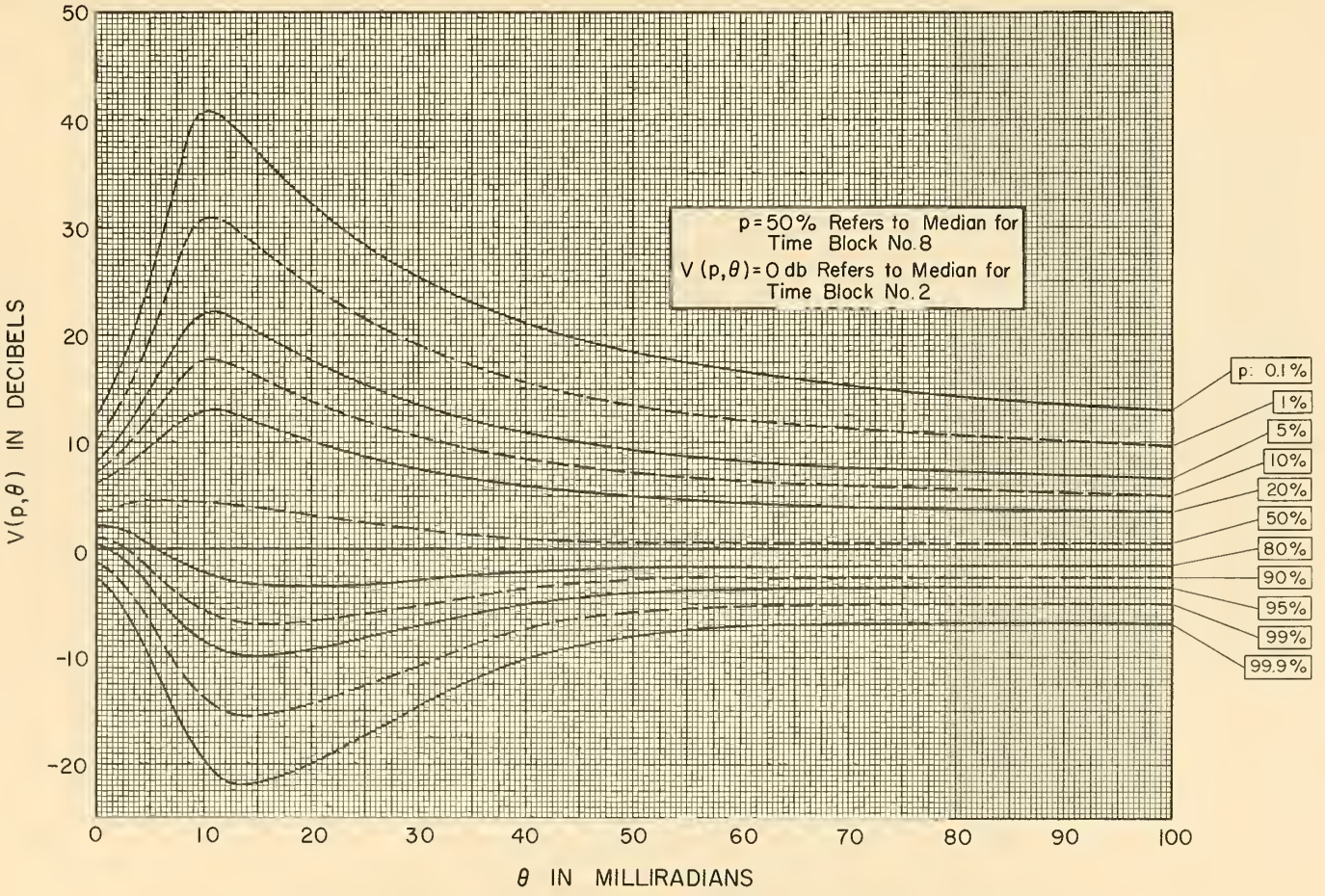

Figure 9

EXPECTED SIGNAL LEVEL, $V(p,\theta)$, EXCEEDED BY p PERCENT OF ALL HOURLY MEDIANS IN TIME BLOCKS 2 AND 5
ALL YEAR, 1 P.M. – 6 P.M.
$L_b(p) = L_{bm} - V(p,\theta)$

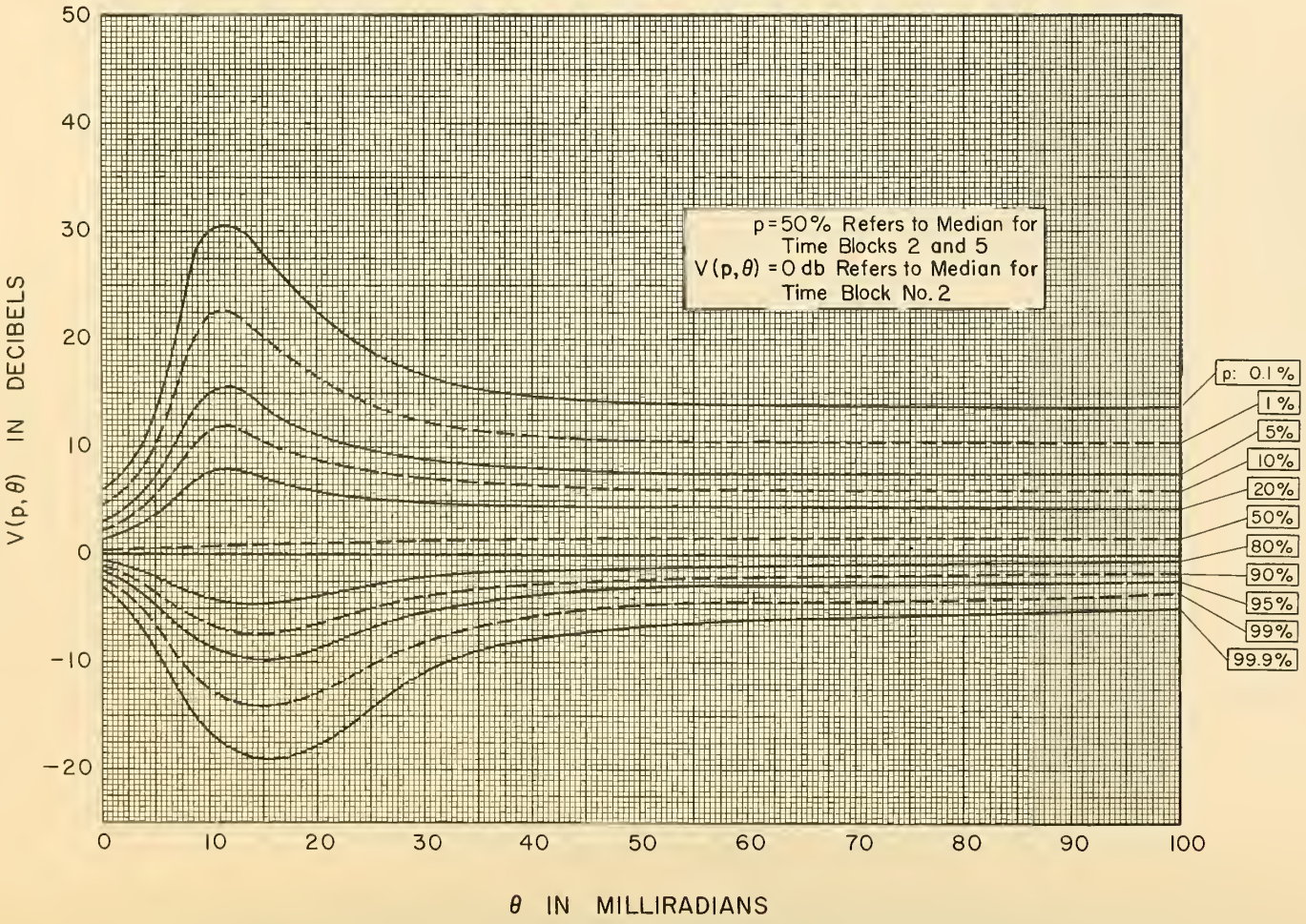

Figure 10

EXPECTED SIGNAL LEVEL, $V(p,\theta)$, EXCEEDED BY p PERCENT OF ALL HOURLY MEDIANS IN TIME BLOCKS 3 AND 6 ALL YEAR, 6 P.M. - MIDNIGHT

$L_b(p) = L_{bm} - V(p,\theta)$

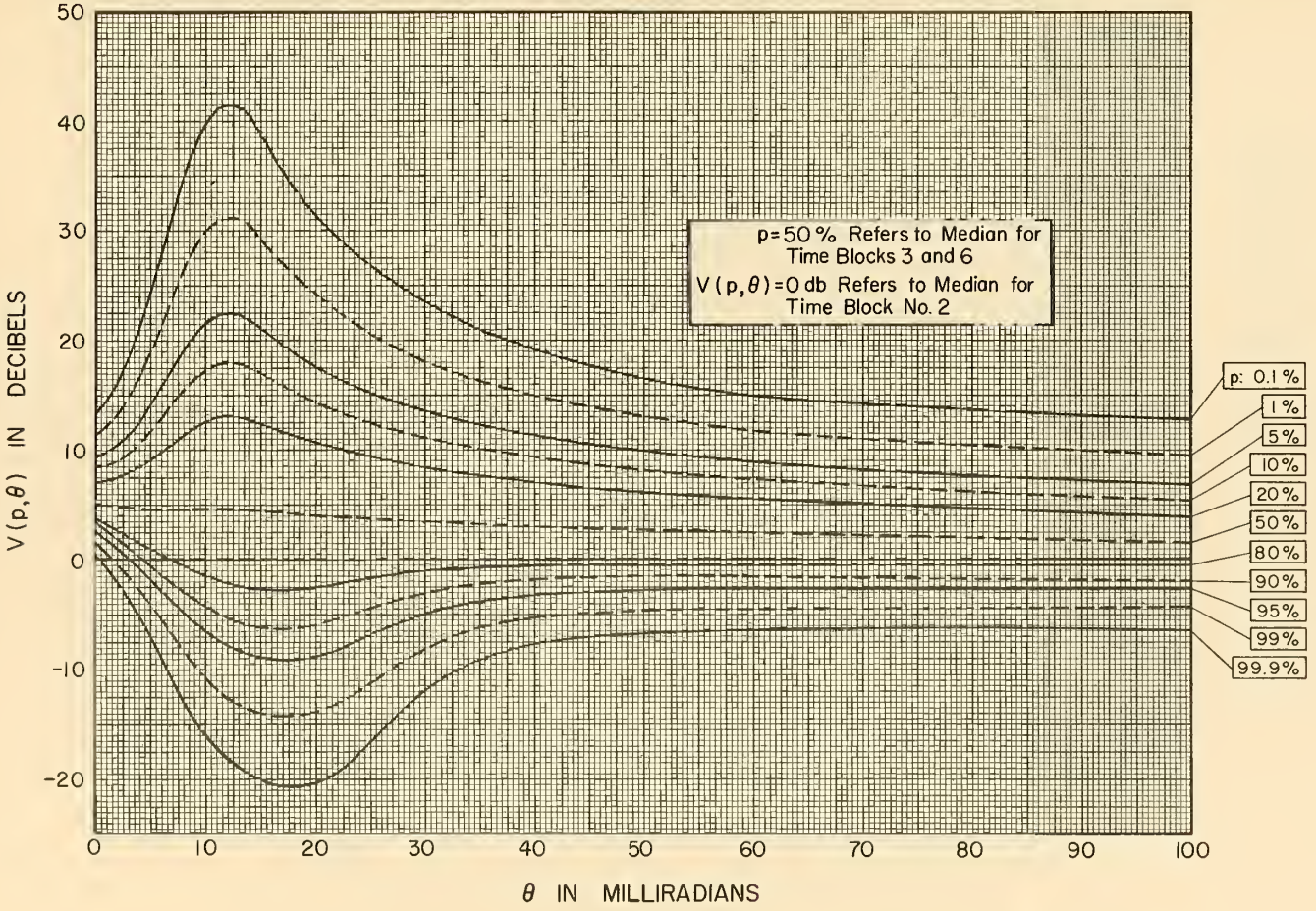

Figure 11

EXPECTED SIGNAL LEVEL, $V(p,\theta)$, EXCEEDED BY p PERCENT OF ALL HOURLY MEDIANS OBSERVED AT ANGULAR DISTANCE θ DURING ALL HOURS OF THE YEAR

$V(p,\theta)$ shows the deviation of all-day, all-year values, $L_b(p,\theta)$, relative to median basic transmission loss, L_{bm}, for the period November-April, 1 P.M.-6 P.M. (Time Block No. 2)

$$L_b(p,\theta) = L_{bm} - V(p,\theta) \text{ decibels}$$

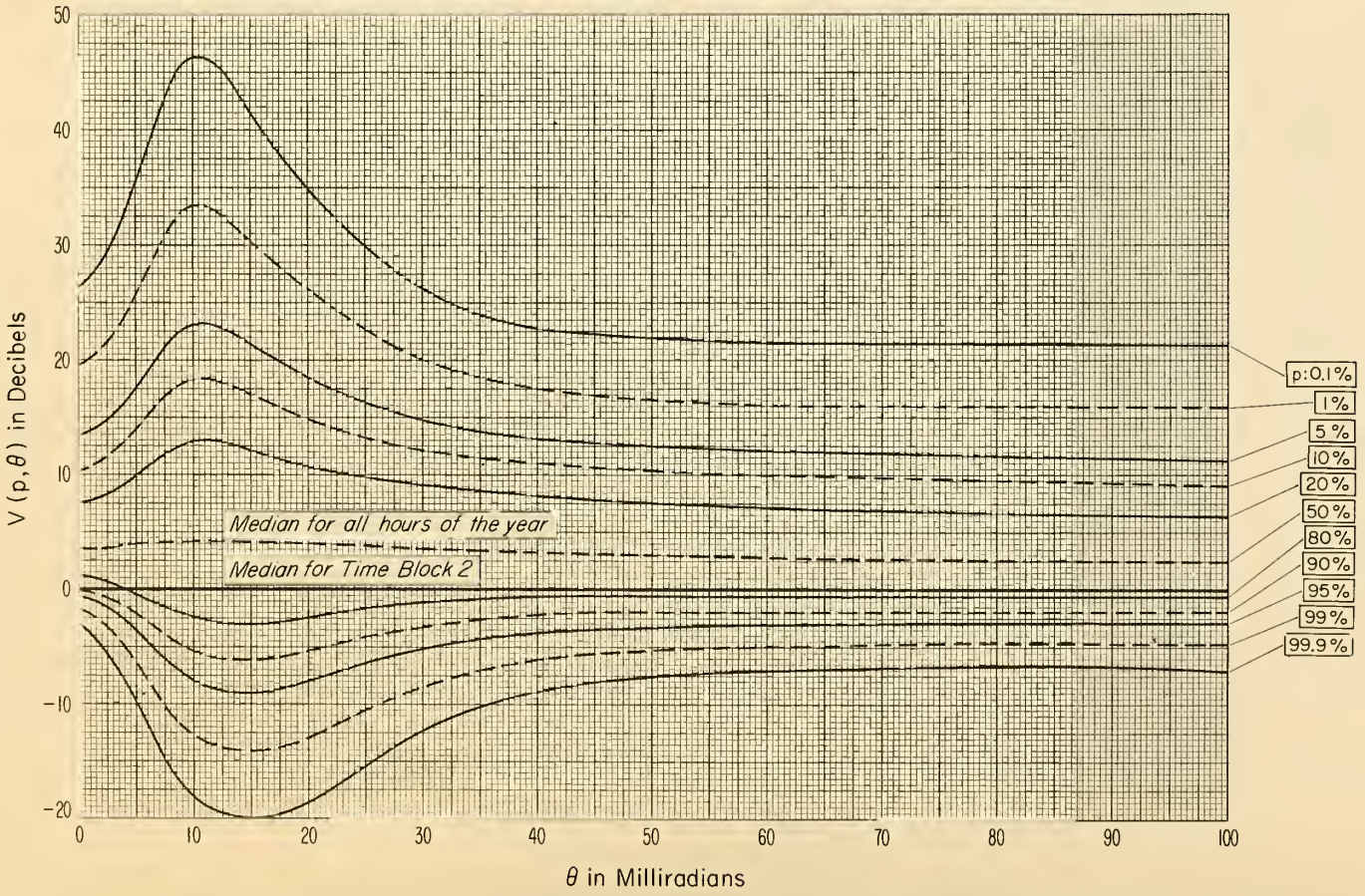

Figure 12

EXPECTED SIGNAL LEVEL, $V(p,\theta)$, EXCEEDED BY p PERCENT OF ALL HOURS, WINTER

November – April, All Hours

$L_b(p,\theta) = L_{bm} - V(p,\theta)$ decibels

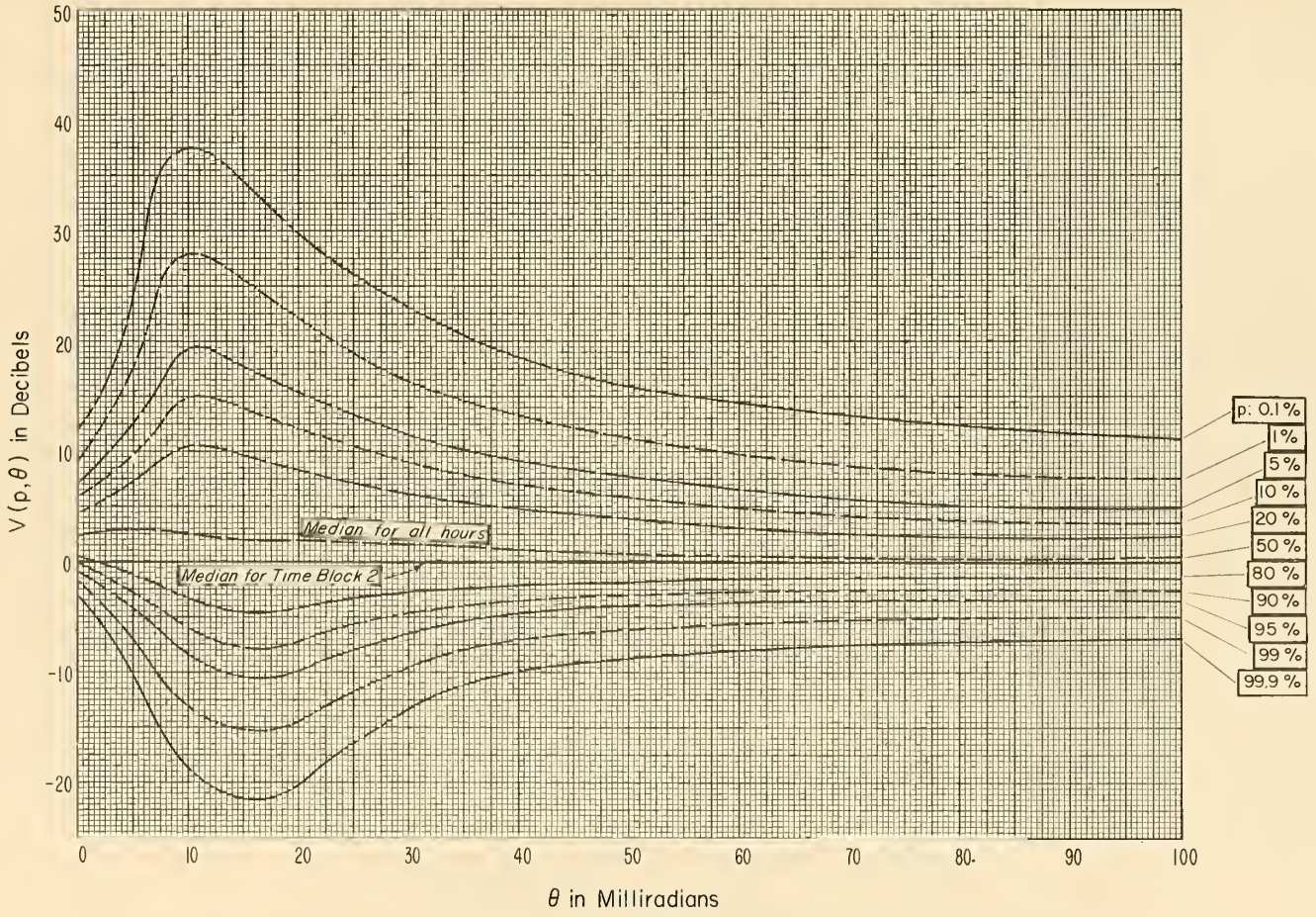

Figure 12a

EXPECTED SIGNAL LEVEL, $V(p,\theta)$, EXCEEDED BY p PERCENT OF ALL HOURS, SUMMER

May - October, All Hours

$L_b(p,\theta) = L_{bm} - V(p,\theta)$ decibels

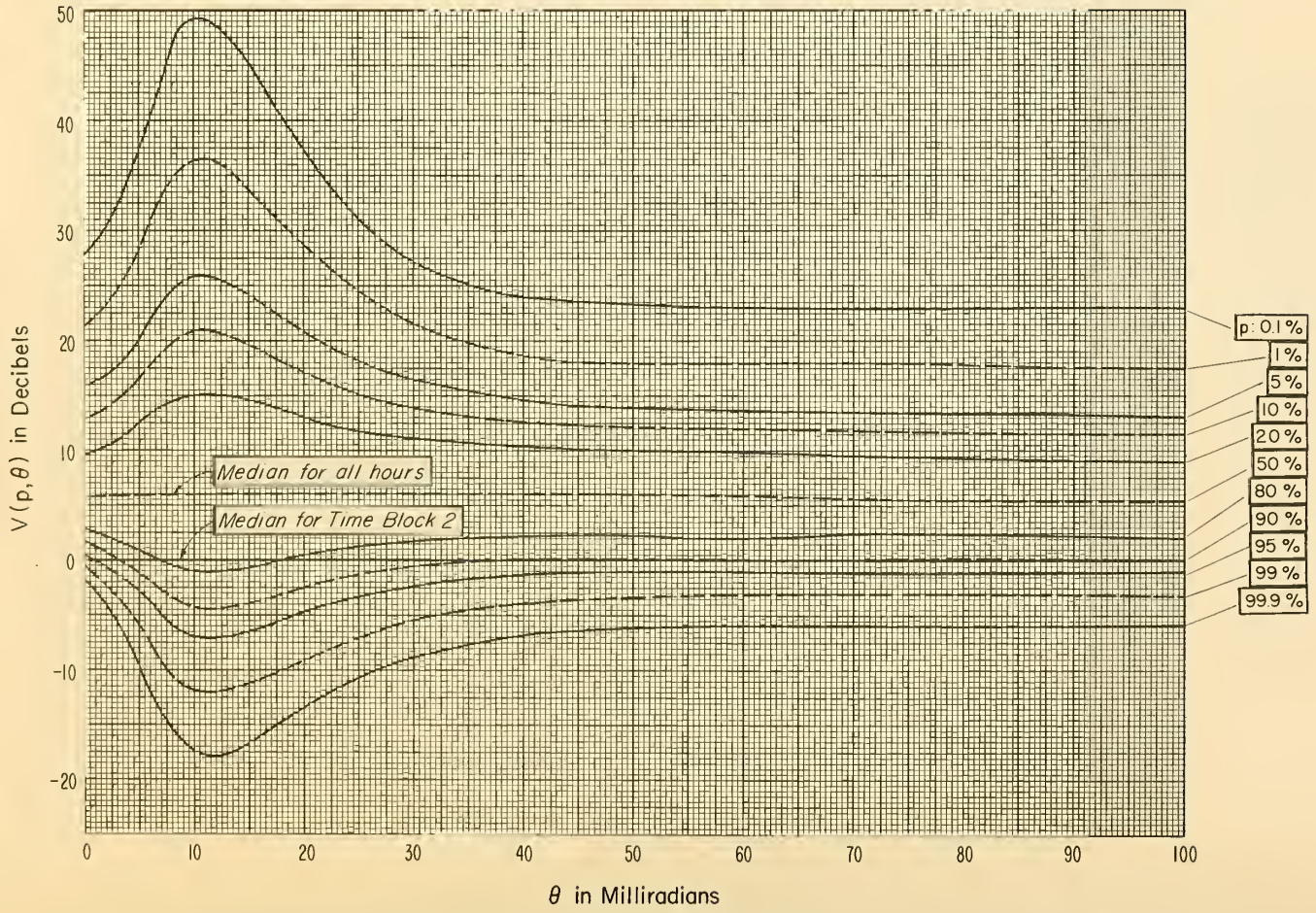

Figure 12 b

Empirical curves, given in Figs. 2 - 12, define a set of time variability factors $V(p, \theta)$ which show, as a function of angular distance, the difference between median fields and fields for other percentages of the time within each time block and for all hours in a year. The angular distance, θ, is the angle between horizon rays from transmitter and receiver; methods for its determination are given in Section 5. The field strength E(p) exceeded by p per cent of the hourly medians in a given time block is given by

$$E(p) = E_m \text{ (Time Block 2)} + V(p, \theta) \tag{3.3}$$

and the corresponding transmission loss L(p) is given by

$$L(p) = L_m \text{ (Time Block 2)} - V(p, \theta) \tag{3.4}$$

where E_m and L_m are median field strength and median transmission loss estimated for winter afternoons, and $V(p, \theta)$ is the time variability factor appropriate for the period of time for which E(p) or L(p) is desired.

Summarizing,

$$L(p) = L_{bd} - R(0.5) - G_p - V(p, \theta) . \tag{3.5}$$

R(0.5) as given by Fig. 1 requires (1) the calculation of L_{bd} by methods explained in Reference 5 and Section 7, and (2) the calculation of L_{bms} as given by (3.1) and explained in Section 9. Formulas for estimating G_p are given for the general case in Reference 9, and in Section 11 of this report for the special case where free space antenna gains are the same for both transmitting and receiving antennas. $V(p, \theta)$ for all hours of the year, winter and summer, appropriately combining the time blocks, is shown in Figs. 12, 12a, 12b. Varying p, (3.5) provides a prediction for the entire cumulative distribution of radio transmission loss for all hours of the year.

A comparison of measured and calculated values for KIXL-FM in Dallas, Texas, recorded by the University of Texas at Austin is shown in Fig. 13 for each time block and for all hours of the year. Several measured cumulative distributions are shown for each calculated one; the station was monitored all day and all night for three and a half years. From Fig. 13 it may be noted that medians for

CUMULATIVE DISTRIBUTION OF HOURLY MEDIAN TRANSMISSION LOSS
for KIXL-FM, Dallas, Texas
d=175.9 miles, fmc = 104.5 Mc, N_s = 306.5

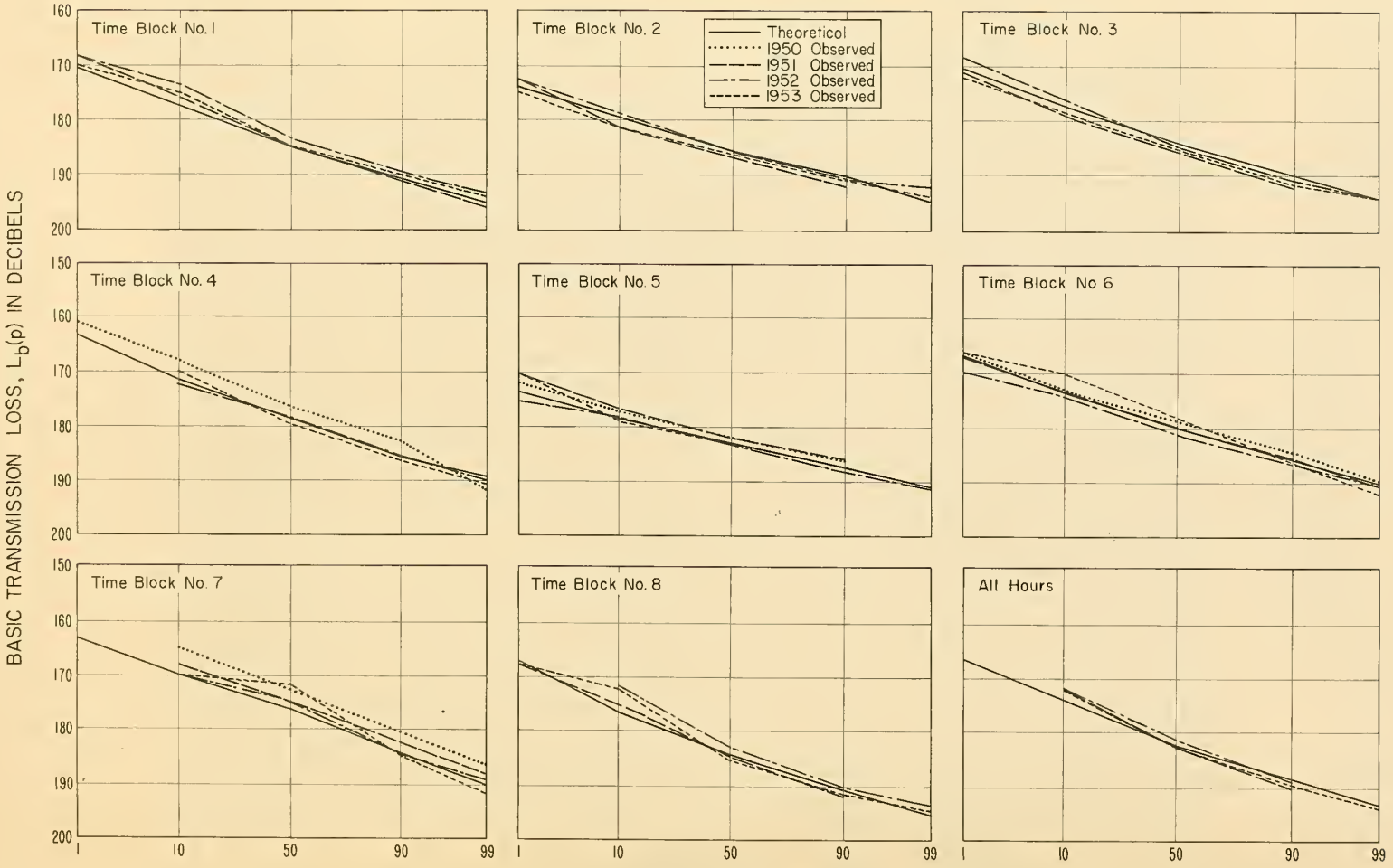

Figure 13

MEDIAN FORWARD SCATTER RADIO TRANSMISSION LOSS RELATIVE TO FREE SPACE CORRESPONDING TO WINTER AFTERNOON CONDITIONS

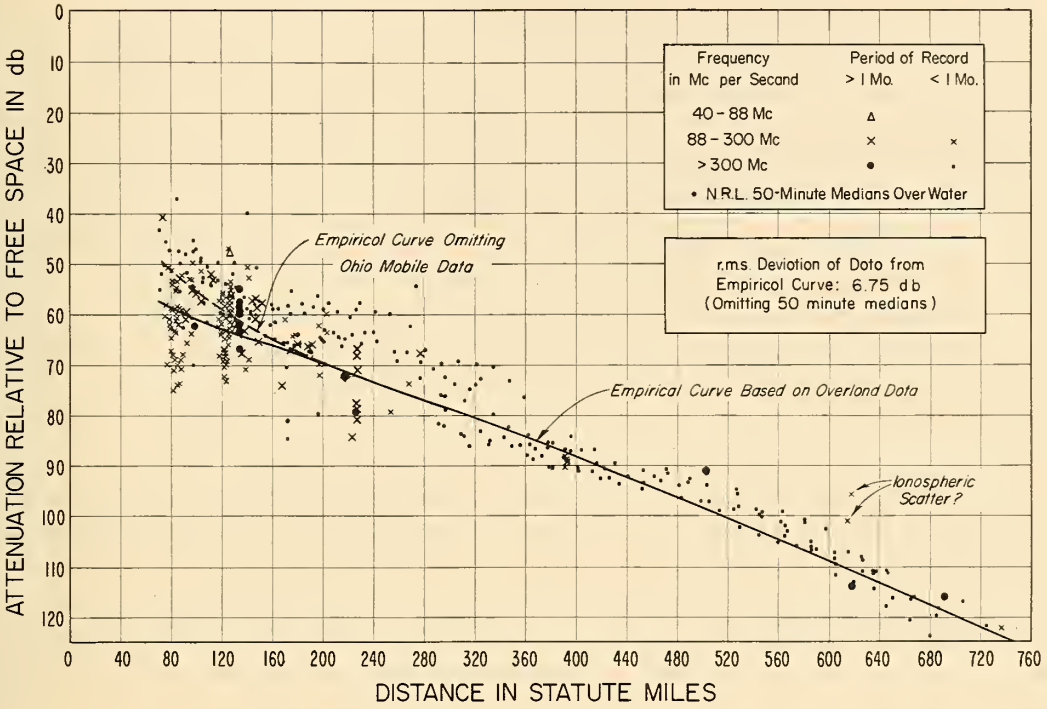

DEVIATION OF THE ABOVE RECORDED MEDIANS FROM VALUES PREDICTED FOR AN EXPONENTIAL ATMOSPHERE USING NBS REPORT No. 5582

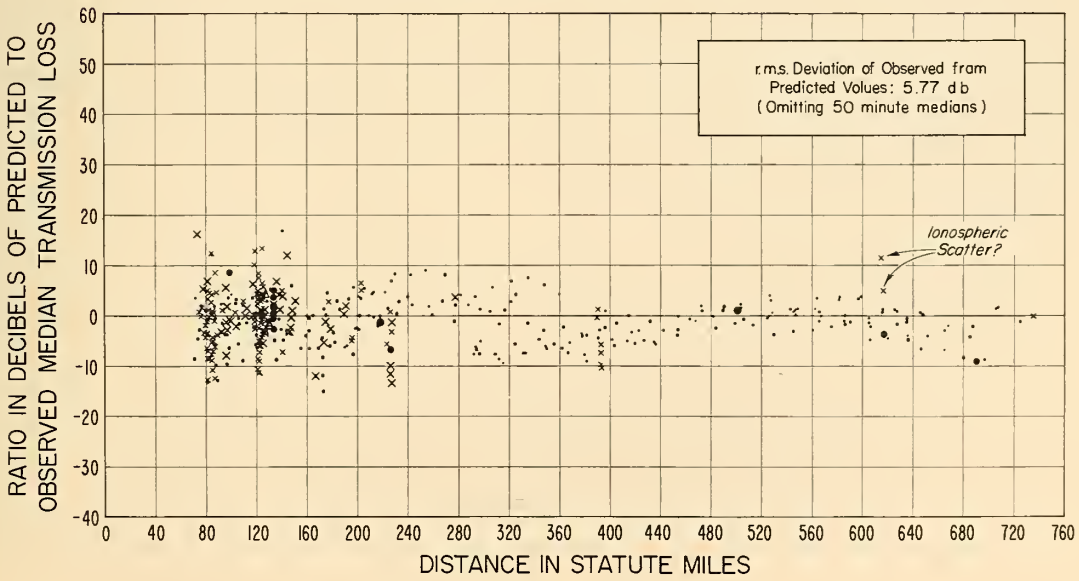

Figure 13a

Explanation of Fig. 13a.

Observed median values of attenuation relative to free space are plotted versus distance in Fig. 13a for a large, heterogeneous sample of data, obtained in most cases with broad beam antennas. No normalization for the effects of frequency, antenna height, loss of antenna gain, terrain or meteorological parameters is included. Almost all recordings were made in the wintertime, and correspond to conditions where tropospheric forward scatter is expected to be the dominant propagation mechanism. Two points are indicated where ionospheric rather than tropospheric scatter may have been recorded at 100 Mc. No data are included for cases where diffraction is expected to be more important than forward scatter, such as short paths where the angular distance is small.

Fig. 13a also shows deviations of data from the point-to-point transmission loss prediction method of this technical note; these deviations are plotted versus distance, using the same data and the same scale. The NRL overwater 50-minute medians shown in Fig. 13a were excluded in calculating the r. m. s. deviation of 6. 75 db from the empirical curve and the r. m. s. deviation of 5. 77 db from the theoretical values.

The data include 80 paths from a special experiment conducted in Ohio with randomly selected receiving sites at 85 and 125 miles. For these paths, long-term median observed transmission loss is slightly greater than when antenna sites are carefully selected to be unobstructed. The prediction method in this report indicates an increase in transmission loss of about 12 db per degree of increase in horizon elevation angles, and these angles were often large for the randomly selected "Ohio mobile" receiving sites.

Time Block No. 4 vary by as much as three and a half decibels from year to year, even though each value represents almost 1300 hours from the same season and time of day each year. Note that our predicted values, for this particular path, depart from the observed values no more than the observed values depart from each other from year to year. In a subsequent part of this report a comparison of our predicted values will be made for all of the paths for which we have both transmission loss and profile information. We conclude from an examination of these data that it is usually safer to base the design of a point-to-point radio relaying system on the transmission losses predicted by our formula than to base this design on a set of transmission loss measurements made over a period of only a few months. It should be noted in this connection that path loss tests are seldom made at the precise locations or with the same antennas as are used in the final systems, and consequently really provide very little pertinent information as to the final performance of the system over a long period of time. Furthermore the prediction formula cannot be used without precise profile information and, when this is obtained, it often leads to the choice of an alternate site which the prediction formula may indicate is somewhat better.

As an example of the use of the formulas in this report, the detailed calculations required to reproduce the theoretical curves of Fig. 13 are given in Section 12.

4. Description of Radio Standard Atmospheres

The forward scatter theory which provides a basis for prediction of radio transmission loss at great distances depends upon work done by Booker and Gordon to explain scattering from the stratosphere. [11] The scattered power is assumed proportional to the square of the mean gradient, (dn/dh), of the refractive index of the atmosphere. In what follows we will use the refractivity $N = (n - 1) \times 10^6$ as a measure of n. Recent work by Bean and Thayer [1] has led to the definition of a set of standard atmospheres which agree with average measured refractivity profiles from the ground to great heights, and which depend upon the average value of the surface refractivity, N_s, and the height of the surface above sea level, h_s. Each of the new standard atmospheres has a linear refractive index gradient for the first kilometer above ground. Refractivity decreases exponentially from this height above the surface to a value N = 105 at a height h = 9 kilometers above sea level. For greater heights the standard atmospheres are the same, with an exponential gradient independent of the surface values of refractivity.

Table II

Reference Atmosphere N_s	ΔN/km	Assumed h_s	a in miles	Range of h_{cg} thousands of feet	Range of h_o in miles	N_e	γ per mile	ΔG in db
250	-29.51	5000'	4878.50	0 to 3.28	0 to 0.463	302.7	0.2021	4.66
				3.28 to 24.5	0.463 to 4.00	294.4	0.1844	6.90
				> 24.5	> 4.00	378.2	0.2292	0
301	-39.23	1000'	5280.00	0 to 3.28	0 to 0.463	314.1	0.2247	2.04
				3.28 to 28.5	0.463 to 4.67	305.6	0.1907	5.84
				> 28.5	> 4.67	378.2	0.2292	0
350	-51.55	0	5896.66	0 to 3.28	0 to 0.463	350.0	0.2564	-1.77
				3.28 to 29.5	0.463 to 4.83	340.1	0.2102	2.80
				> 29.5	> 4.83	378.2	0.2292	0
400	-68.13	0	6996.67	0 to 3.28	0 to 0.463	400.0	0.3005	-6.37
				3.28 to 29.5	0.463 to 4.83	383.2	0.2314	-0.32
				> 29.5	> 4.83	378.2	0.2292	0

The average refractivity gradient near the ground, $\Delta N/km$, is specified by the following empirical relationship in terms of the average surface refractivity, N_s:

$$\Delta N \text{ per kilometer} = -7.32 \exp(0.005577\, N_s) \qquad (4.1a)$$

When a good estimate of the average gradient ΔN is available from refractivity profiles, the average surface refractivity N_s to be used in the calculations should be obtained from (4.1b):

$$N'_s = 412.87 \log_{10} |\Delta N/km| - 356.93 \qquad (4.1b)$$

rather than using the observed average value of N_s in case it differs appreciably from N'_s. Transmission loss L(p) is obtained for a given N_s by linear db interpolation or extrapolation from calculations for two adjacent values selected from the four reference values, N_s = 250, 301, 350, and 400.

The refractivity gradient, ΔN, largely determines radio ray bending through the atmosphere. For each ΔN, an effective earth's radius, a, is defined in such a way that rays drawn above an earth with this effective radius will not bend until they reach heights exceeding one kilometer. Table II shows for the four reference atmospheres the values of the effective earth's radius, a, in statute miles, and the corresponding linear gradient, $\Delta N/km$, for the first kilometer above the surface. Also tabulated are the logarithmic gradients, γ, appropriate for greater heights where the refractivity N decreases exponentially with height.

Fig. 14 illustrates for both rough and smooth earth conditions the geometry of a forward scatter link in a linear gradient atmosphere. The most important parameters shown are the propagation path distance, d, and elevation angles of the radio horizons, α_{oo} and β_{oo},

GEOMETRY FOR A LINEAR GRADIENT ATMOSPHERE

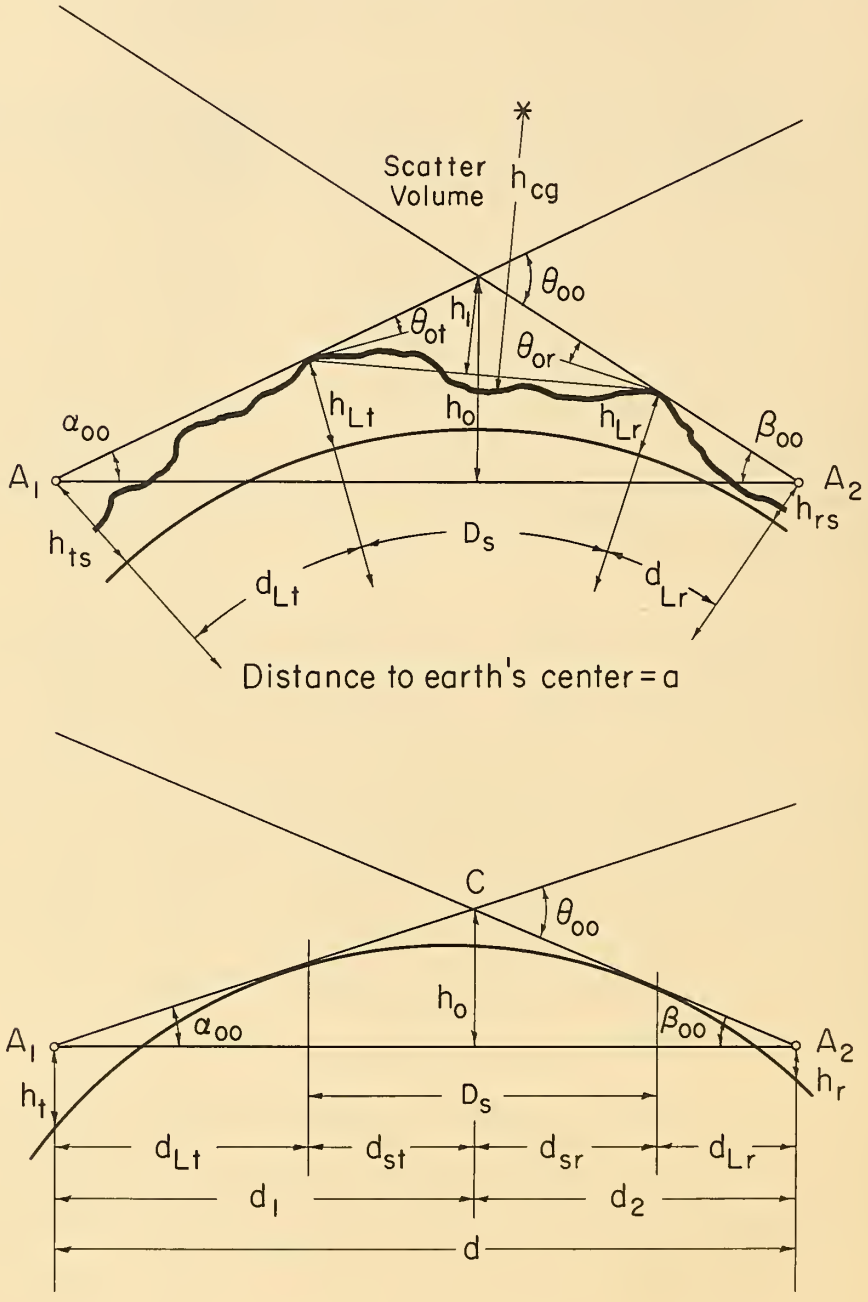

Distances are measured in statute miles along a great circle arc

$$\theta_{oo} = \frac{D_s}{a} + \theta_{ot} + \theta_{or}$$

Figure 14

for a linear gradient atmosphere. Section 5 of this report shows how the true elevation angles α_o and β_o are obtained for the longer paths and for very large antenna heights, using the standard exponential atmospheres of Table II.

Within the scattering volume pictured in Fig. 14, the relationship between refractivity, N, and height above ground, $h - h_s$, is taken to be

$$N(h - h_s) = N_e \exp[-\gamma (h - h_s)] \qquad (4.2)$$

where h is the height of a scatterer above sea level and h_s is the average height of the surface above sea level:

$$h_s = (h_{Lt} + h_{Lr})/2 \qquad (4.3)$$

Where h_s cannot be determined, the values assumed in Table II may be used. The parameters h_{Lt} and h_{Lr} are heights of radio horizon obstacles above sea level, as illustrated in Fig. 14. Extrapolated refractivity values, N_e, and the logarithmic gradients, γ per mile, are listed in Table II for various ranges of the height of the "scattering center" above ground, h_{cg}. An approximation to this height has been derived in terms of the height, h_o, of the crossover of radio horizon rays above the reference axis A_1A_2 from transmitter to receiver:

$$h_{cg} \cong 6\, h_o + 0.5 \qquad (4.4)$$

Here, h_{cg} is in thousands of feet and h_o is in miles; note the difference in units. Section 8 contains a further discussion of these parameters.

5. Path Geometry

The steps required to obtain accurate estimates of the geometrical parameters defined in Fig. 14 for an equivalent earth of radius a are as follows:

a. Plotting a Terrain Profile

Plot a great circle path terrain profile between transmitter and receiver locations. If topographic maps are used, denote by (N_1, W_1) and (N_2, W_2) the latitude and longitude of antennas at

A_1 and A_2 on the surface of a spherical earth of radius 3960 miles. Let (N, W) be the geographical coordinates of any point on the great circle between A_1 and A_2. Then,

$$A \cos (W - W_1) \cos N + B \sin (W - W_1) \cos N + \sin N = 0 \qquad (5.1)$$

is the general equation for a plane through the center of the earth and a point (x, y, z), where $x = \cos (W - W_1) \cos N$, $y = \sin(W - W_1) \cos N$, $z = \sin N$. This is a cartesian coordinate system with z in the direction of the earth's axis, x - y the equatorial plane, and the x-z plane passing through the antenna location A_1. Geographical coordinates of (x, y, z) and (N, W), and the constants A and B are evaluated by substituting the known coordinates (N_1, W_1) and (N_2, W_2) in (5.1):

$$A = - \tan N_1 \qquad (5.2)$$

$$B = \tan N_1 \cot (W_2 - W_1) - \tan N_2 \csc (W_2 - W_1). \qquad (5.3)$$

A great circle path is plotted on a contour map by choosing values for N and solving (5.1) for W, or vice versa. The great circle distance d between points with coordinates (N, W) and (N', W') is given by

$$\cos (d/a') = \sin N \sin N' + \cos N \cos N' \cos (W - W'), \qquad (5.4)$$

where a' is the actual earth's radius.

b. Determining Radio Horizons

Having obtained a great circle path terrain profile, the next step is to determine the location of radio horizon obstacles at each end of the path. Where a smooth earth is involved, over the sea for instance, the methods described in subsection (5d) for calculating α_o and β_o are easier than methods described in subsections (5b) and (5c). For an antenna less than one kilometer above ground, the location of the equivalent earth radio horizon is used in the calculations. The correct horizons maximize the horizon elevation angles θ_{et} and θ_{er}:

$$\theta_{et} = \frac{h_{Lt} - h_{ts}}{5280\, d_{Lt}} - \frac{d_{Lt}}{2a} \text{ radians}, \qquad (5.5)$$

$$\theta_{er} = \frac{h_{Lr} - h_{rs}}{5280\, d_{Lr}} - \frac{d_{Lr}}{2a} \text{ radians} \qquad (5.6)$$

where heights are in feet and distances in miles. Having approximately located the radio horizons by inspection, the values of h_{Lt} and d_{Lt} or h_{Lr} and d_{Lr} corresponding to nearby high points are substituted into (5.5) and (5.6); values which maximize θ_{et} and θ_{er} are the correct ones. If θ_{et} or θ_{er} is negative, choose the value nearest zero.

As illustrated in Fig. 14, h_{ts} and h_{rs} are transmitting and receiving antenna heights above sea level, and d_{Lt} and d_{Lr} are distances to radio horizon obstacles from transmitting and receiving antennas. The effective earth's radius, a, is found in Table II.

c. Computation of Angular Distance

The angles α_o, β_o, and $\theta = \alpha_o + \beta_o$ for a reference atmosphere are in general larger than the angles α_{oo}, β_{oo}, and θ_{oo} computed for the corresponding linear gradient atmosphere if either antenna or the scatter volume is more than one kilometer above the surface. Accordingly, θ is computed in two steps; first, α_{oo} and β_{oo} are calculated for a linear gradient atmosphere, and then α_o and β_o are obtained by adding small corrections, $\Delta\alpha_o$ and $\Delta\beta_o$ to α_{oo} and β_{oo}. It will be seen that these corrections are either zero or negligible for short paths if $|h_{ts} - h_{Lt}|$ and $|h_{rs} - h_{Lr}|$ are less than one kilometer.

$$\alpha_{oo} = \frac{d}{2a} + \theta_{et} + \frac{h_{ts} - h_{rs}}{5280\, d} \text{ radians} \qquad (5.7)$$

$$\beta_{oo} = \frac{d}{2a} + \theta_{er} - \frac{h_{ts} - h_{rs}}{5280\, d} \text{ radians} \qquad (5.8)$$

These angles α_{oo} and β_{oo} are positive for beyond-the-horizon paths.

$$\theta_{ot} = \theta_{et} + \frac{d_{Lt}}{a} \text{ radians} \qquad (5.9)$$

$$\theta_{or} = \theta_{er} + \frac{d_{Lr}}{a} \text{ radians} \tag{5.10}$$

These angles may be positive or negative, and over a smooth spherical earth are zero, as may be seen from Fig. 14.

$$D_s = d - d_{Lt} - d_{Lr} \tag{5.11}$$

$$\theta_{oo} = \alpha_{oo} + \beta_{oo} = \frac{D_s}{a} + \theta_{ot} + \theta_{or} = \frac{d}{a} + \theta_{et} + \theta_{er} \text{ radians} \tag{5.12}$$

Over a smooth spherical earth,

$$d_{Lt} = \sqrt{(a/5280)\ (2\ h_{te})}, \tag{5.13}$$

$$d_{Lr} = \sqrt{(a/5280)\ (2\ h_{re})}, \tag{5.14}$$

and the angular distance, θ_{oo}, is the distance between radio horizons, D_s, divided by the effective earth's radius, a, as may be seen using (5.12). Exact expressions relating d_{Lt}, d_{Lr} and h_{te}, h_{re} in a linear gradient atmosphere are given by (7.3) and (7.4) in Section 7.

Next, correcting α_{oo} and β_{oo} to values expected in a reference atmosphere:

$$\alpha_o = \alpha_{oo} + \Delta\alpha_o\ (d_{st},\ \theta_{ot},\ N_s) \tag{5.15}$$

$$\beta_o = \beta_{oo} + \Delta\beta_o\ (d_{sr},\ \theta_{or},\ N_s) \tag{5.16}$$

The correction $\Delta\alpha_o$ in milliradians is plotted in Figs. 15 - 22 for the four reference atmospheres of Table II, as a function of d_{st}, θ_{ot}, and N_s. These same figures are used to read $\Delta\beta_o$, given d_{sr} in statute miles and θ_{or} in milliradians.

$$d_{st} = \frac{d\beta_o}{\theta} - d_{Lt} \cong \frac{d\beta_{oo}}{\theta_{oo}} - d_{Lt} \tag{5.17}$$

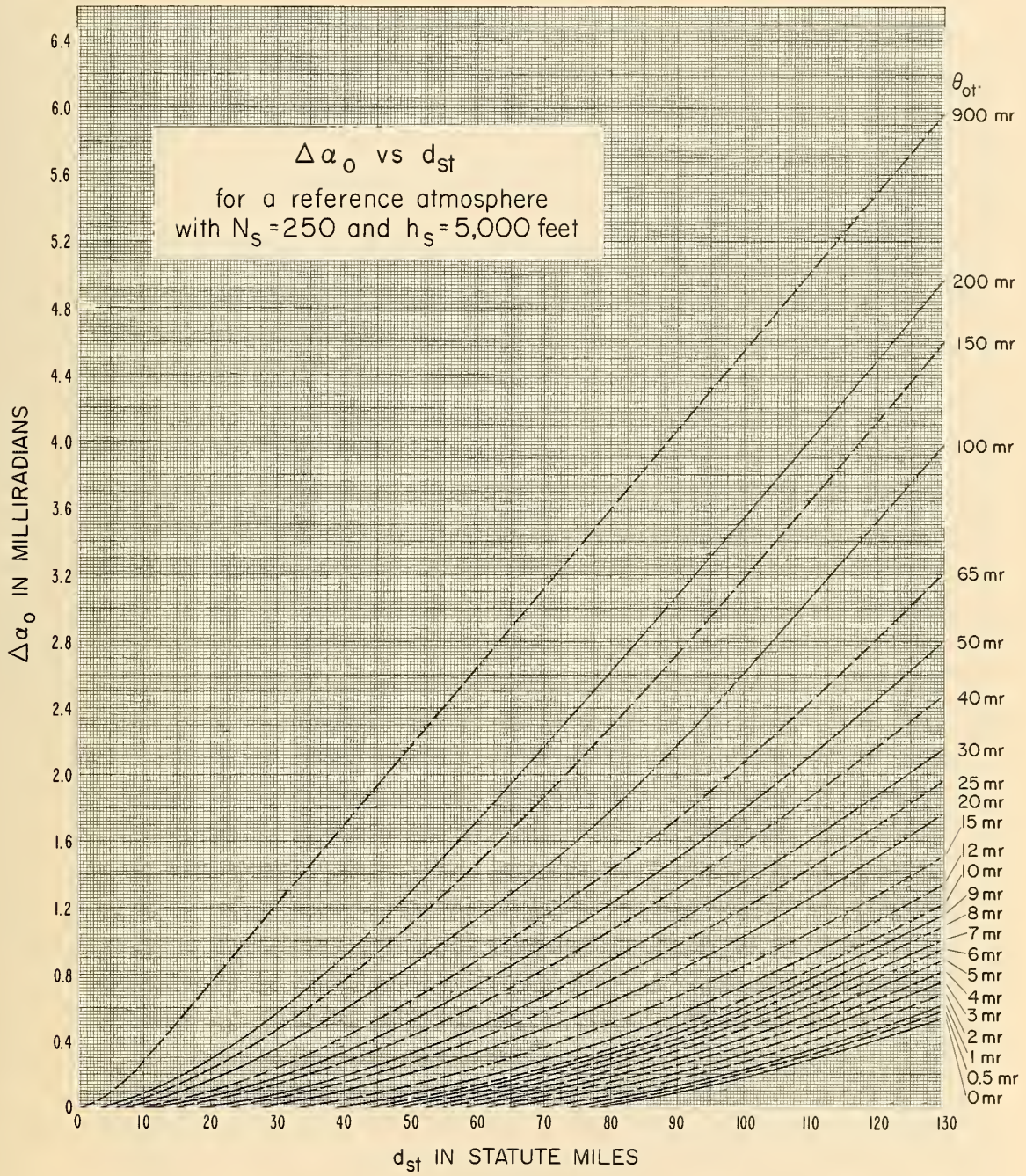
$\Delta\alpha_o$ vs d_{st}
for a reference atmosphere
with N_s = 250 and h_s = 5,000 feet
$\Delta\alpha_o$ IN MILLIRADIANS
d_{st} IN STATUTE MILES
θ_{ot}
900 mr
200 mr
150 mr
100 mr
65 mr
50 mr
40 mr
30 mr
25 mr
20 mr
15 mr
12 mr
10 mr
9 mr
8 mr
7 mr
6 mr
5 mr
4 mr
3 mr
2 mr
1 mr
0.5 mr
0 mr
0
0.4
0.8
1.2
1.6
2.0
2.4
2.8
3.2
3.6
4.0
4.4
4.8
5.2
5.6
6.0
6.4
0
10
20
30
40
50
60
70
80
90
100
110
120
130

Figure 15

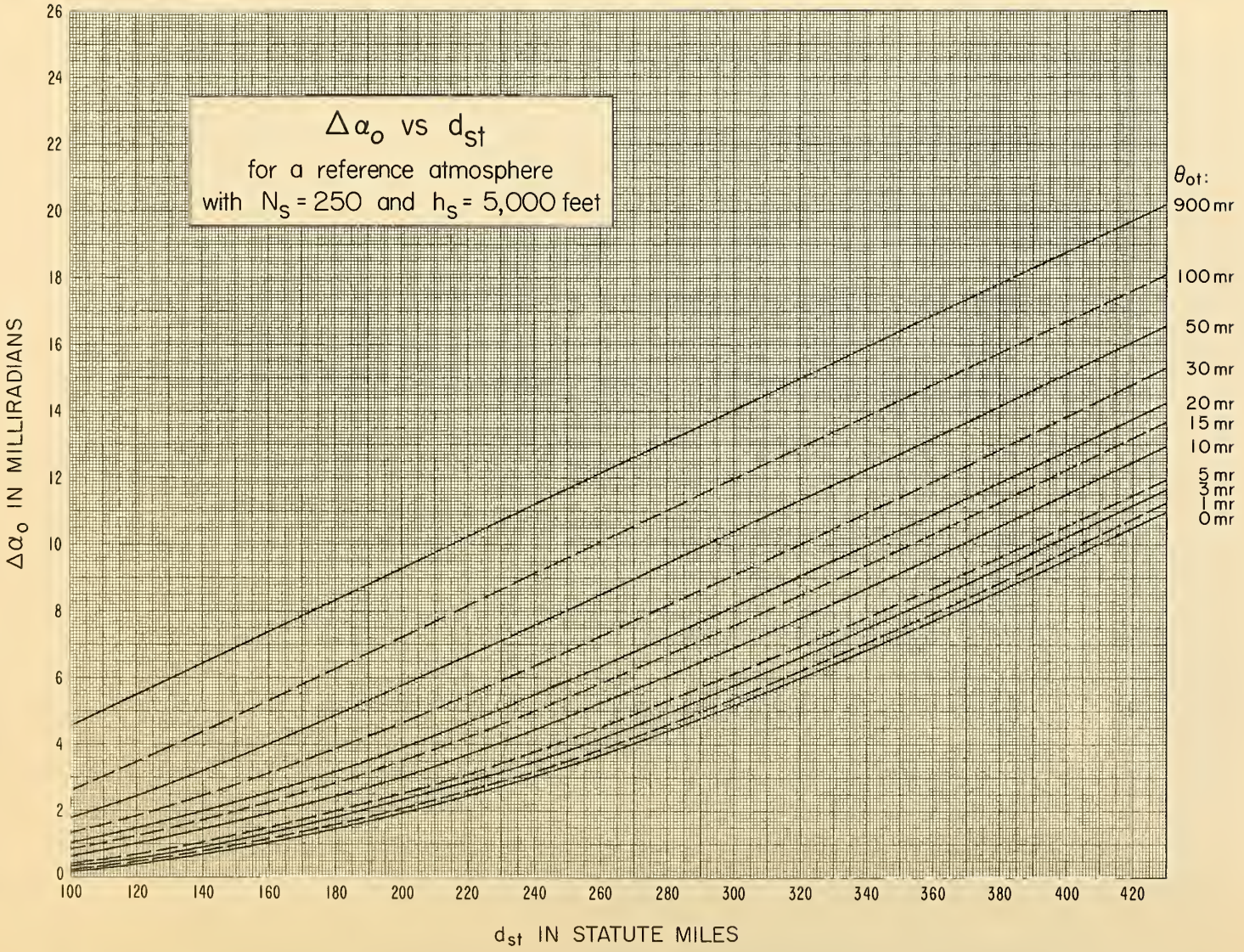
$\Delta\alpha_o$ vs d_{st}
for a reference atmosphere
with N_s = 250 and h_s = 5,000 feet
$\Delta\alpha_o$ IN MILLIRADIANS
d_{st} IN STATUTE MILES
θ_{ot}:
900 mr
100 mr
50 mr
30 mr
20 mr
15 mr
10 mr
5 mr
3 mr
1 mr
0 mr
0
2
4
6
8
10
12
14
16
18
20
22
24
26
100
120
140
160
180
200
220
240
260
280
300
320
340
360
380
400
420

Figure 16

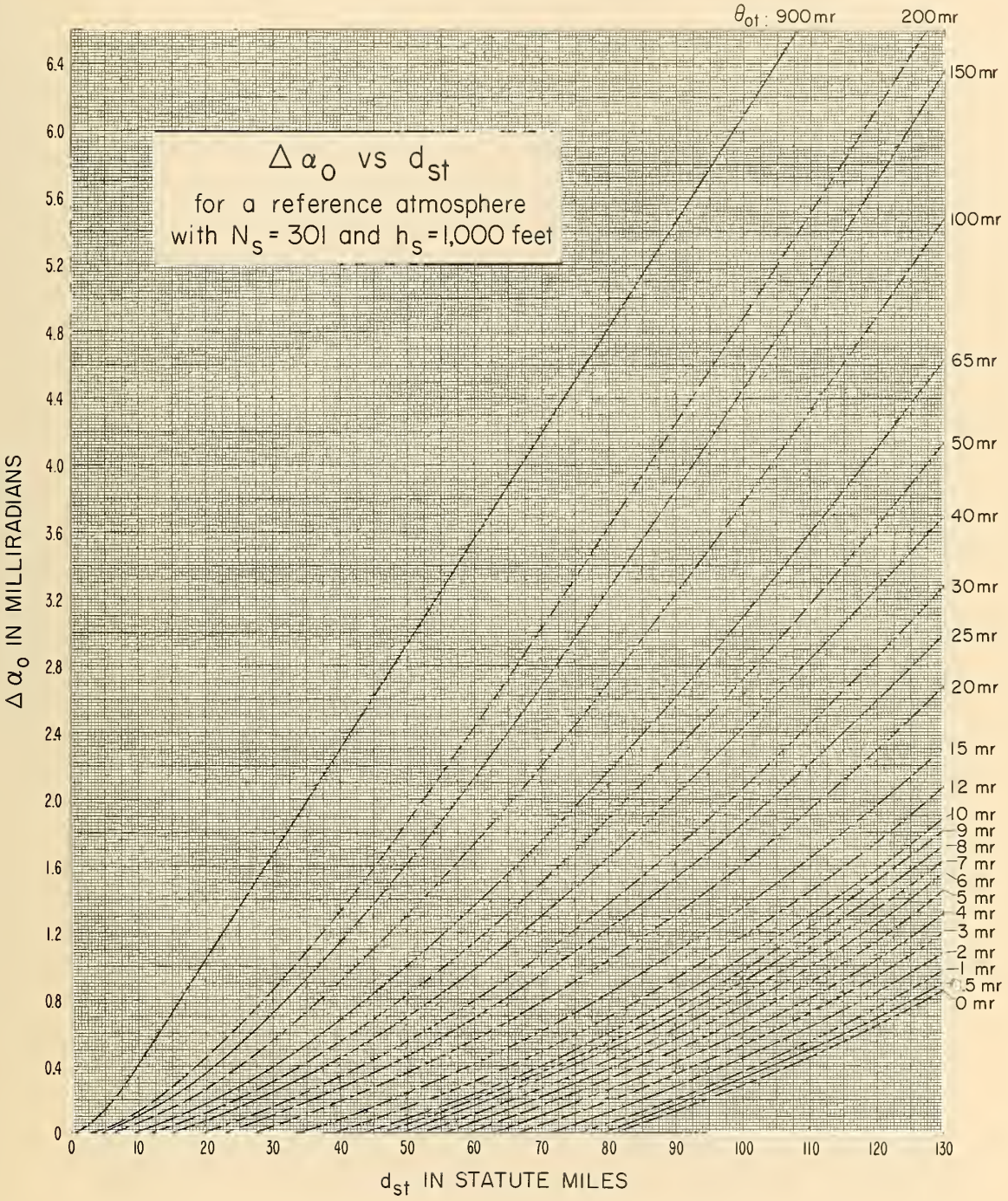
θ_{ot}: 900 mr
200 mr
150 mr
100 mr
65 mr
50 mr
40 mr
30 mr
25 mr
20 mr
15 mr
12 mr
10 mr
9 mr
8 mr
7 mr
6 mr
5 mr
4 mr
3 mr
2 mr
1 mr
.5 mr
0 mr
$\Delta \alpha_o$ vs d_{st}
for a reference atmosphere
with N_s = 301 and h_s = 1,000 feet
$\Delta \alpha_o$ IN MILLIRADIANS
d_{st} IN STATUTE MILES
0
0.4
0.8
1.2
1.6
2.0
2.4
2.8
3.2
3.6
4.0
4.4
4.8
5.2
5.6
6.0
6.4
0
10
20
30
40
50
60
70
80
90
100
110
120
130

Figure 17

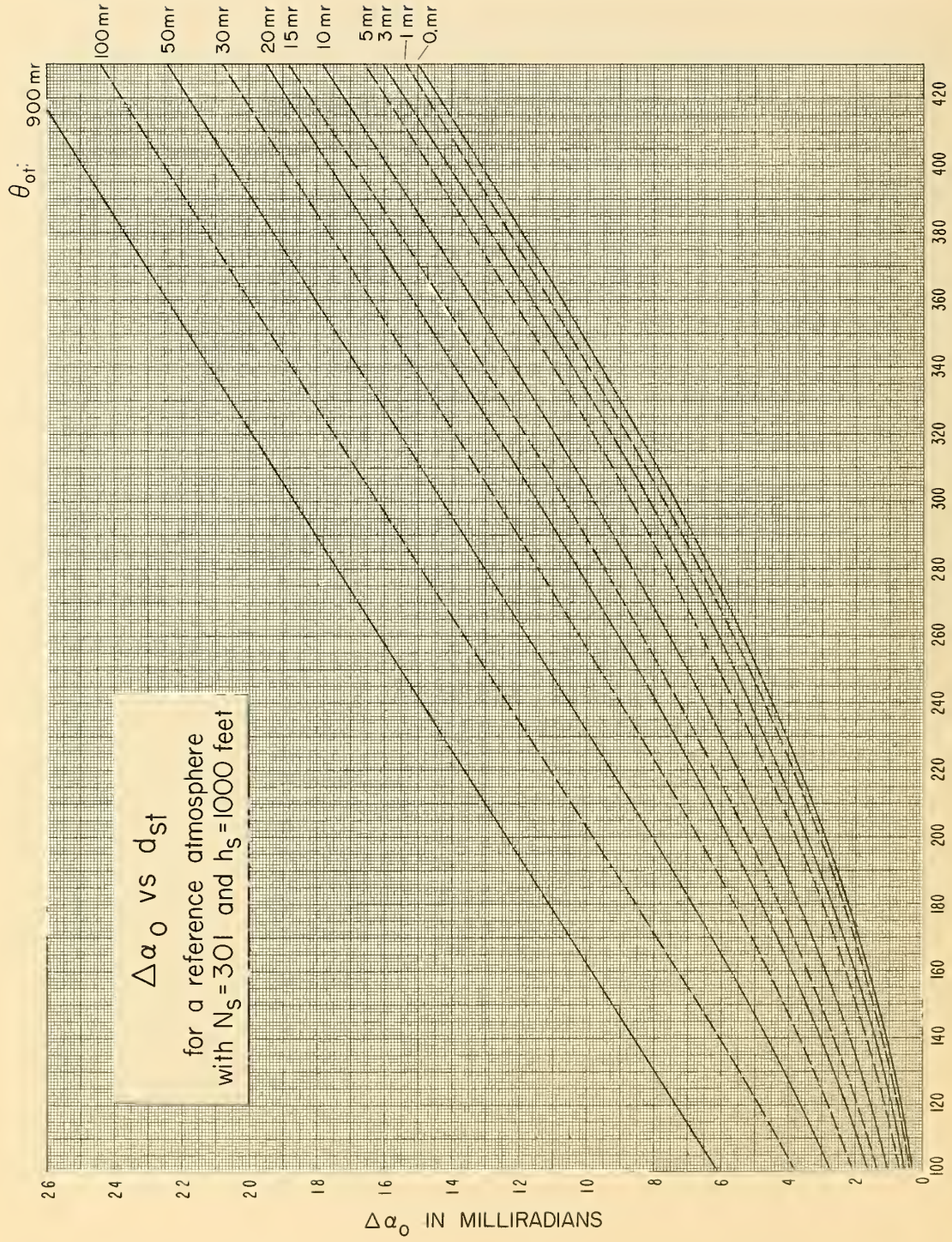

Figure 18

Figure 18

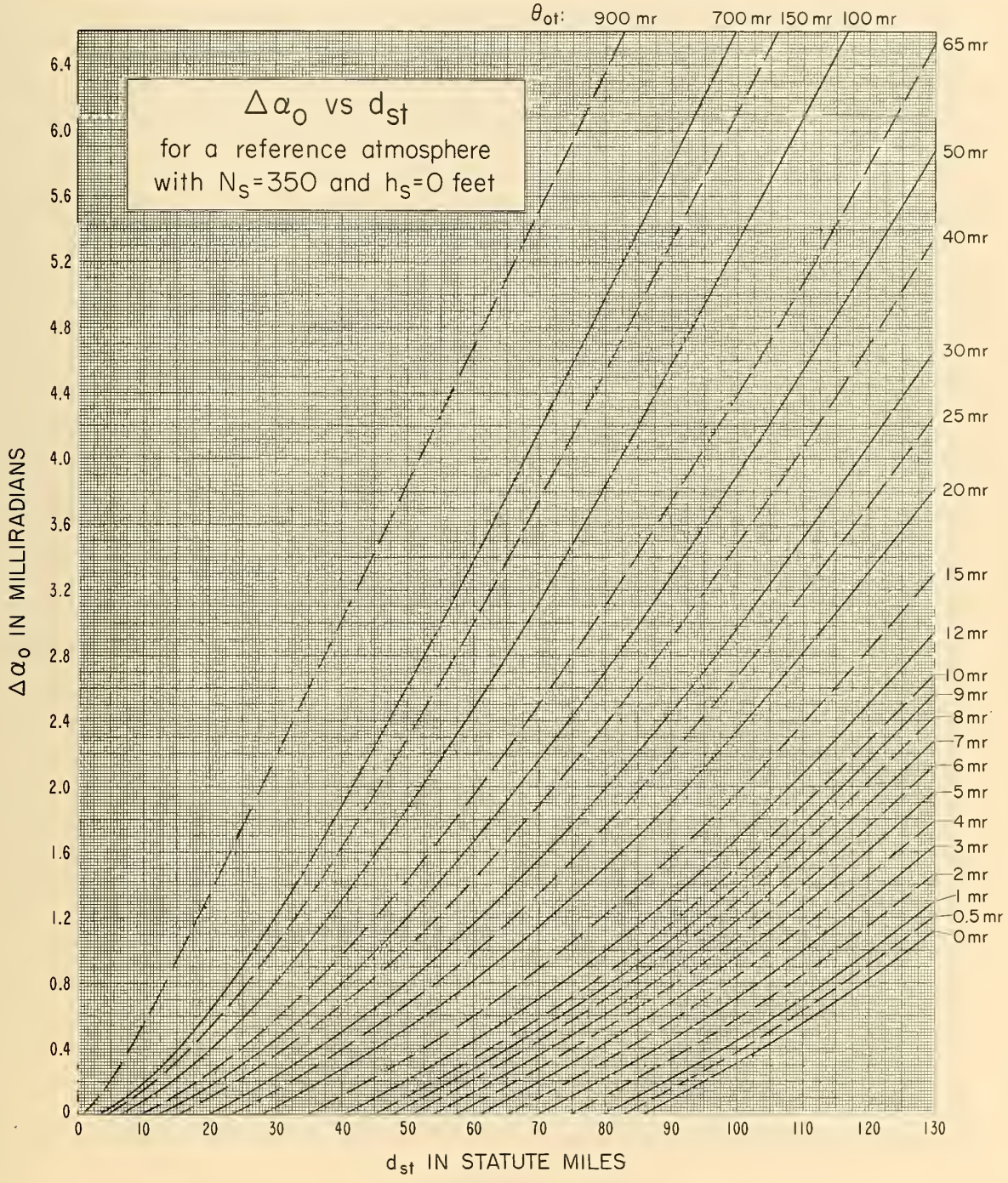
θ_{ot}: 900 mr 700 mr 150 mr 100 mr
$\Delta\alpha_o$ vs d_{st}
for a reference atmosphere
with N_s=350 and h_s=0 feet
65 mr
50 mr
40 mr
30 mr
25 mr
20 mr
15 mr
12 mr
10 mr
9 mr
8 mr
7 mr
6 mr
5 mr
4 mr
3 mr
2 mr
1 mr
0.5 mr
0 mr
$\Delta\alpha_o$ IN MILLIRADIANS
0 0.4 0.8 1.2 1.6 2.0 2.4 2.8 3.2 3.6 4.0 4.4 4.8 5.2 5.6 6.0 6.4
0 10 20 30 40 50 60 70 80 90 100 110 120 130
d_{st} IN STATUTE MILES

Figure 19

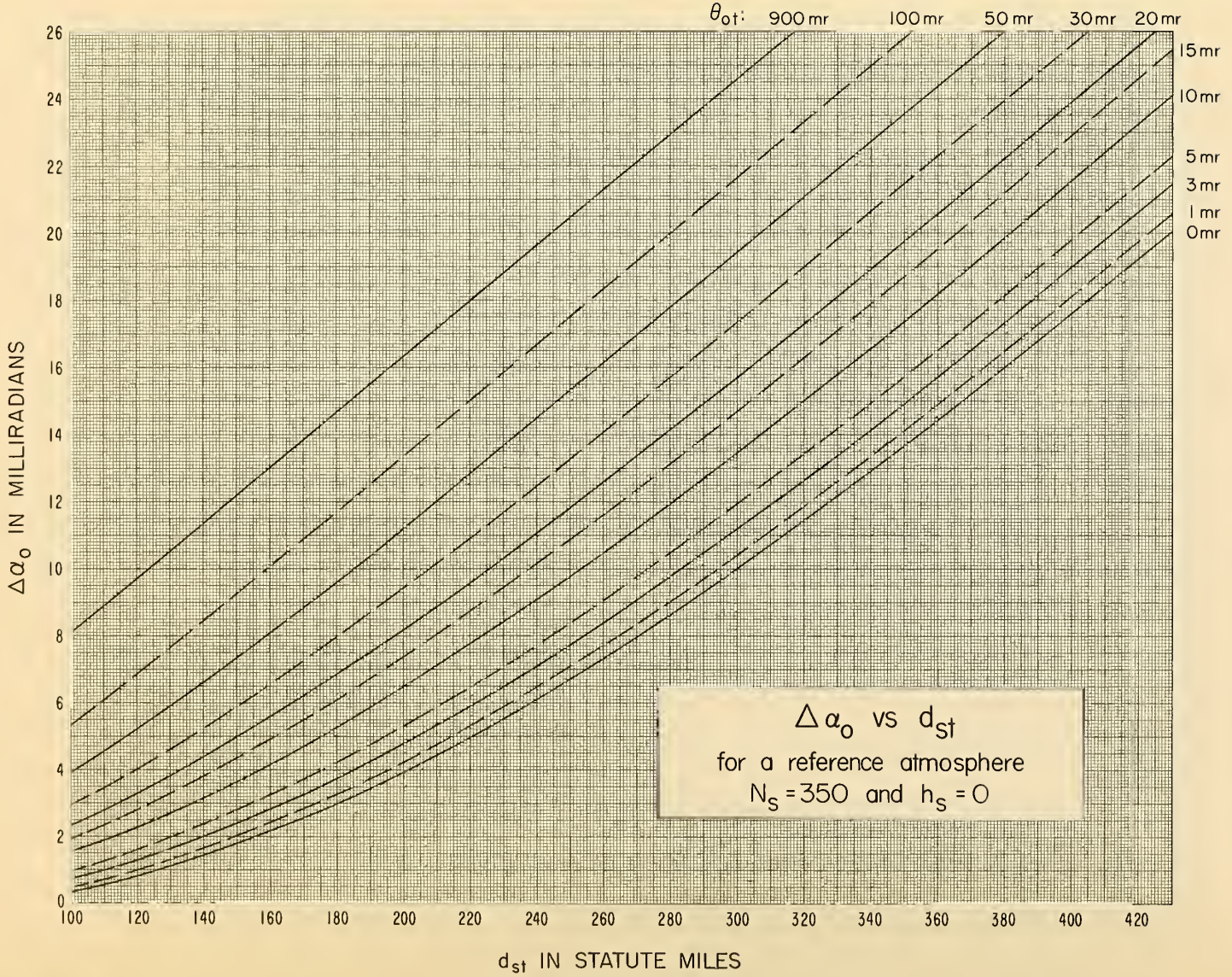
θ_{ot}: 900 mr
100 mr
50 mr
30 mr
20 mr
15 mr
10 mr
5 mr
3 mr
1 mr
0 mr
$\Delta\alpha_o$ IN MILLIRADIANS
d_{st} IN STATUTE MILES
$\Delta\alpha_o$ vs d_{st}
for a reference atmosphere
$N_s = 350$ and $h_s = 0$

Figure 20

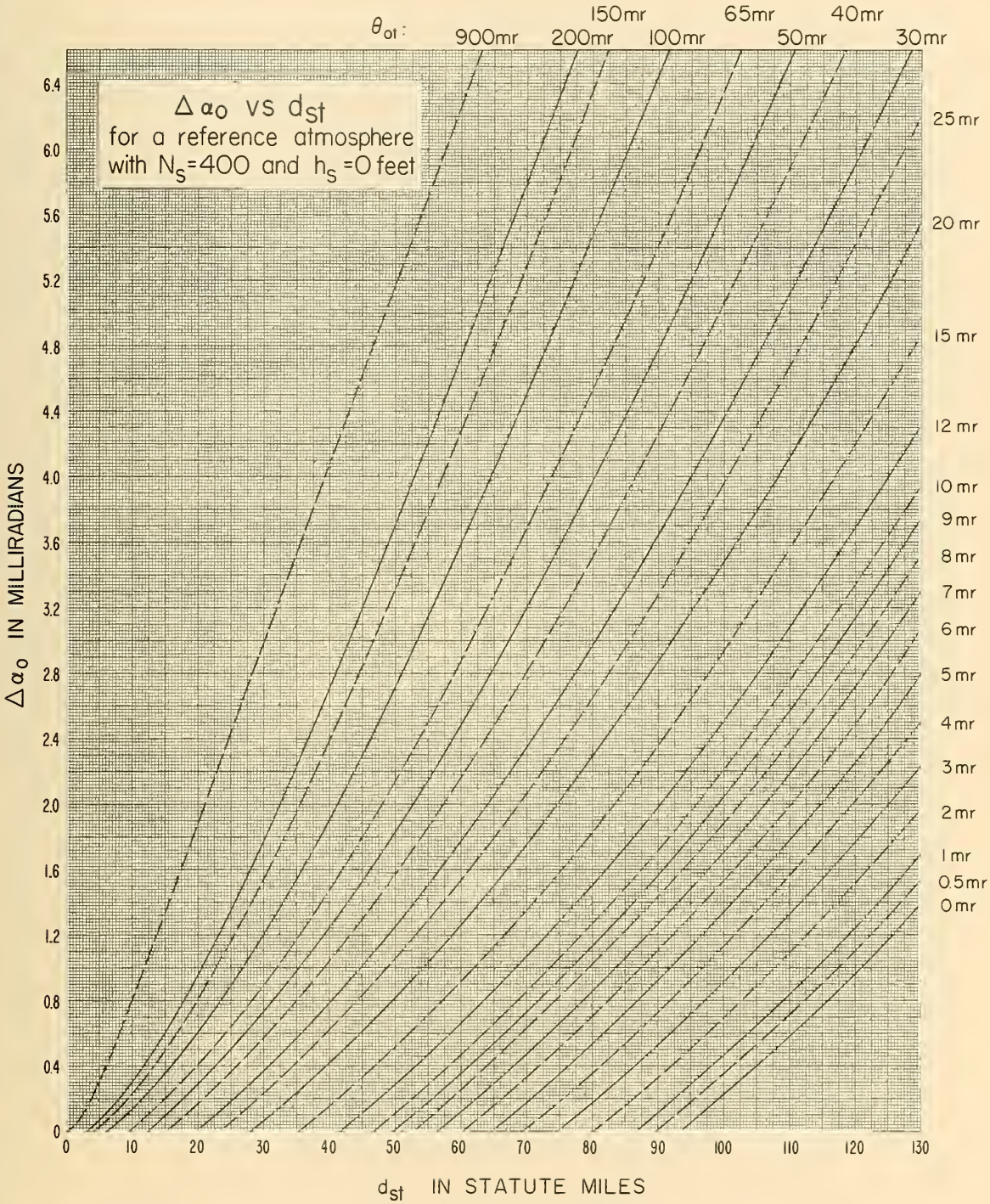
θ_{ot}:
900mr
200mr
150mr
100mr
65mr
50mr
40mr
30mr
$\Delta\alpha_o$ vs d_{st}
for a reference atmosphere
with N_s=400 and h_s=0 feet
25 mr
20 mr
15 mr
12 mr
10 mr
9 mr
8 mr
7 mr
6 mr
5 mr
4 mr
3 mr
2 mr
1 mr
0.5mr
0 mr
$\Delta\alpha_o$ IN MILLIRADIANS
0
0.4
0.8
1.2
1.6
2.0
2.4
2.8
3.2
3.6
4.0
4.4
4.8
5.2
5.6
6.0
6.4
0
10
20
30
40
50
60
70
80
90
100
110
120
130
d_{st} IN STATUTE MILES

Figure 21

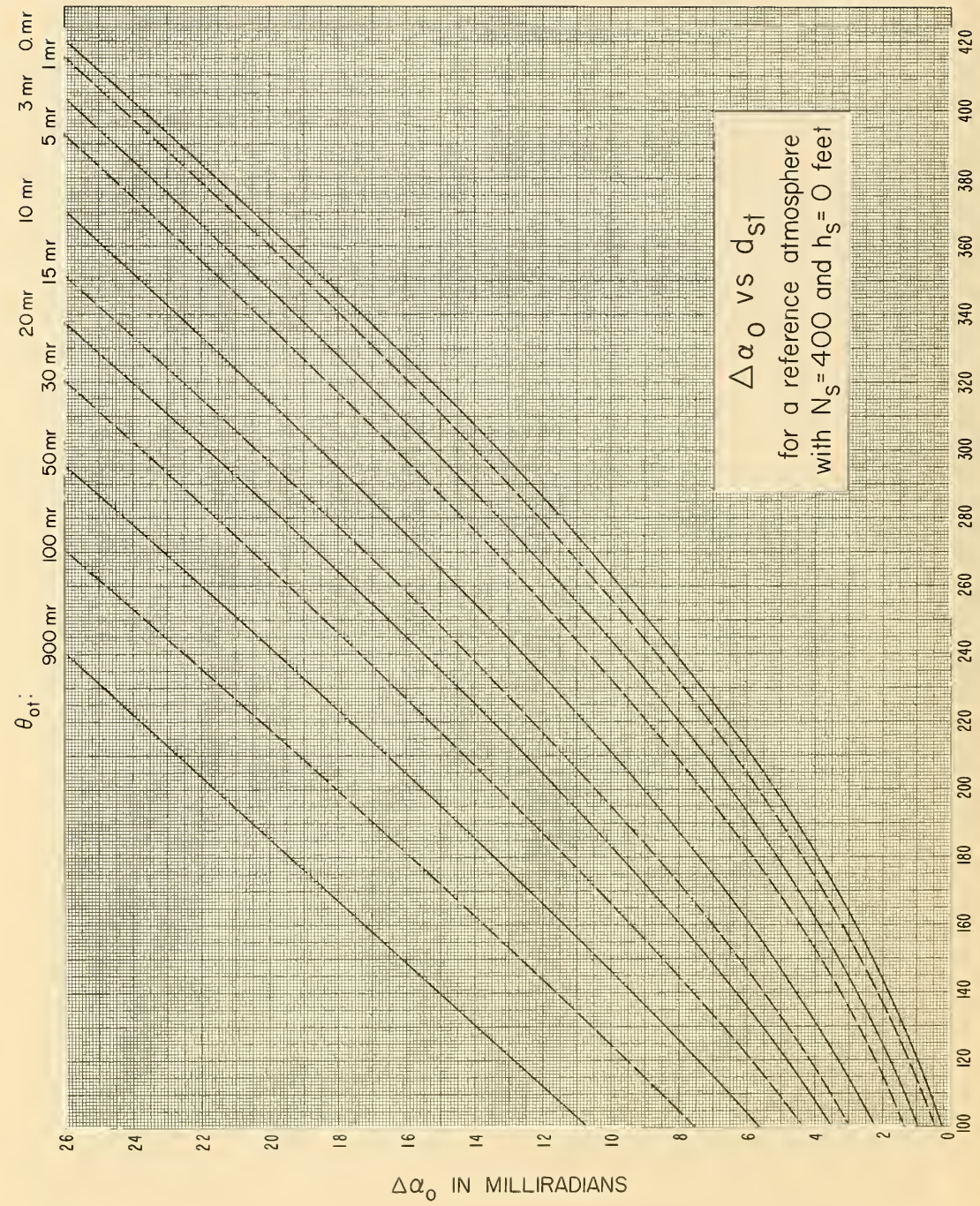
θ_{ot}:
900 mr
100 mr
50 mr
30 mr
20 mr
15 mr
10 mr
5 mr
3 mr
1 mr
0 mr
$\Delta\alpha_o$ vs d_{st}
for a reference atmosphere
with N_s = 400 and h_s = 0 feet
$\Delta\alpha_o$ IN MILLIRADIANS
d_{st} IN STATUTE MILES
0
2
4
6
8
10
12
14
16
18
20
22
24
26
100
120
140
160
180
200
220
240
260
280
300
320
340
360
380
400
420

Figure 22

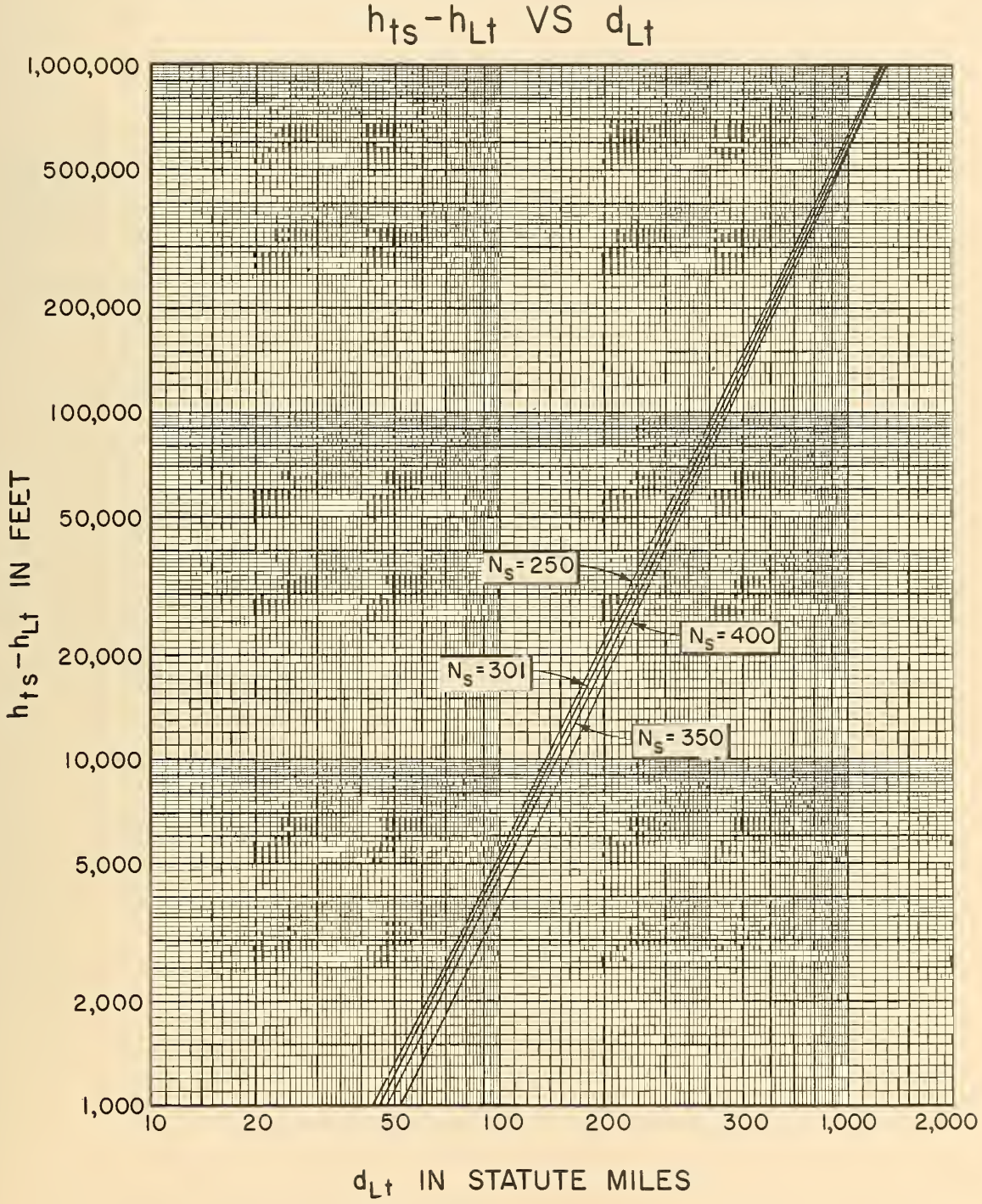
$h_{ts}-h_{Lt}$ VS d_{Lt}
1,000,000
500,000
200,000
100,000
50,000
20,000
10,000
5,000
2,000
1,000
$h_{ts}-h_{Lt}$ IN FEET
N_s = 250
N_s = 400
N_s = 301
N_s = 350
10
20
50
100
200
300
1,000
2,000
d_{Lt} IN STATUTE MILES

Figure 23

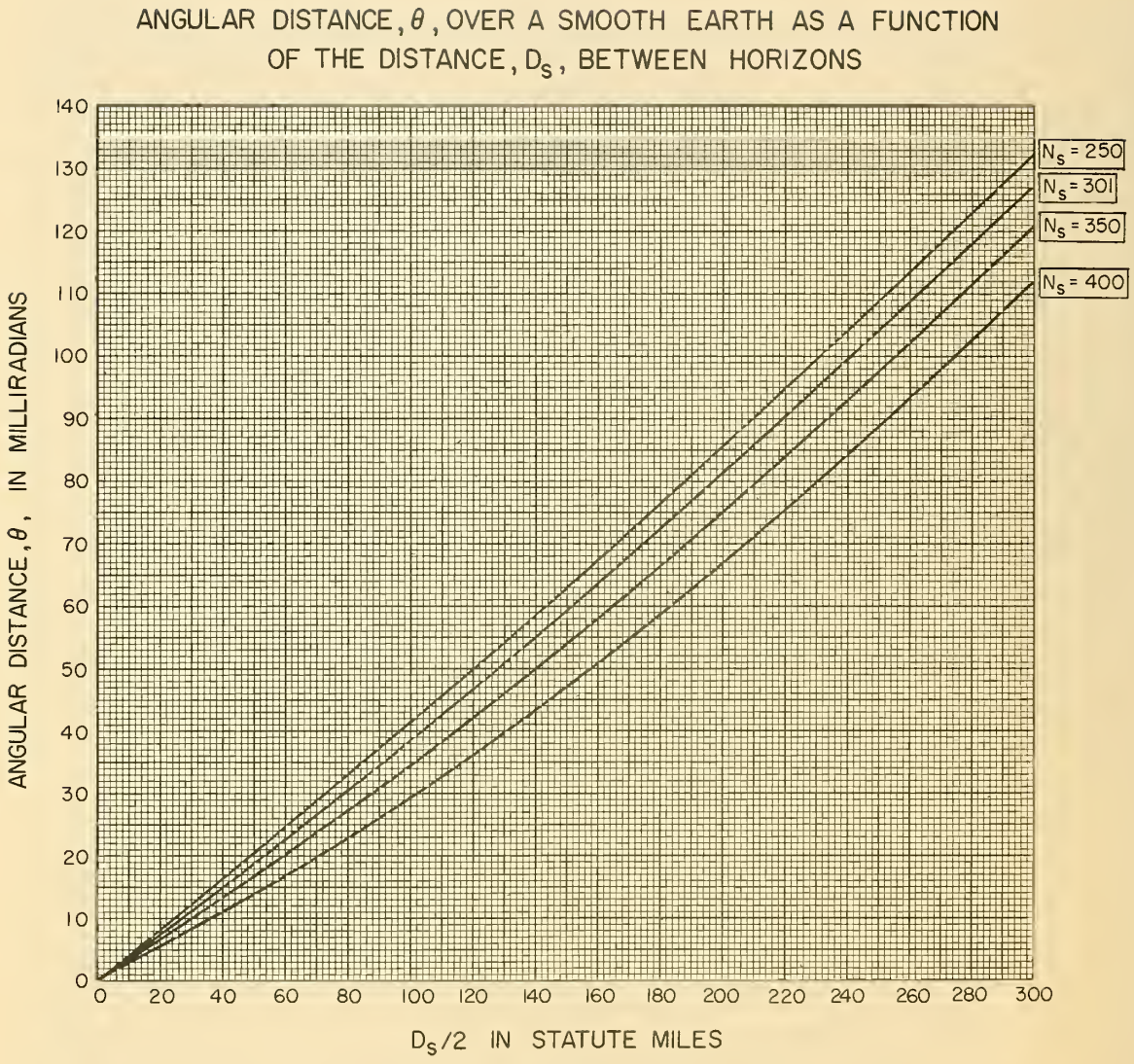
ANGULAR DISTANCE, θ, OVER A SMOOTH EARTH AS A FUNCTION OF THE DISTANCE, D_S, BETWEEN HORIZONS
ANGULAR DISTANCE, θ, IN MILLIRADIANS
0
10
20
30
40
50
60
70
80
90
100
110
120
130
140
0
20
40
60
80
100
120
140
160
180
200
220
240
260
280
300
$D_S/2$ IN STATUTE MILES
N_S = 250
N_S = 301
N_S = 350
N_S = 400

Figure 24

$$d_{sr} = \frac{da_o}{\theta} - d_{Lr} \cong \frac{da_{oo}}{\theta_{oo}} - d_{Lr} \qquad (5.18)$$

In practice, the approximate expressions in (5.17) and (5.18) are used to find distances d_{st} or d_{sr} from a horizon obstacle to the crossover of radio horizon rays.

In Figs. 15 - 22, when θ_{ot} is negative, replace d_{st} by $|\, d_{st} - a\,(|\,\theta_{ot}\,|)\,|$ and read the curve for $\theta_{ot} = 0$ to obtain Δa_o. Similarly, if θ_{or} is negative and $\Delta\beta_o$ is required, replace d_{sr} by $|\, d_{sr} - a\,(|\,\theta_{or}\,|)\,|$ and read the curve for $\theta_{or} = 0$. In these formulas θ_{ot} and θ_{or} are expressed in radians.

d. Computation of θ with Very High Antennas Over a Smooth Earth

If the difference $|\, h_{ts} - h_{Lt}|$ or $|\, h_{rs} - h_{Lr}\,|$ greatly exceeds one kilometer, equivalent earth geometry may not locate the radio horizon correctly. In this case, refraction between the antenna and its horizon departs from what is expected in a linear gradient atmosphere. The problem is still simple for a smooth earth, but becomes quite complex over a very rough terrain profile. Fig. 23 shows d_{Lt} plotted versus $h_{ts} - h_{Lt}$ for each of the four reference atmospheres of Table II, for the case $\theta_{ot} = 0$. For a smooth earth and $h_{ts} > h_{Lt}$, read d_{Lt} from Fig. 23, compute d_{Lr}, and compute D_s from (5.11). For a smooth earth, $\theta_{ot} = \theta_{or} = 0$, $d_{st} = d_{sr} = D_s/2$, and θ may be read from Fig. 24 as a function of $D_s/2$. Then,

$$d_1 = d_{Lt} + D_s/2, \qquad d_2 = d_{Lr} + D_s/2,$$

$$s = d_2/d_1, \qquad a_o = s\theta/(1+s), \qquad \beta_o = \theta/(1+s). \qquad (5.19)$$

This subsection (d) should apply for the case of aircraft flying high over rough terrain, wherever the assumption of an average smooth earth seems reasonable. Figs. 23 and 24, with (5.19) make the computation of a_o and β_o easier than it is when terrain profiles must be plotted.

e. Computation of θ with Very High Antennas over a Rough Earth

Over a rough terrain profile with either $|h_{ts} - h_{Lt}|$ or $|h_{rs} - h_{Lr}|$ greater than one kilometer, it is possible to trace rays carefully in any one of the four reference atmospheres by using one of Figs. 26 - 29. This was necessary in only one situation among paths analyzed by CRPL, where one antenna was located on top of Pike's Peak in Colorado. Fig. 25 shows the path of a radio ray and the parameters used in Figs. 26 - 29. Figs. 30 - 33 are helpful for interpolating values from Figs. 26 - 29.

Only extreme situations should require the use of this latter set of figures, so their use is not explained in detail. Tracing a ray from the transmitting antenna to its horizon, identify $h_{ts} - h_{Lt}$ with h, d_{Lt} with d, and θ_{ot} with α. The figures are also used to trace a ray from this horizon to the crossover of horizon rays.

6. Determination of Surface Refractivity, N_s

Where measured values of N_s are not available, estimates of N_s for the U.S. may be obtained for Time Block 2 from Fig. 34. For other areas, refer to a recent report by Bean and Horn [12]. In Fig. 34, N_s is not plotted directly, but is obtained from the reduced-to-sea-level refractivity, N_o:

$$N_s = N_o \exp(-0.03222\, h_s), \tag{6.1}$$

where h_s is the elevation of the ground above mean sea level, in thousands of feet, as given by (4.3). A world map of minimum monthly mean N_o values is shown as Fig. 34a; these values may be substituted for Time Block 2 values if the latter are not available.

7. Effective Antenna Heights, h_{te} and h_{re}

The definition of h_{te} and h_{re} given in this section is used in this paper to calculate L_{bms}, and in Reference 5 to calculate L_{bd}.

RAY TRACING DIAGRAM

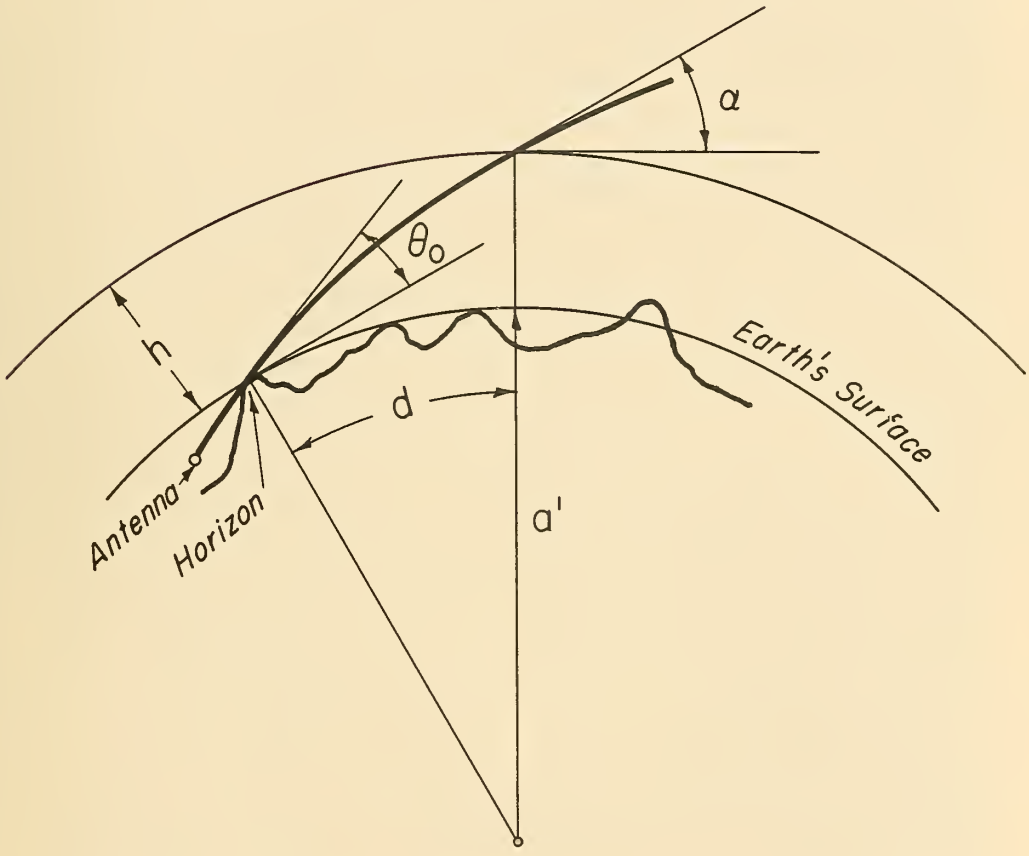

Figure 25

RAY TRACING IN A REFERENCE ATMOSPHERE

with $N_s = 250$ and $h_s = 5{,}000$ feet

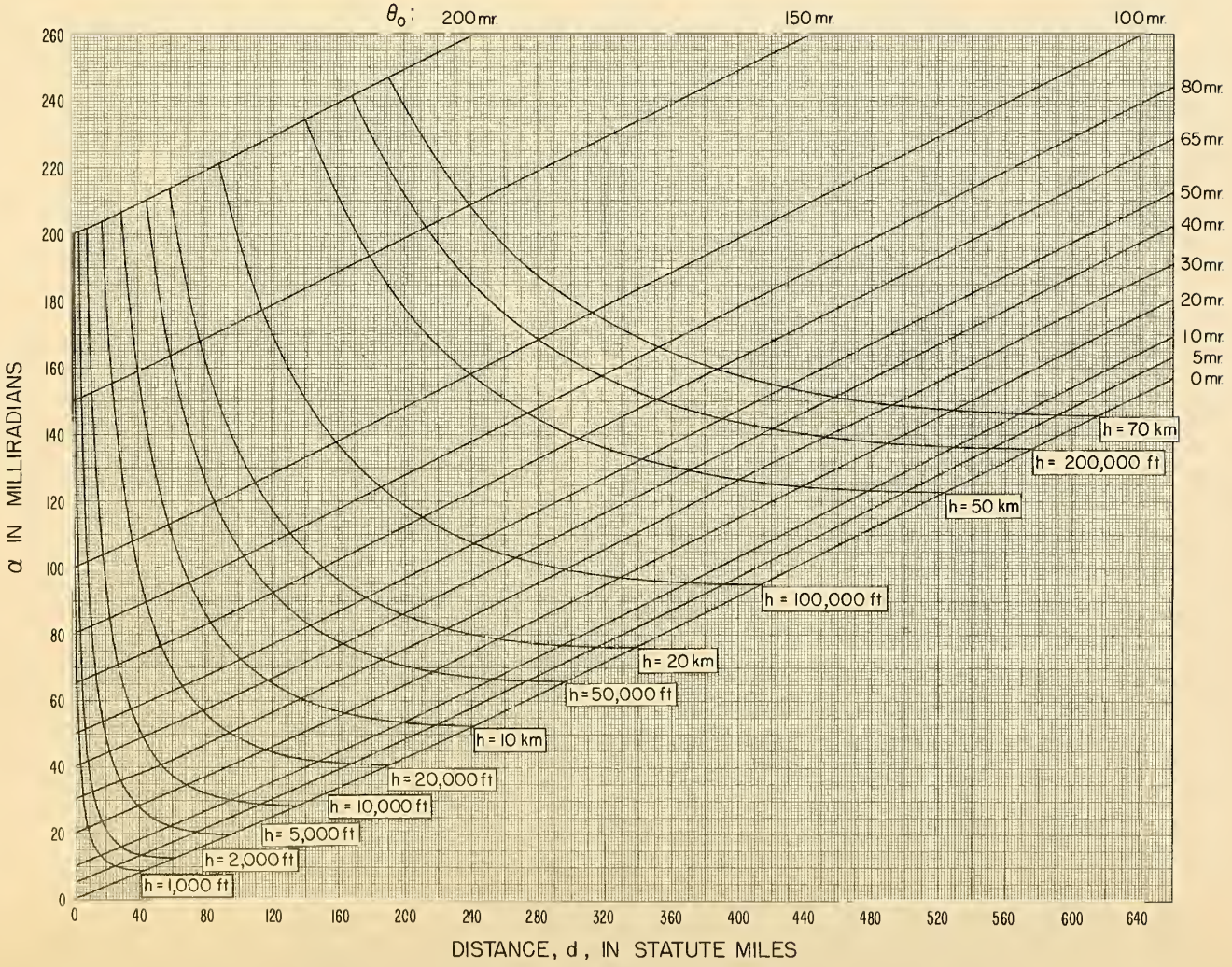

Figure 26

RAY TRACING IN A REFERENCE ATMOSPHERE

with $N_s = 301$ and $h_s = 1{,}000$ feet

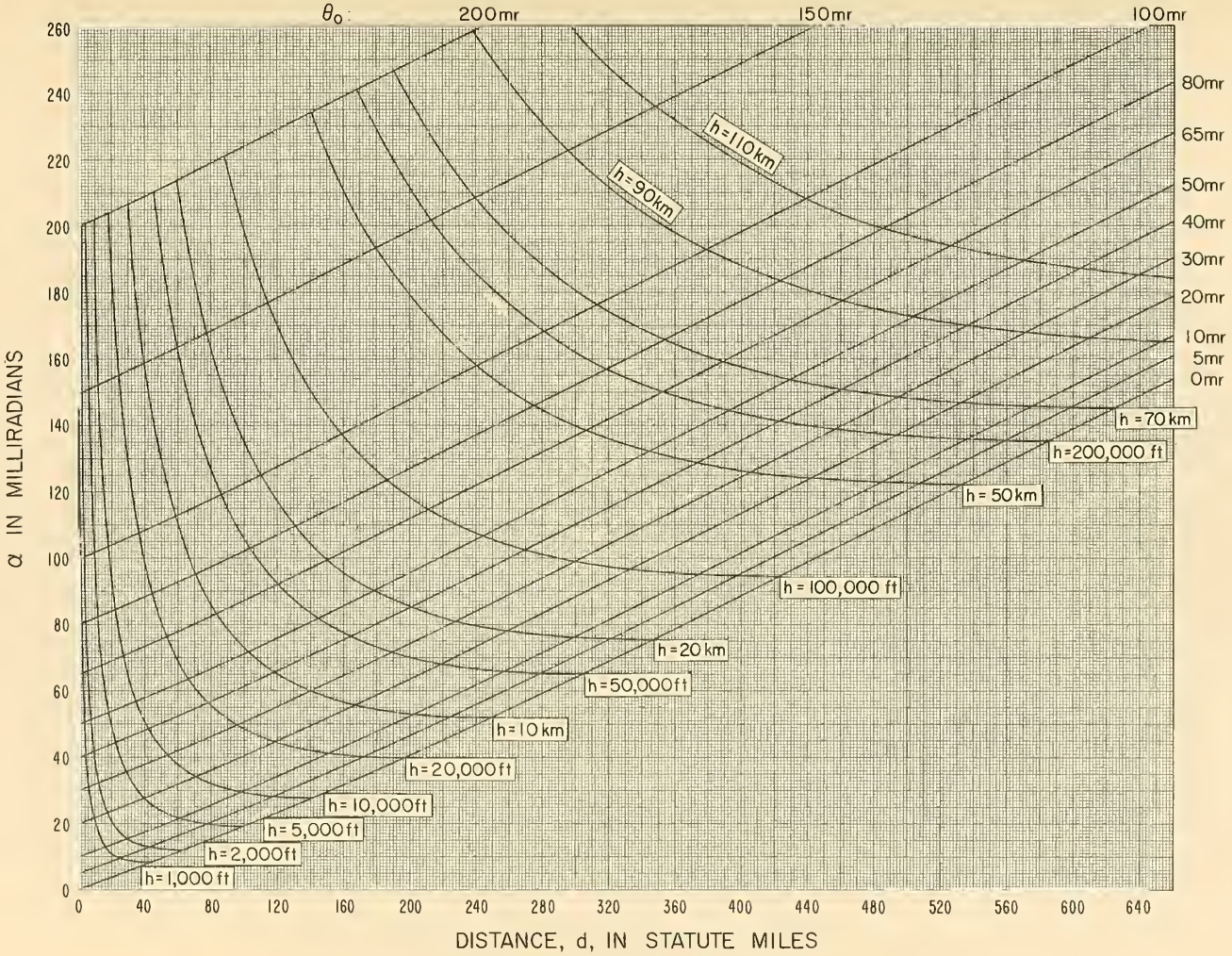

Figure 27

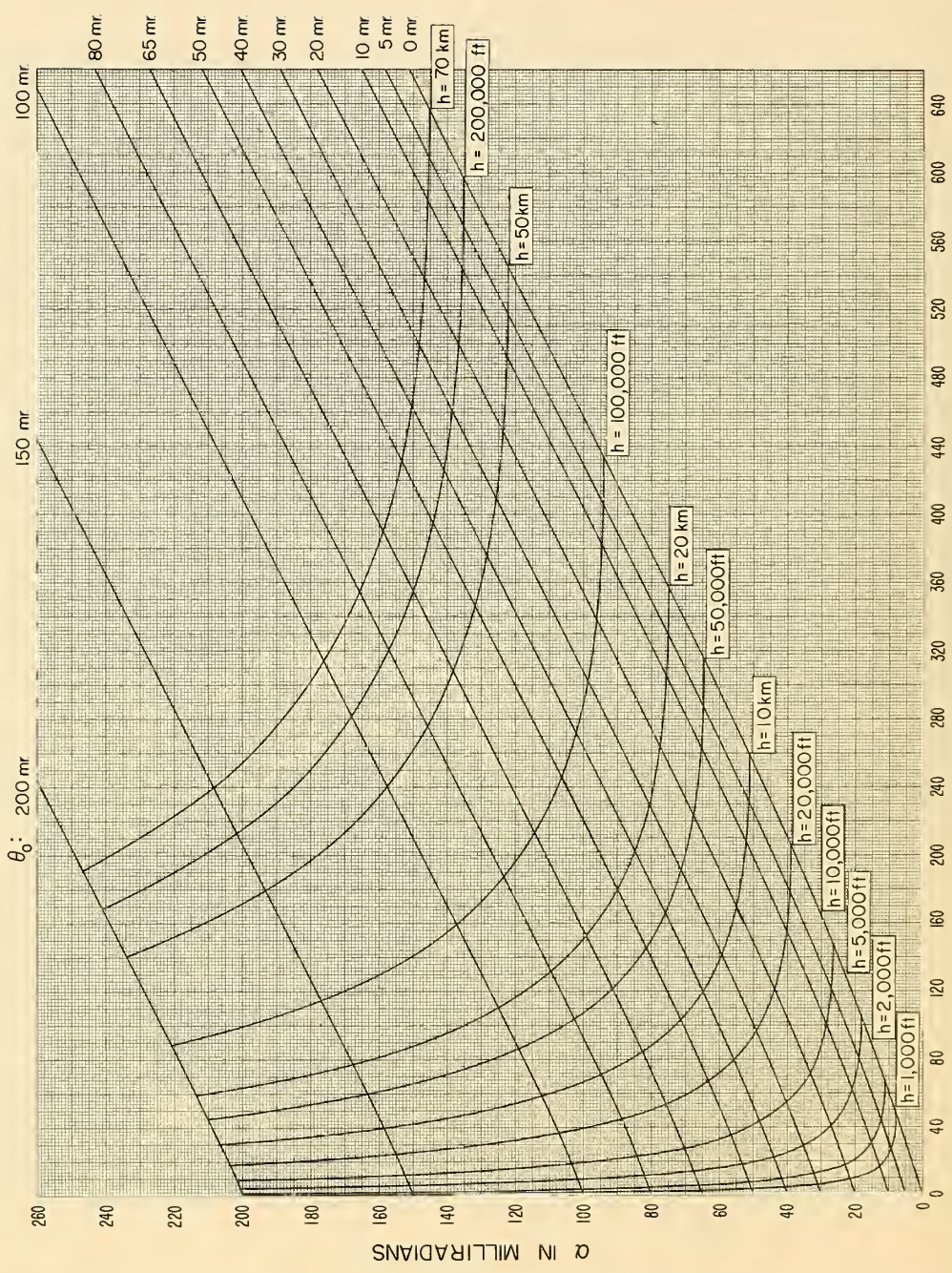
RAY TRACING IN A REFERENCE ATMOSPHERE
with N_s = 350 and h_s = 0 feet
θ_o: 200 mr
150 mr
100 mr
80 mr
65 mr
50 mr
40 mr
30 mr
20 mr
10 mr
5 mr
0 mr
h = 70 km
h = 200,000 ft
h = 50km
h = 100,000 ft
h = 20 km
h = 50,000ft
h = 10km
h = 20,000ft
h = 10,000ft
h = 5,000ft
h = 2,000ft
h = 1,000ft
α IN MILLIRADIANS
DISTANCE, d, IN STATUTE MILES

Figure 28

RAY TRACING IN A REFERENCE ATMOSPHERE

with $N_s = 400$ and $h_s = 0$ feet

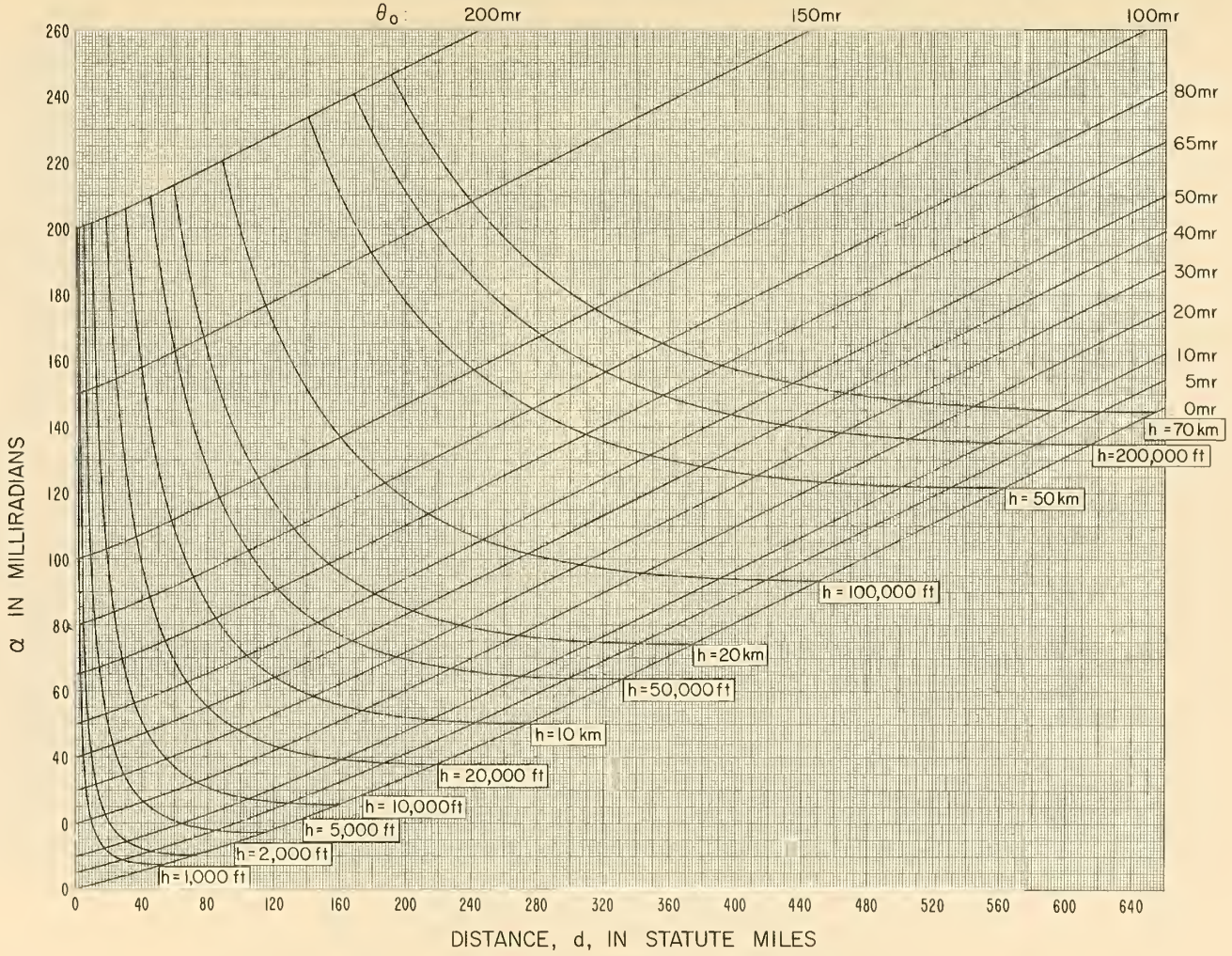

Figure 29

RAY TRACING IN A REFERENCE ATMOSPHERE

With $N_s = 250$ and $h_s = 5000$ feet

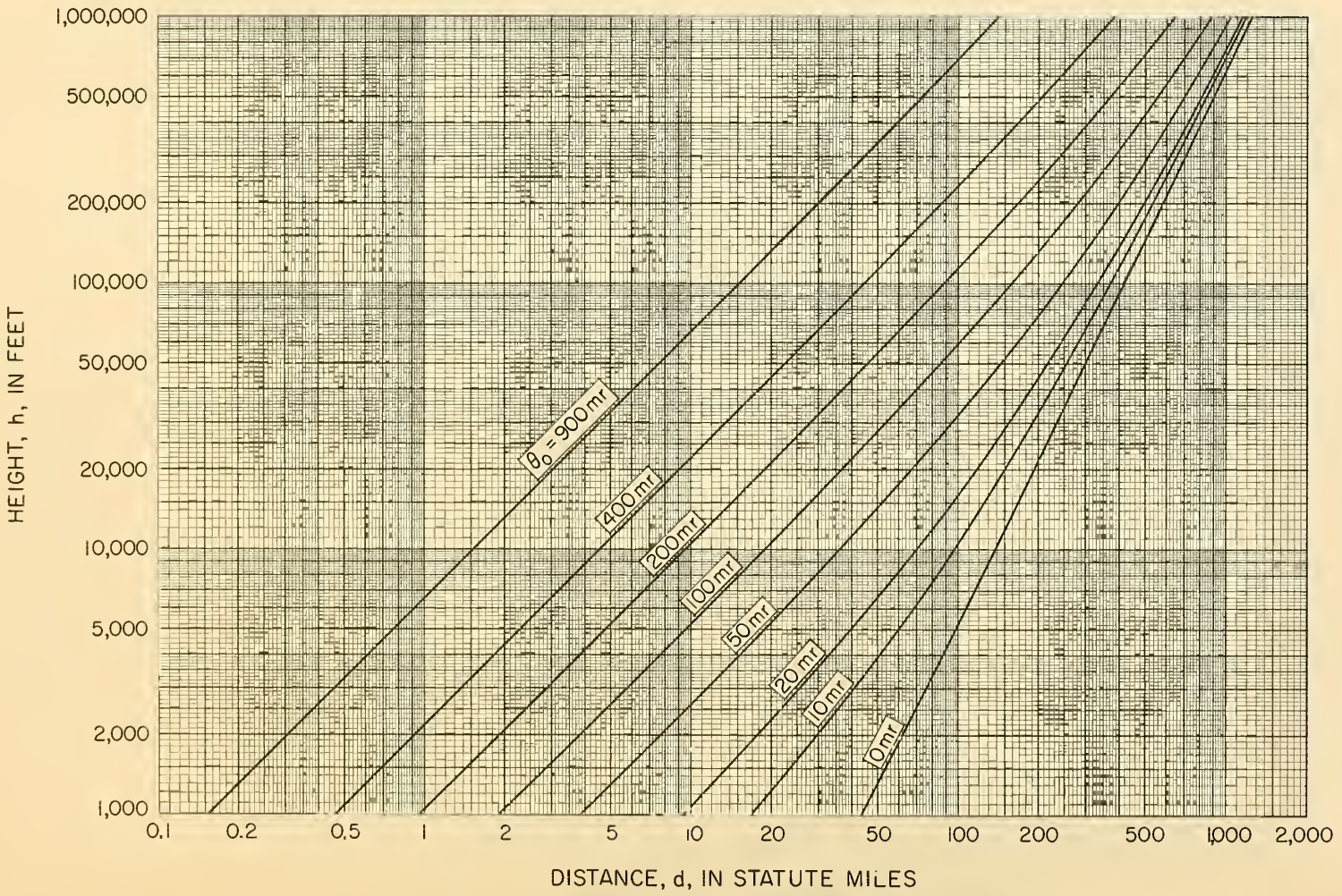

Figure 30

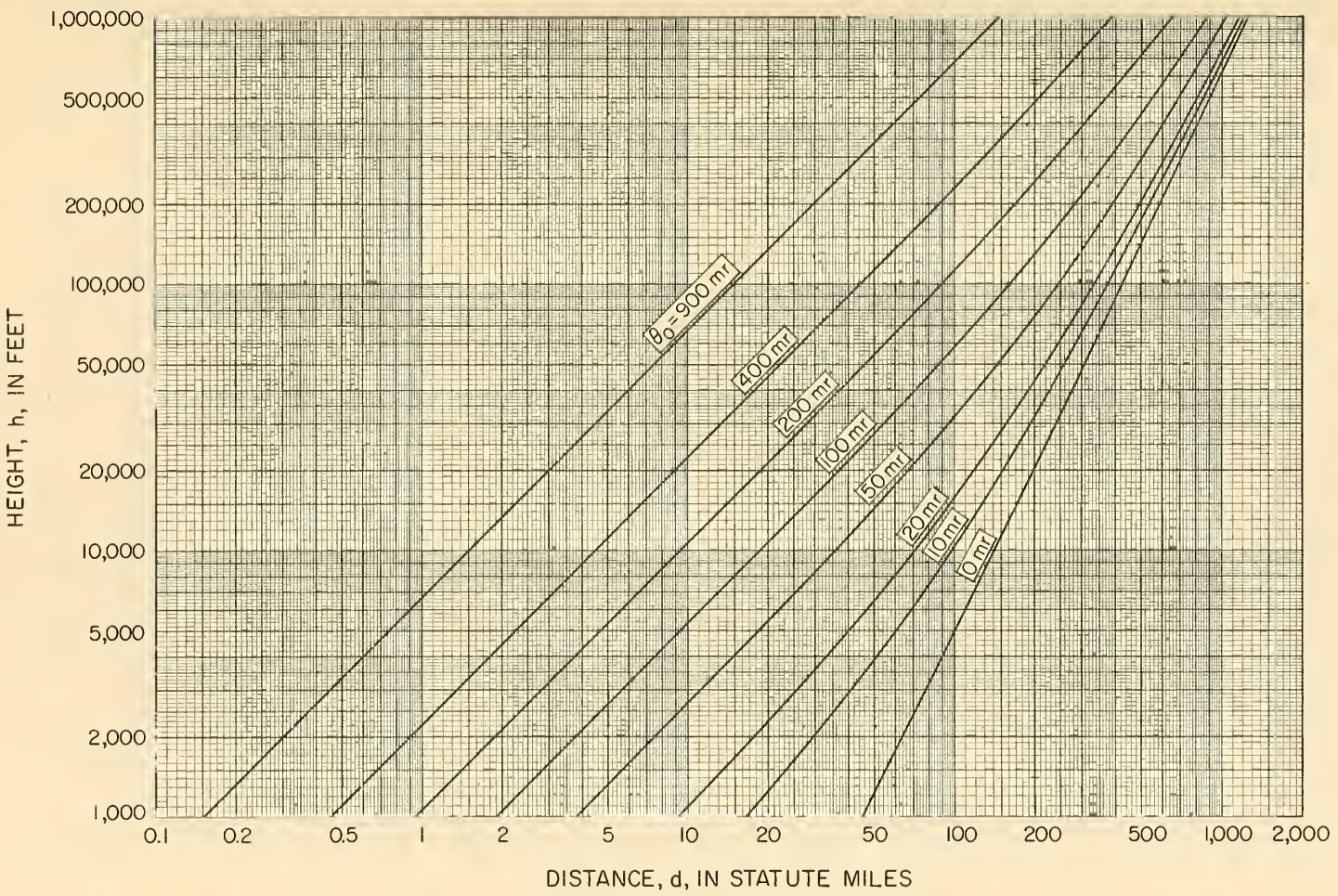
RAY TRACING IN A REFERENCE ATMOSPHERE
With N_s = 301 and h_s = 1000 feet
HEIGHT, h, IN FEET
1,000,000
500,000
200,000
100,000
50,000
20,000
10,000
5,000
2,000
1,000
0.1
0.2
0.5
1
2
5
10
20
50
100
200
500
1,000
2,000
DISTANCE, d, IN STATUTE MILES
θ_0=900 mr
400 mr
200 mr
100 mr
50 mr
20 mr
10 mr
0 mr

Figure 31

RAY TRACING IN A REFERENCE ATMOSPHERE

With $N_S = 350$ and $h_S = 0$

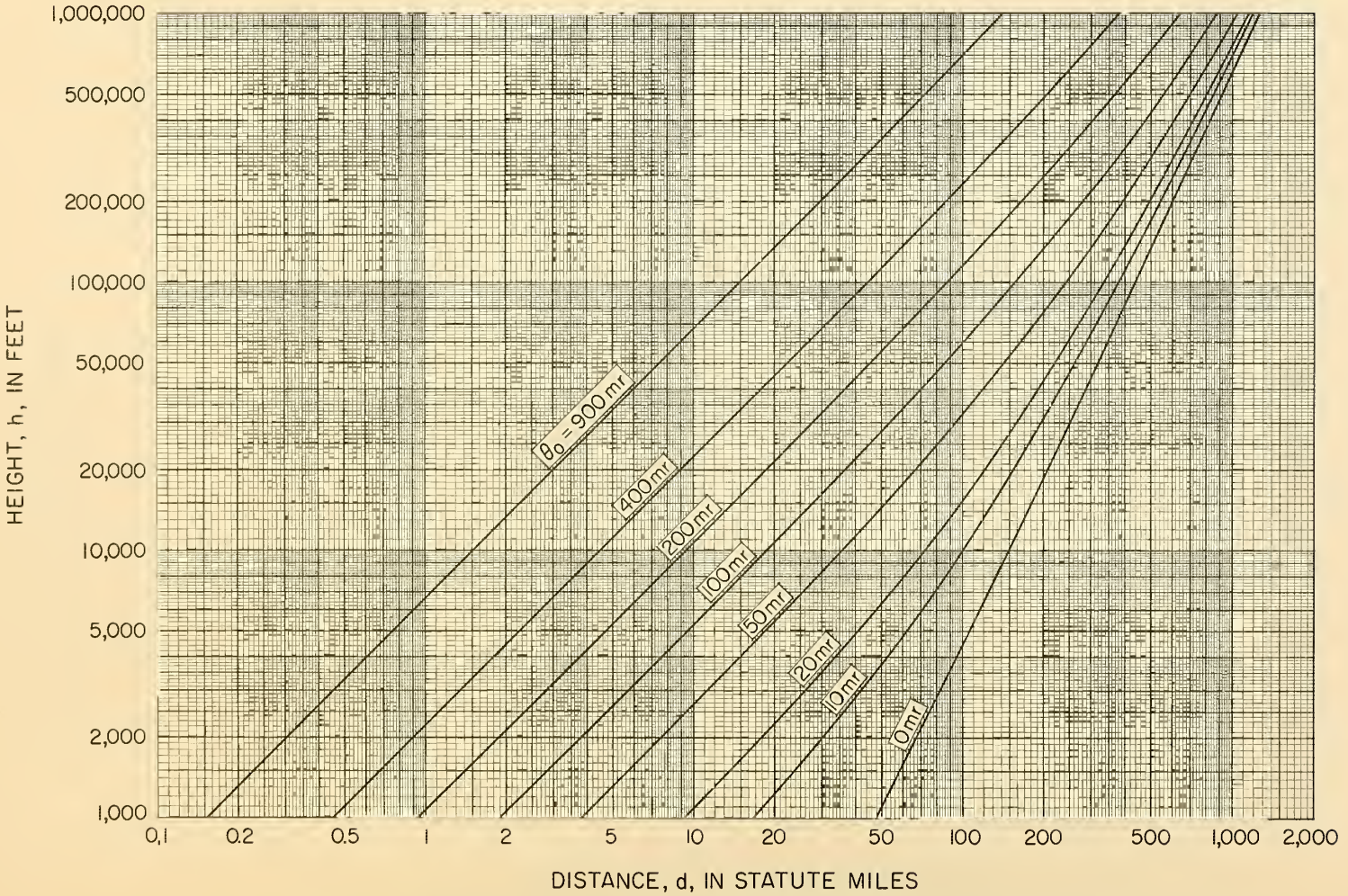

Figure 32

RAY TRACING IN A REFERENCE ATMOSPHERE

With $N_s = 400$ and $h_s = 0$ feet

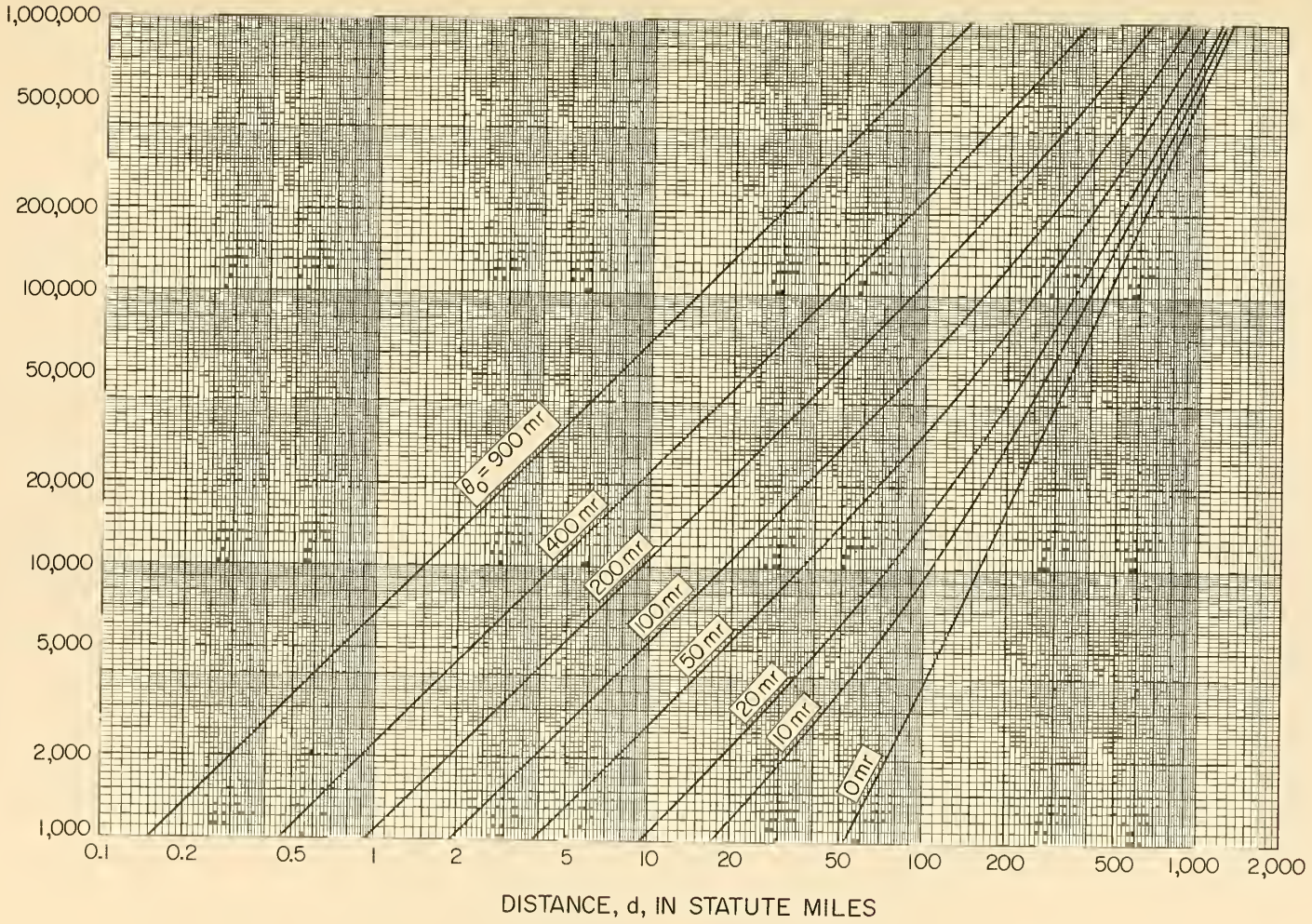

Figure 33

SURFACE REFRACTIVITY, NOVEMBER - APRIL, 1 P.M. - 6 P.M. (TIME BLOCK Nº 2)
Contours Show Reduced-to-Sea-Level Values, N_0

SURFACE REFRACTIVITY $N_S = N_0 \exp(-0.032218\, h_S)$,
h_S Is the Height Of the Surface Above Mean Sea Level, In Thousands Of Feet

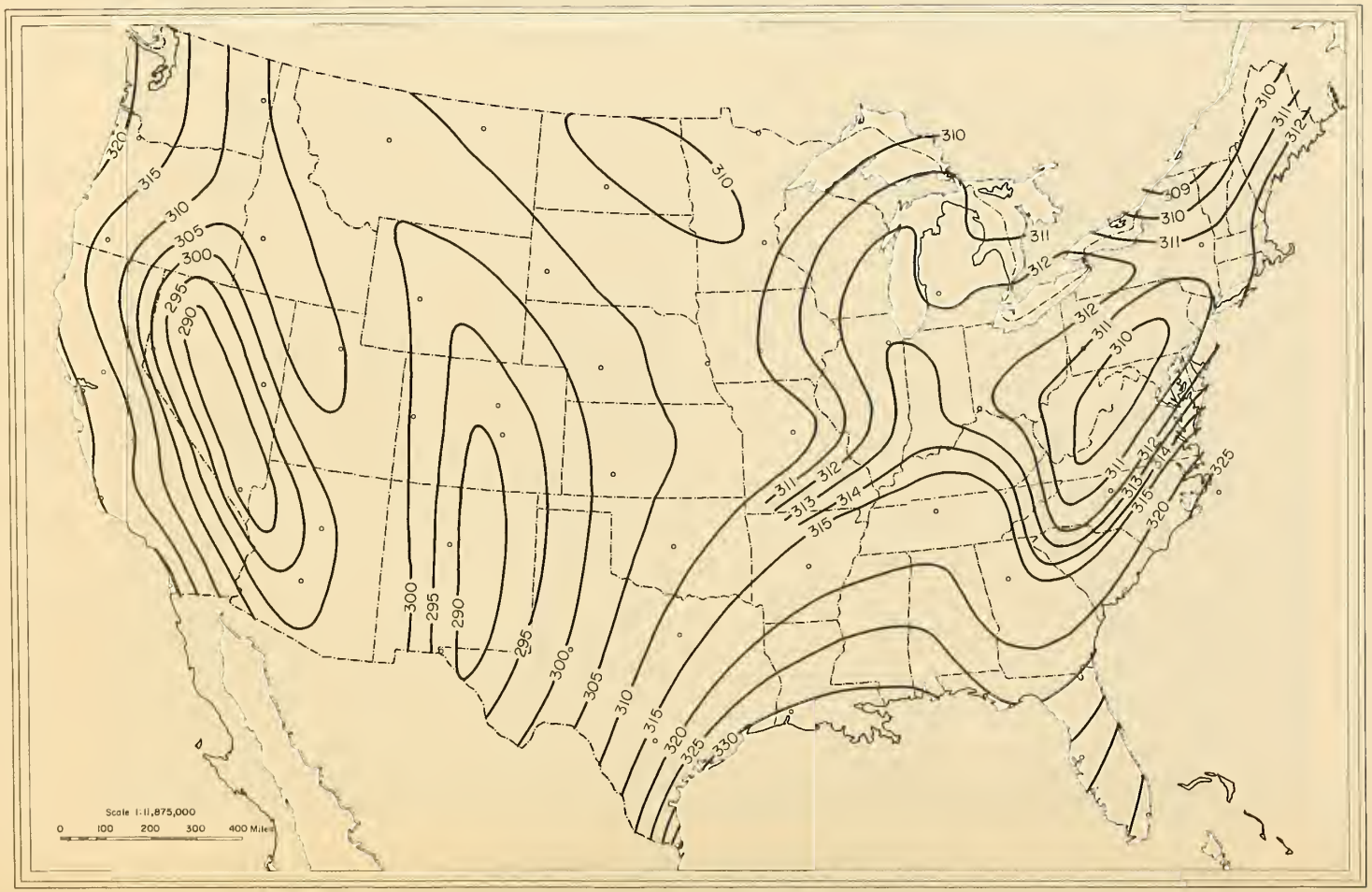

Figure 34

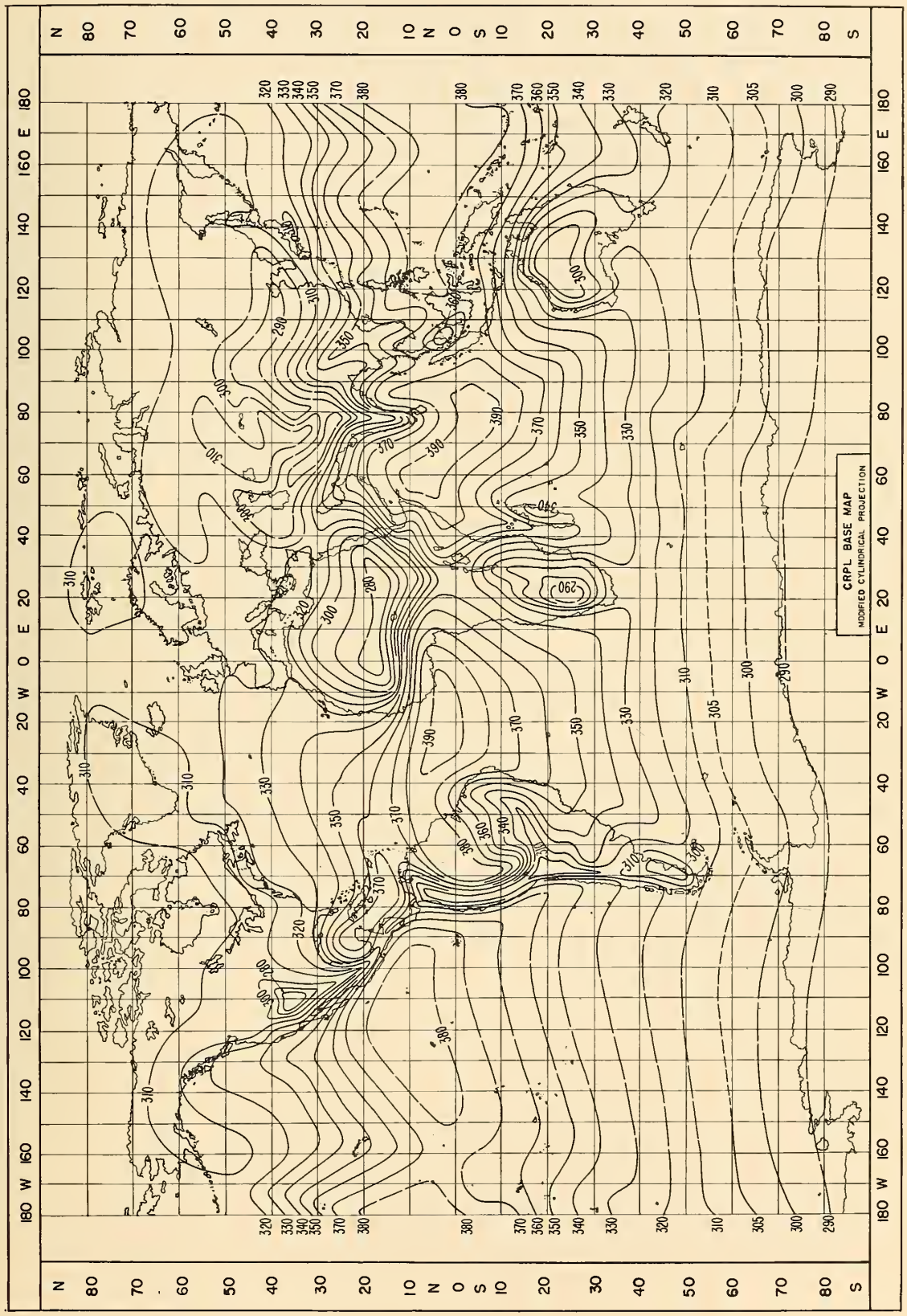
MINIMUM MONTHLY MEAN $\overline{N}_0$
CRPL BASE MAP
MODIFIED CYLINDRICAL PROJECTION

Fig. 34a

a. Antenna Heights h'_{te} and h'_{re} Less than One Kilometer Above the Surface

For antennas elevated more than a hundred feet above ground, the effective height was defined as the height of the antenna above a circular arc fitted by least squares to a portion of the terrain. This was chosen to be eight-tenths of the terrain along the great circle path extending from the antenna to its four-thirds earth radio horizon. It is assumed that critical ground reflection lobery in the lower regions of the scattering volume is unaffected by terrain near either the antenna or its radio horizon.

This definition of effective antenna height is not satisfactory for most receiving antennas if their height above ground is small with respect to average terrain irregularities. Some effective heights in such cases are an order of magnitude greater than the structural antenna heights. The structural height is used, therefore, for receiving antennas, and the more complicated definition of effective antenna height is used for antennas higher than 100 feet above ground.

Except for the ambiguity of such a definition, the structural height of an antenna, sometimes including a building, cliff, or hill as part of the structure, might have been used to define h'_{te} and h'_{re} for both high and low antennas.

b. Antennas More than One Kilometer above the Surface

If h'_{te} as defined in subsection (a) is less than one kilometer, it is used as the effective transmitting antenna height h_{te} in the prediction formulas, since radio ray refraction from the antenna to its horizon is then what is expected in a linear gradient atmosphere. For higher antennas, Fig. 35 is used to obtain a correction Δh, which reduces h'_{te} to the value h_{te} to be used in the formulas of Reference 5 and this report. The same comments apply to h'_{re} and h_{re}:

$$h_{te} = h'_{te} - \Delta h\,(h'_{te},\ N_s) \qquad (7.1)$$

$$h_{re} = h'_{re} - \Delta h\,(h'_{re},\ N_s) \qquad (7.2)$$

Over a smooth earth, the actual antenna heights, h'_{te} and h'_{re} correspond to horizon distances d_{Lt} and d_{Lr} in a reference atmosphere. Effective antenna heights h_{te} and h_{re} are defined

in such a way as to preserve these correct horizon distances over a smooth earth in a linear gradient atmosphere. Except for extremely high antennas, (5.13) and (5.14) show the simple relationship that holds between antenna height and horizon distance over a smooth earth in a linear gradient atmosphere; exact expressions are

$$h_{te} = a[\sec (d_{Lt}/a) - 1] \tag{7.3}$$

$$h_{re} = a[\sec (d_{Lr}/a) - 1] \tag{7.4}$$

8. Parameters Required to Compute L_{bms}

Tabulate the following parameters, for use in Section 9. Refer to Fig. 14 for illustrations of path geometry. Section 9 explains the individual terms in (3.1), used to calculate L_{bms} for each of two reference atmospheres.

N_s = surface refractivity, obtained from (4.1b) if possible, or from direct measurement of winter afternoon conditions, or from Fig. 34 and (6.1), or from Reference 12.

a = equivalent earth's radius. Choose two values from Table II, for reference atmospheres corresponding to N_s values above and below the correct N_s. Calculate the following parameters for each reference atmosphere.

θ = angular distance. (Tabulate two values.)

s = path asymmetry parameter:

$$s = \alpha_o/\beta_o \tag{8.1}$$

It is helpful to identify antennas in such a way that $s \leq 1$.

h_o = height of horizon ray crossover above a straight line between the antennas:

$$h_o = sd\theta/(1 + s)^2 = \alpha_o \beta_o d/\theta = d_1 \alpha_o = d_2 \beta_o \text{ miles} \tag{8.2}$$

where d, d_1, d_2 are in statute miles, and angles α_o, β_o, θ are in radians. (5.19) defines d_1 and d_2.

REDUCTION Δh OF EFFECTIVE ANTENNA HEIGHT

for very high antennas

$$h_{te} = h'_{te} - \Delta h(h'_{te}, N_s)$$

$$h_{re} = h'_{re} - \Delta h(h'_{re}, N_s)$$

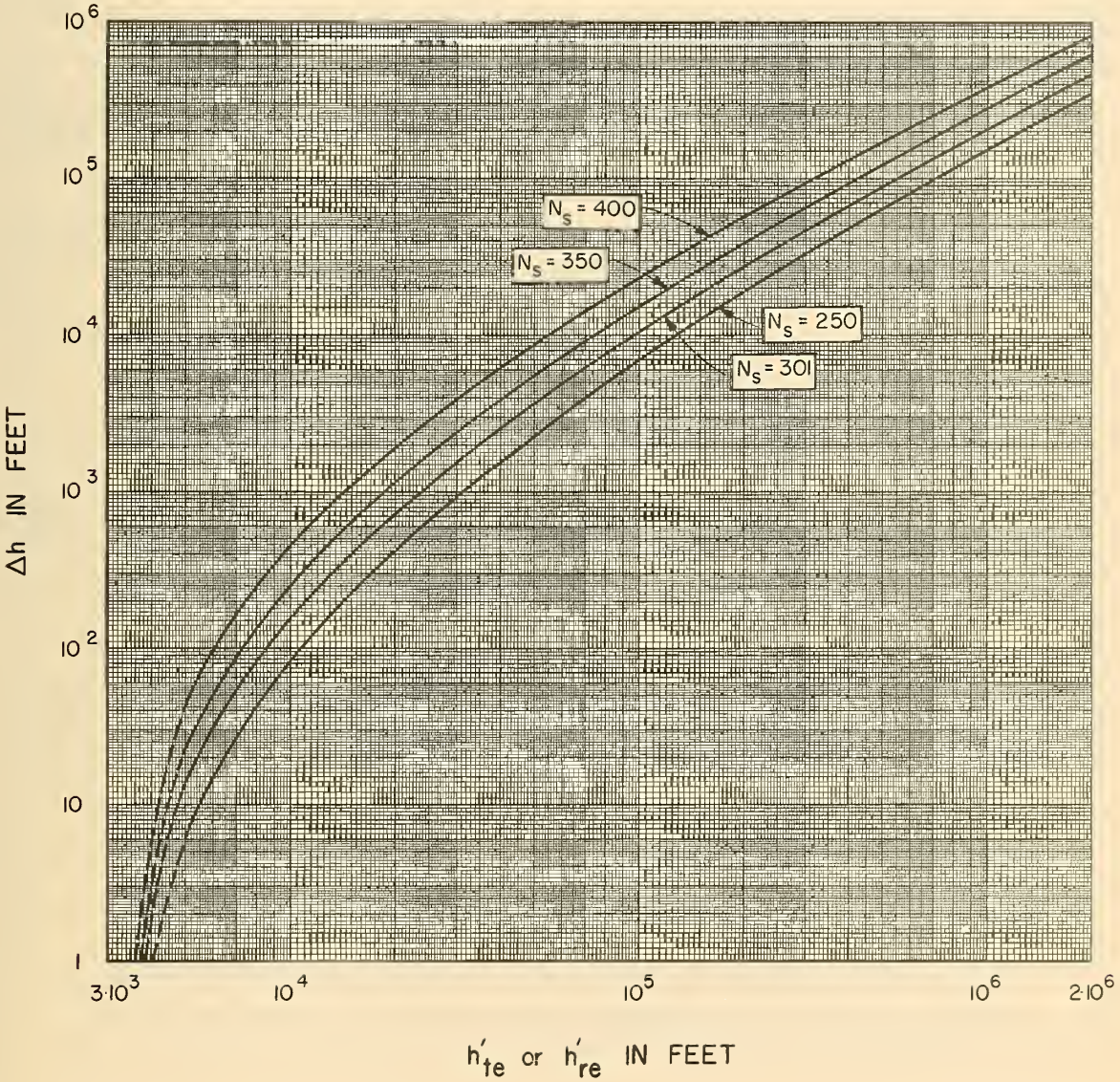

Figure 35

h_l = height of horizon ray crossover above a straight line between the radio horizons:

$$h_l = d_{st}\, d_{sr}\, \theta / D_s \text{ miles} \tag{8.3}$$

where d_{st} and d_{sr} as illustrated in Fig. 14 are defined by (5.17) and (5.18). θ is in radians in (8.3)

h_{cg} = height of scattering center above ground, in thousands of feet. Accuracy of this determination is not important for the formulas in this paper, so a careful derivation of h_{cg} is not given. Use (4.4) from Section 4 when no better estimate of h_{cg} is available.

γ per mile = logarithmic gradient of refractivity with height, determined from Table II as a function of N_s and h_{cg}.

h_s = average height of a propagation path above mean sea level. Where terrain profiles are available, use (4.3); otherwise, use the values in Table II.

$$h_s = (h_{Lt} + h_{Lr})/2 \tag{4.3}$$

η_s = normalized height of horizon ray crossover:

$$\eta_s = 4\gamma\, h_o, \tag{8.4}$$

a dimensionless parameter. Use γ per mile and h_o in miles in (8.4).

$$\eta = \gamma\, d\, \theta \tag{8.5}$$

This is another dimensionless parameter, the most important one in the theory. Use γ per mile, path distance d in miles, and angular distance θ in radians in (8.5). If the asymmetry parameter $s = 1$, then $\eta = \eta_s$. Note that equal antenna heights do not necessarily imply a symmetrical path, except over a smooth earth.

Comparing (8.4) and (8.5):

$$\eta_s = 4s\eta/(1 + s)^2 \tag{8.6}$$

Effects of energy reflected from the ground are a function of η_s and of effective antenna height in wavelengths multiplied by the elevation angle of the radio horizon:

$$v_t = 4\pi h_{te} \alpha_o / \lambda \ , \tag{8.7}$$

$$v_r = 4\pi h_{re} \beta_o / \lambda \ , \tag{8.8}$$

where h_{te} and h_{re} are effective antenna heights above the reflecting surface between each antenna and its radio horizon, as discussed in Section 7. These heights and the free space radio wavelength, λ, are expressed in feet in this report, and the angles α_o and β_o are in radians.

Computations described in the next section also require

$$q = v_r / v_t, \quad r_1 = v_t [1 + (1/s)] , \quad r_2 = qsr_1 = v_r (1 + s). \tag{8.9}$$

These parameters are required only when $\eta_s < 1$.

9. The Scatter Prediction Formula

Repeating (3.1), median basic transmission loss due to forward scatter in Time Block No. 2, winter afternoons, is given by

$$L_{bms} = G(\eta) + 30 \log_{10} f_{mc} - 20 \log_{10} d_{mi} + A_a$$

$$+ H_o - F_o - F_s - F(h_{cg}, N_s) \ . \tag{3.1}$$

In this section, terms of (3.1) are explained in detail.

a. The Attenuation Function, $G(\eta)$

$G(\eta)$ shows the decibel attenuation of field strength with increasing $\gamma d\theta$, and is the most important term in (3.1). At very great distances, the last four terms are negligible. For 500' and 30' antennas at 100 Mc, (3.1) corresponds to an attenuation rate of about 0.12 db per mile from two to five hundred miles over a smooth earth.

$$G(\eta) = G_o(\eta) + \Delta G \tag{9.1}$$

$G_o(\eta)$ is plotted as Fig. 36, η is given by (8.5), and ΔG is tabulated for the reference atmospheres in Table II for various ranges of the height of the scattering center h_{cg} above ground, given in thousands of feet.

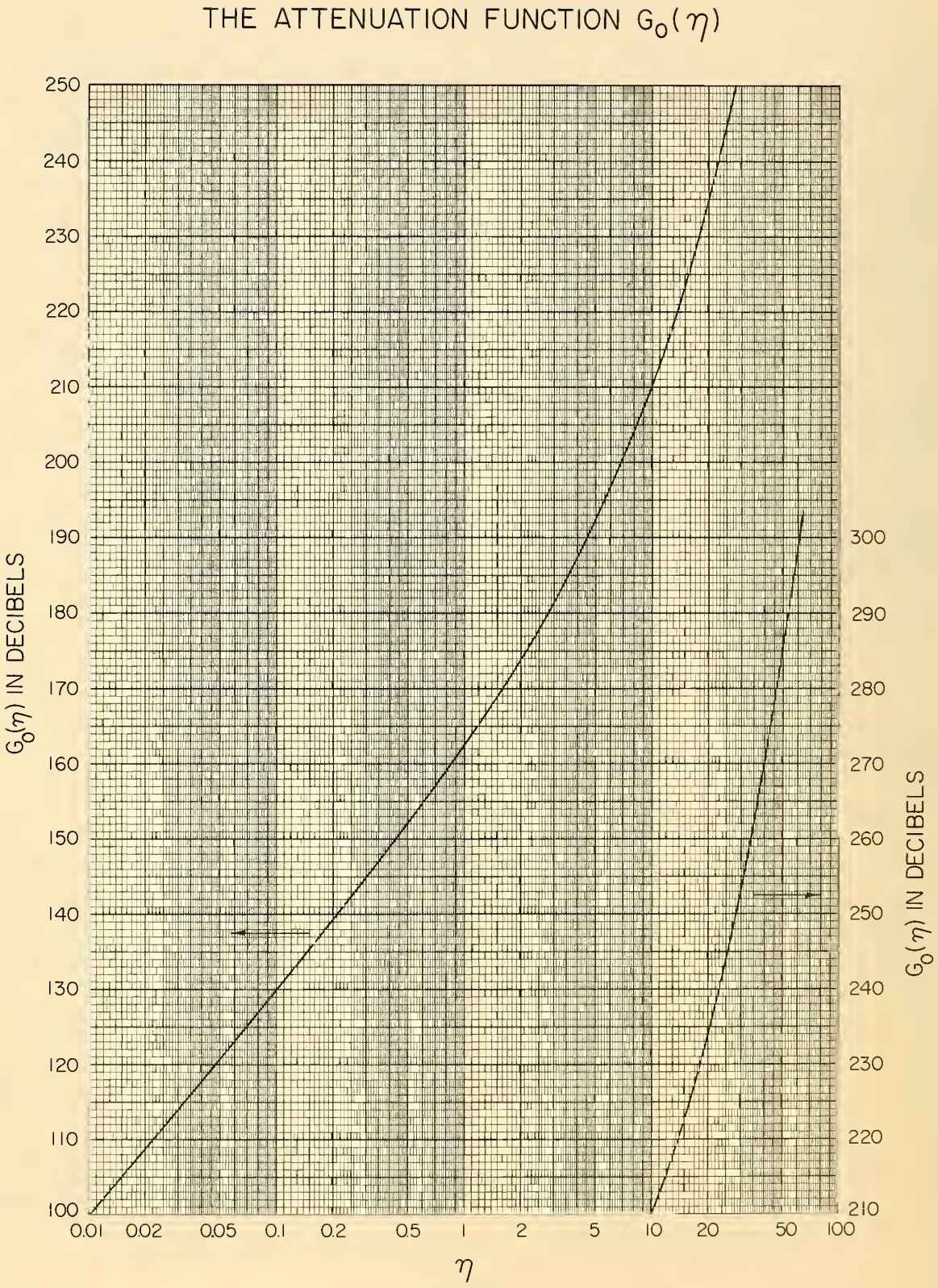
THE ATTENUATION FUNCTION $G_0(\eta)$
$G_0(\eta)$ IN DECIBELS
250
240
230
220
210
200
190
180
170
160
150
140
130
120
110
100
300
290
280
270
260
250
240
230
220
210
0.01
0.02
0.05
0.1
0.2
0.5
1
2
5
10
20
50
100
η

Figure 36

b. The Sea Level Correction, F_o

The "sea level correction", F_o, allows for increased fields expected when $h_1 < h_o$. See Fig. 14. For antenna both at sea level, $h_1 = h_o$ and $F_o = 0$; in general,

$$F_o = 4.343\ \gamma\ (h_o - h_1) \tag{9.2}$$

where γ per mile is tabulated in Table II, h_o and h_1 are given in miles by (8.2) and (8.3). The terms F_o and F_s are usually negligible.

c. The Asymmetry Correction, F_s

The "asymmetry correction", F_s, allows for departures of the asymmetry parameter s from unity. F(s) is the product of the functions C(s) and M(η) shown in Figs. 37 and 38. Note that C(1/s) = C(s).

d. The Frequency Gain Function, H_o

The "frequency gain function", H_o, in (3.1) is a measure of how much energy is sent well above the crossover of radio horizon rays by reflection from the earth. Scattering efficiency is reduced at higher altitudes. For most commonly occurring antenna heights, the field strength at the horizon ray crossover should be 10 to 20 decibels below free space [13], corresponding to maximum values for H_o of 16 to 26 db at great distances. For low antennas and short paths, H_o may be much larger.

The computation of H_o is different for the two special cases, $\eta_s \geq 1$ and $\eta_s < 1$, corresponding to large and small distances. In either case, values $H_o(v_t)$ and $H_o(v_r)$ are read from Fig. 39 as a function of η_s, v_t, and v_r as defined by (8.4), (8.7), (8.8), and these readings are averaged:

$$H_o(\eta_s \geq 1) = \frac{1}{2}[H_o(v_t) + H_o(v_r)] + \Delta H_o \tag{9.3}$$

$$\Delta H_o = 6\ (0.6 - \log_{10}\ \eta_s)\ \log_{10}\ s\ \log_{10}\ q \tag{9.4}$$

ΔH_o is defined only for $\eta_s \geq 1$. For $\eta_s < 1$, ΔH_o is calculated from (9.4) with η_s set equal to 1.

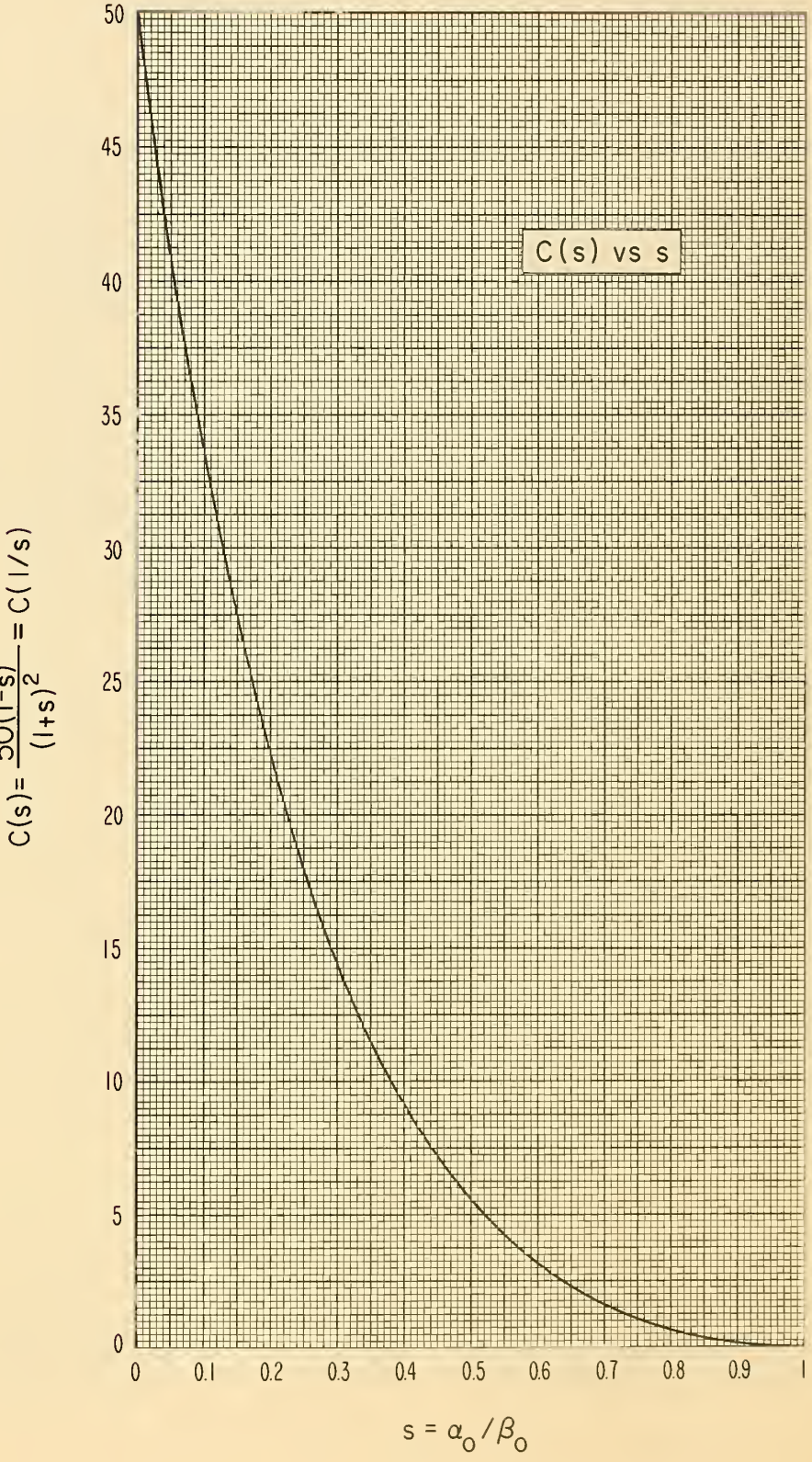
C(s) vs s
$C(s)=\frac{50(1-s)^2}{(1+s)^2}=C(1/s)$
50
45
40
35
30
25
20
15
10
5
0
0
0.1
0.2
0.3
0.4
0.5
0.6
0.7
0.8
0.9
1
$s=\alpha_0/\beta_0$

Figure 37

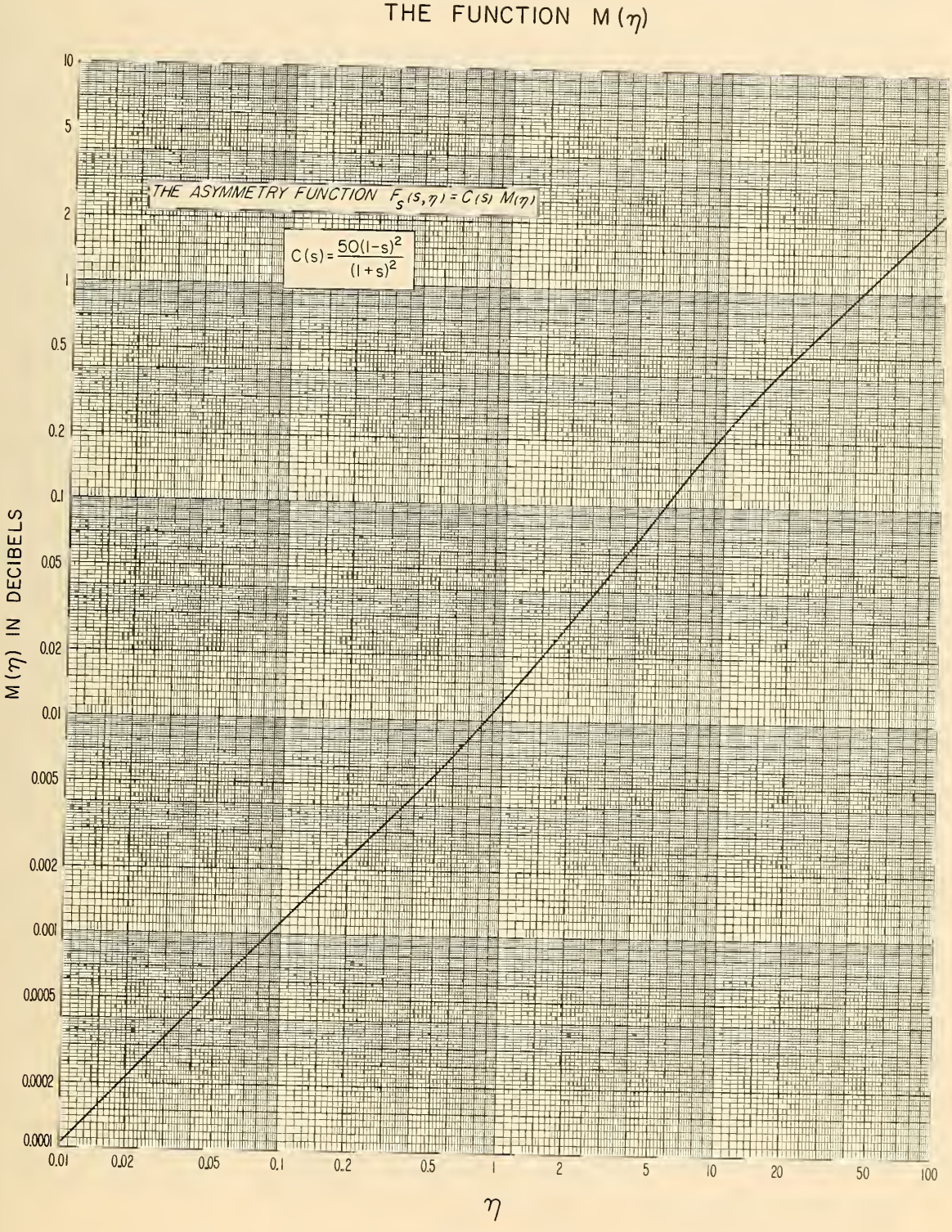
THE FUNCTION M(η)
THE ASYMMETRY FUNCTION $F_s(s,\eta) = C(s)\, M(\eta)$
$C(s) = \frac{50(1-s)^2}{(1+s)^2}$
M(η) IN DECIBELS
10
5
2
1
0.5
0.2
0.1
0.05
0.02
0.01
0.005
0.002
0.001
0.0005
0.0002
0.0001
0.01
0.02
0.05
0.1
0.2
0.5
1
2
5
10
20
50
100
η

Figure 38

[See (8.1) and (8.9) for definitions of s and q.] ΔH_o is an approximate correction factor, valid if s and q are each within the limits 0.1 to 10. For values of s or q outside these limits, use the nearest limit for s or q in (9.4). The frequency gain, H_o, is always positive, so if ΔH_o overcorrects, assume $H_o = 0$. Also, ΔH_o must not exceed $1/2[H_o(v_t) + H_o(v_r)]$.

Fig. 39 is drawn for the special case where s = 1 and q = 1, and (9.3) implicitly assumes that frequency gain effects at the two ends of a propagation path are independent. This is nearly true for $\eta_s \geq 1$ (large distances), but at the shorter distances it is not true. Accordingly, an asymptotic expression which is exact for $\gamma = 0$ (no bending of radio rays) is evaluated, and $H_o(\eta_s < 1)$ is obtained by linear db interpolation between $H_o(1) \equiv H_o(\eta_s = 1)$ and $H_o(0) \equiv H_o(\eta_s = 0)$:

$$H_o(0) = 10 \log_{10} \frac{2(1 - s^2 q^2)}{r_2^2 [h(r_1) - h(r_2)]}, \qquad (9.5)$$

where $h(r_1)$ and $h(r_2)$ are read from Fig. 40, and r_1, r_2, and q are defined by (8.9). The function h(r) is also shown on Fig. 40a.

If sq = 1, read $H_o(0)$ from Fig. 41. For $v_t > 10$, $v_r > 10$, $H_o(0) = 0$.

Then, for $\eta_s < 1$,

$$H_o(\eta_s) = H_o(0) + \eta_s [H_o(1) - H_o(0)] \qquad (9.6)$$

where $H_o(1)$ is determined from (9.3) and Fig. 39, with $\eta_s = 1$, and $H_o(0)$ is determined from (9.5).

For equal effective antenna heights, sq = 1. Graphs of H_o versus v_t, η_s, and s are given in Figs. 39a - 39f. This special case occurs frequently in system design calculations.

e. Atmospheric Absorption, A_a

Atmospheric absorption is important at long distances and at frequencies above 1000 Mc. Table III, Section 10, lists values of A_a appropriate for the calculation of weak fields, E(99), corresponding to L(p) for p = 99%.

THE FREQUENCY GAIN FUNCTION H_o FOR $\eta_s \geq 1$

for $\alpha_o = \beta_o$ and $v_t = v_r$ $(s=1, q=1)$

$v_t = 4\pi h_{te} \alpha_o / \lambda$, $v_r = 4\pi h_{re} \beta_o / \lambda$

$\eta_s = 4\gamma h_o$ has the values indicated on the curves

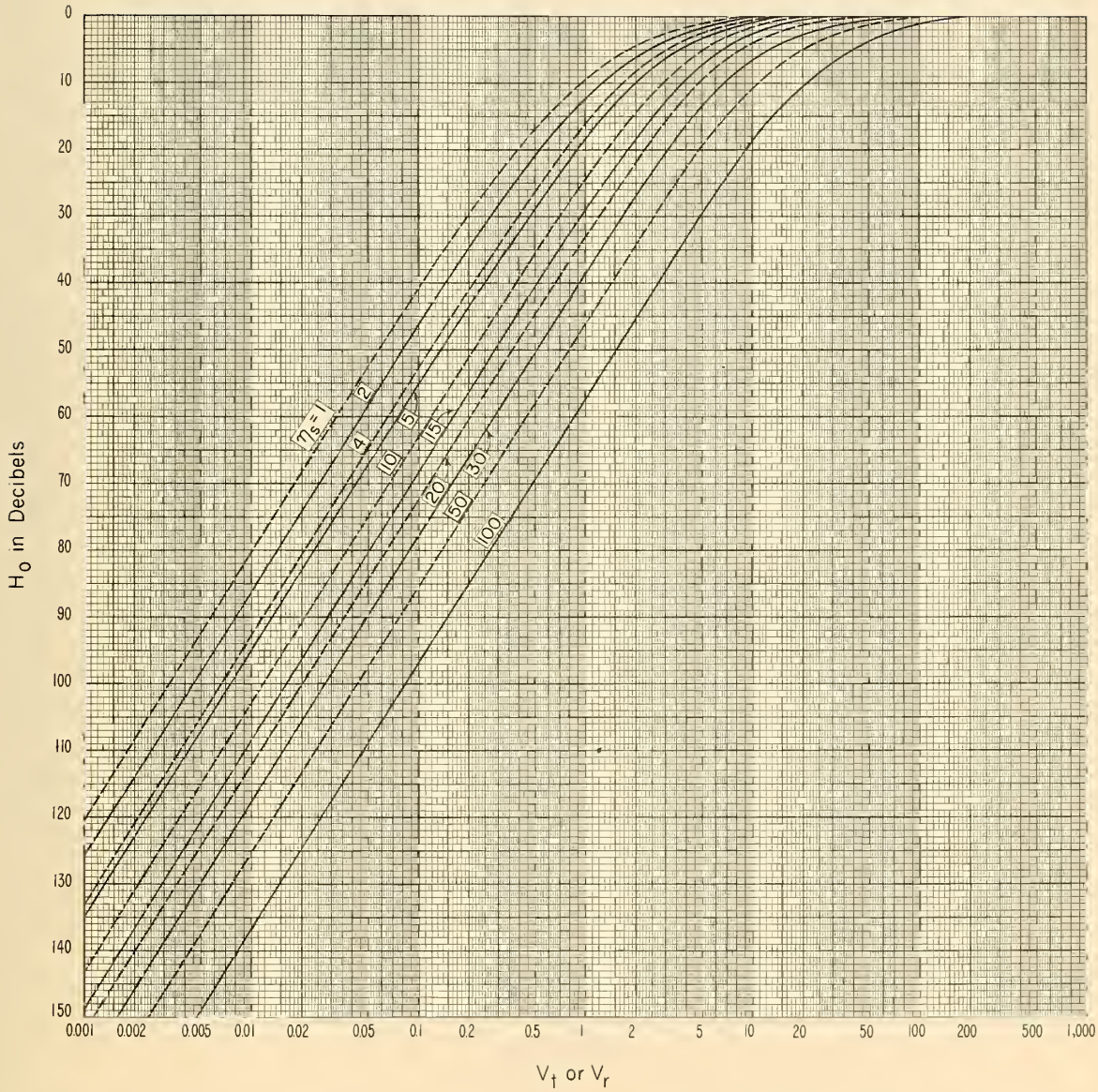

Figure 39

THE FREQUENCY GAIN FUNCTION H_o FOR $h_{te} = h_{re}$ (sq = 1)

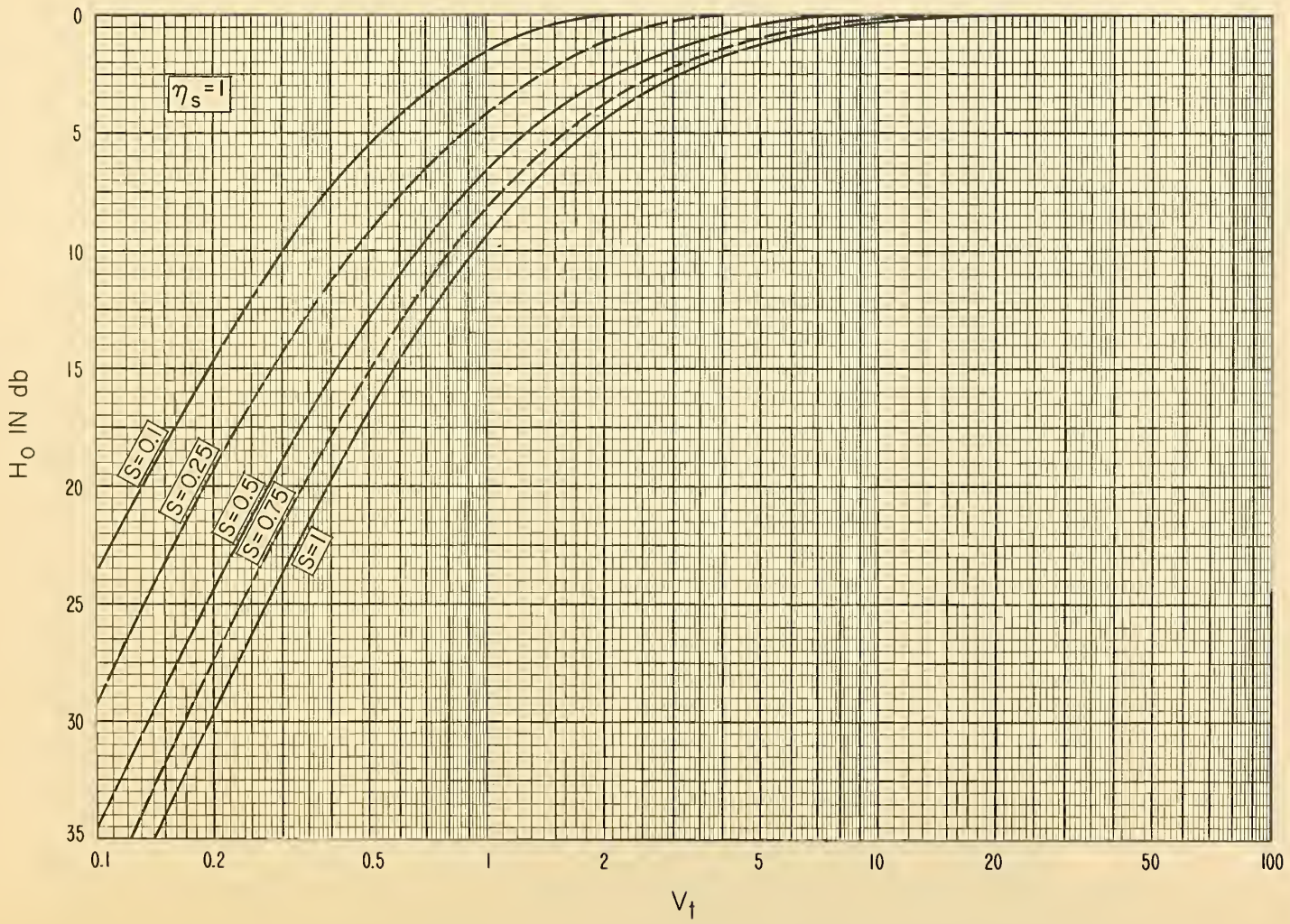

Figure 39a

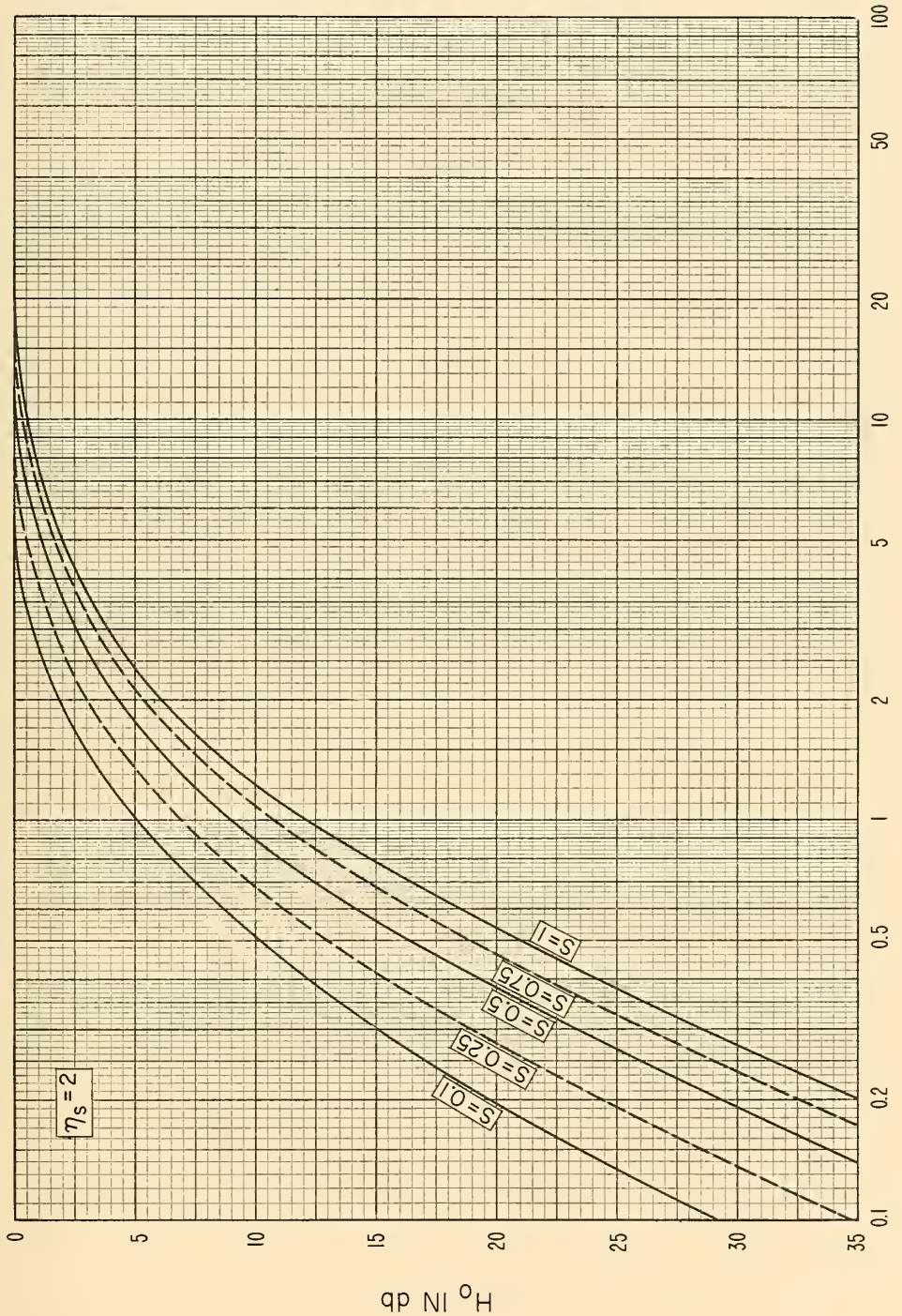
THE FREQUENCY GAIN FUNCTION H_o FOR $h_{te} = h_{re}$ (sq=1)
H_o IN db
0
5
10
15
20
25
30
35
0.1
0.2
0.5
1
2
5
10
20
50
100
V_f
$\eta_s = 2$
S=0.1
S=0.25
S=0.5
S=0.75
S=1

Figure 39b

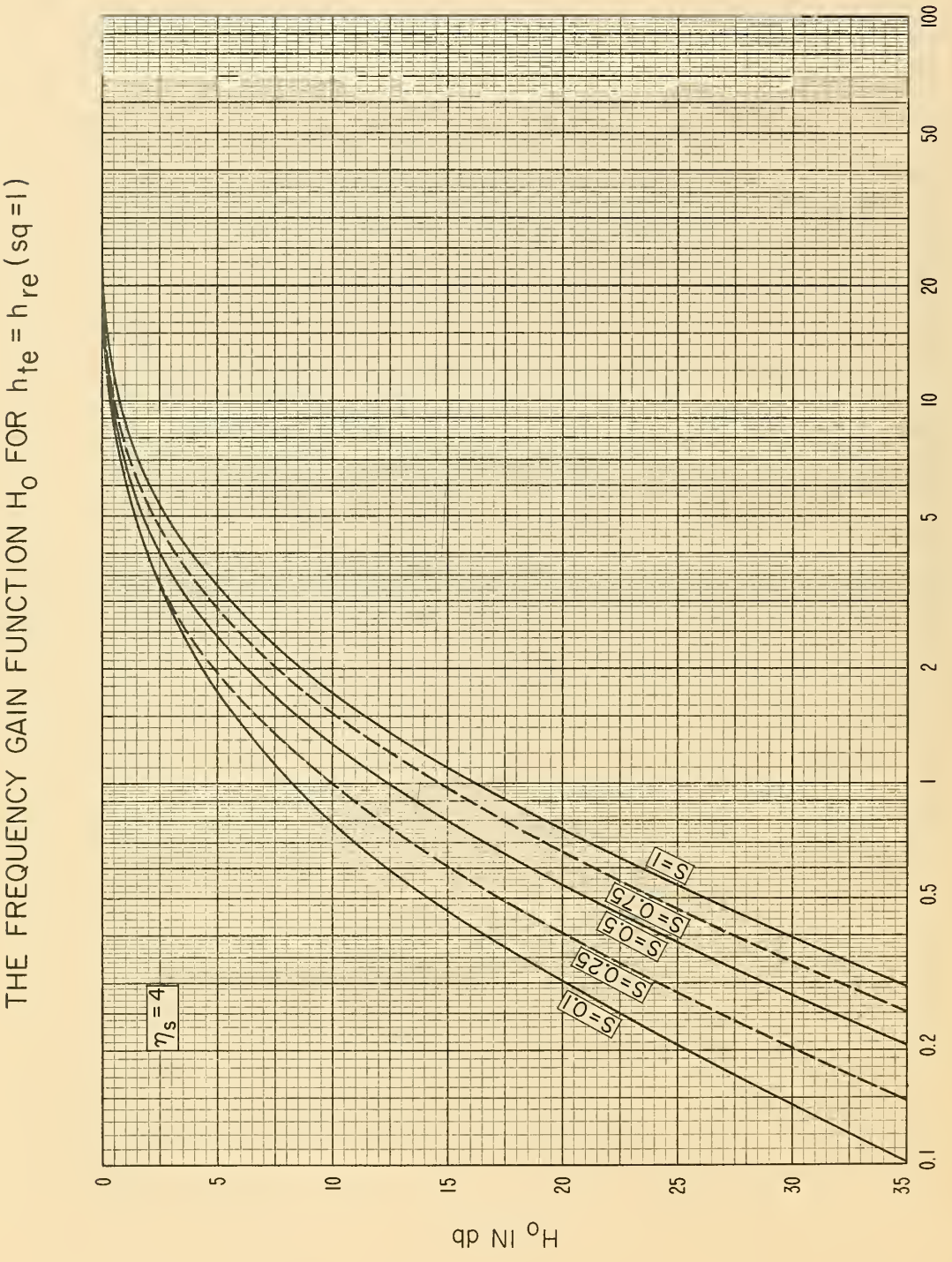
THE FREQUENCY GAIN FUNCTION H_o FOR $h_{te} = h_{re}$ (sq=1)
H_o IN db
0
5
10
15
20
25
30
35
$\eta_s = 4$
S=0.1
S=0.25
S=0.5
S=0.75
S=1
0.1
0.2
0.5
1
2
5
10
20
50
100
V_t

Figure 39c

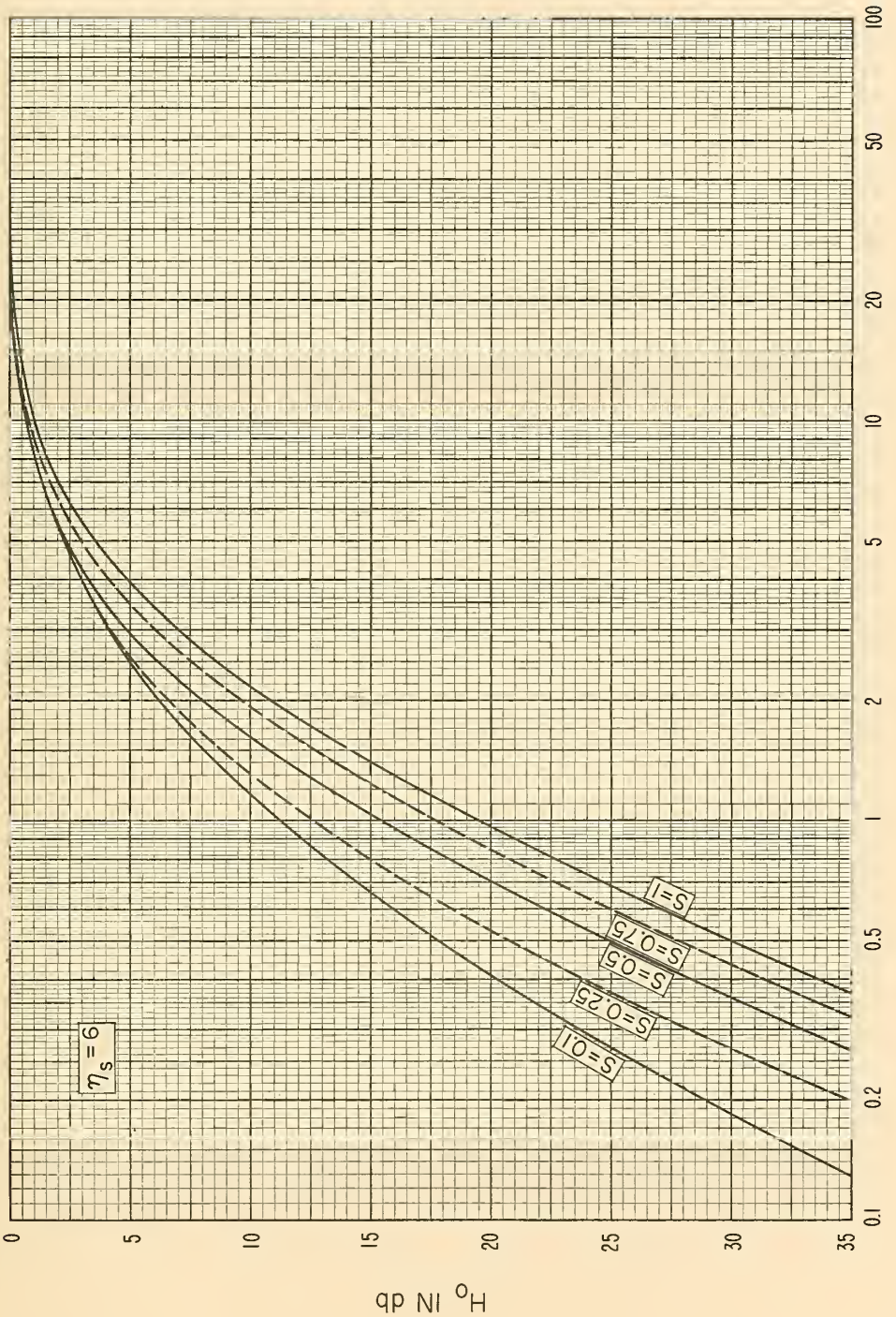
THE FREQUENCY GAIN FUNCTION H_o FOR $h_{te} = h_{re}$ (sq=1)
H_o IN db
0
5
10
15
20
25
30
35
0.1
0.2
0.5
1
2
5
10
20
50
100
V_t
$\eta_s = 9$
S=0.1
S=0.25
S=0.5
S=0.75
S=1

Figure 39d

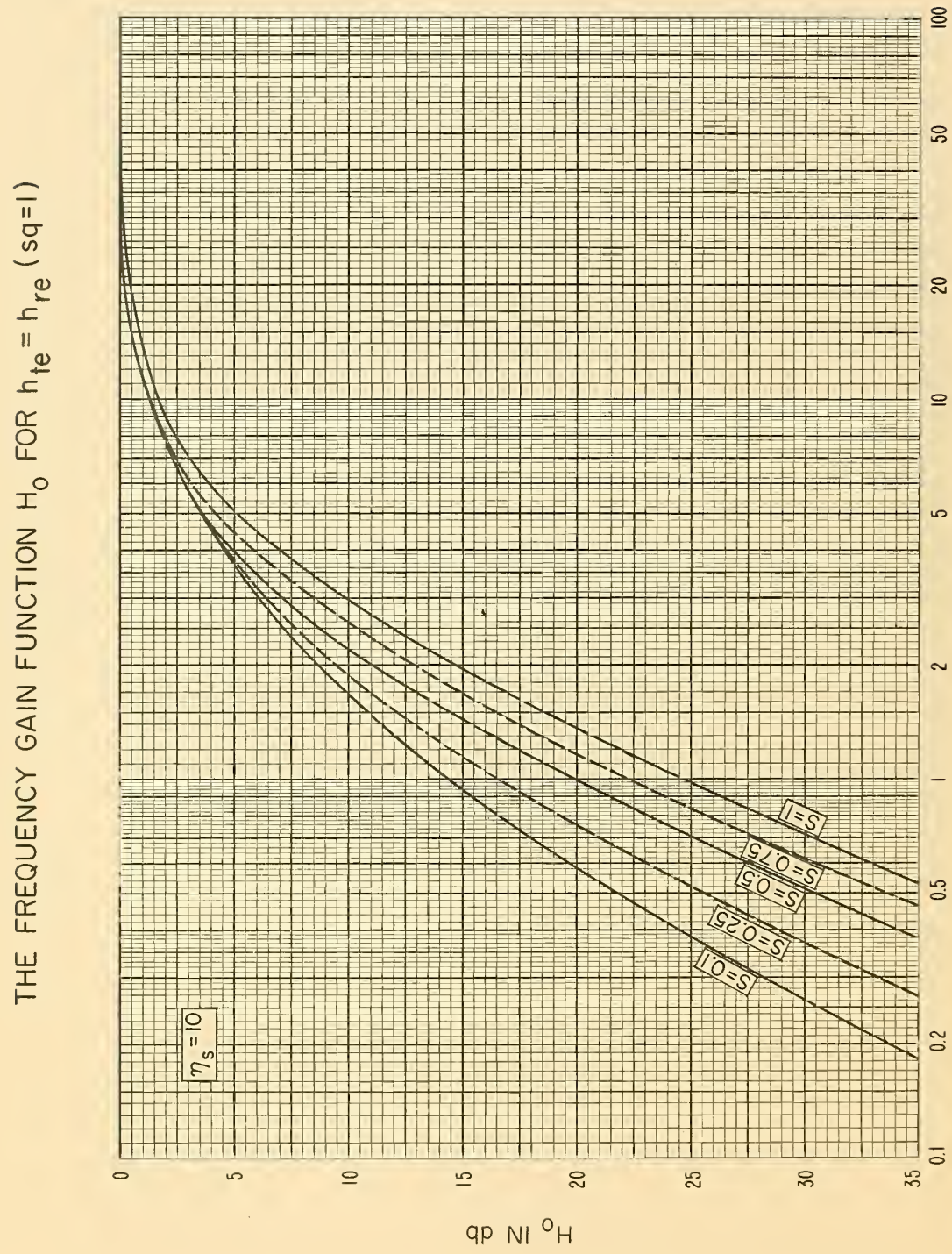
THE FREQUENCY GAIN FUNCTION H_o FOR $h_{te} = h_{re}$ (sq=1)
H_o IN db
V_t
$\eta_s = 10$
S=1
S=0.75
S=0.5
S=0.25
S=0.1
0
5
10
15
20
25
30
35
0.1
0.2
0.5
1
2
5
10
20
50
100

Figure 39e

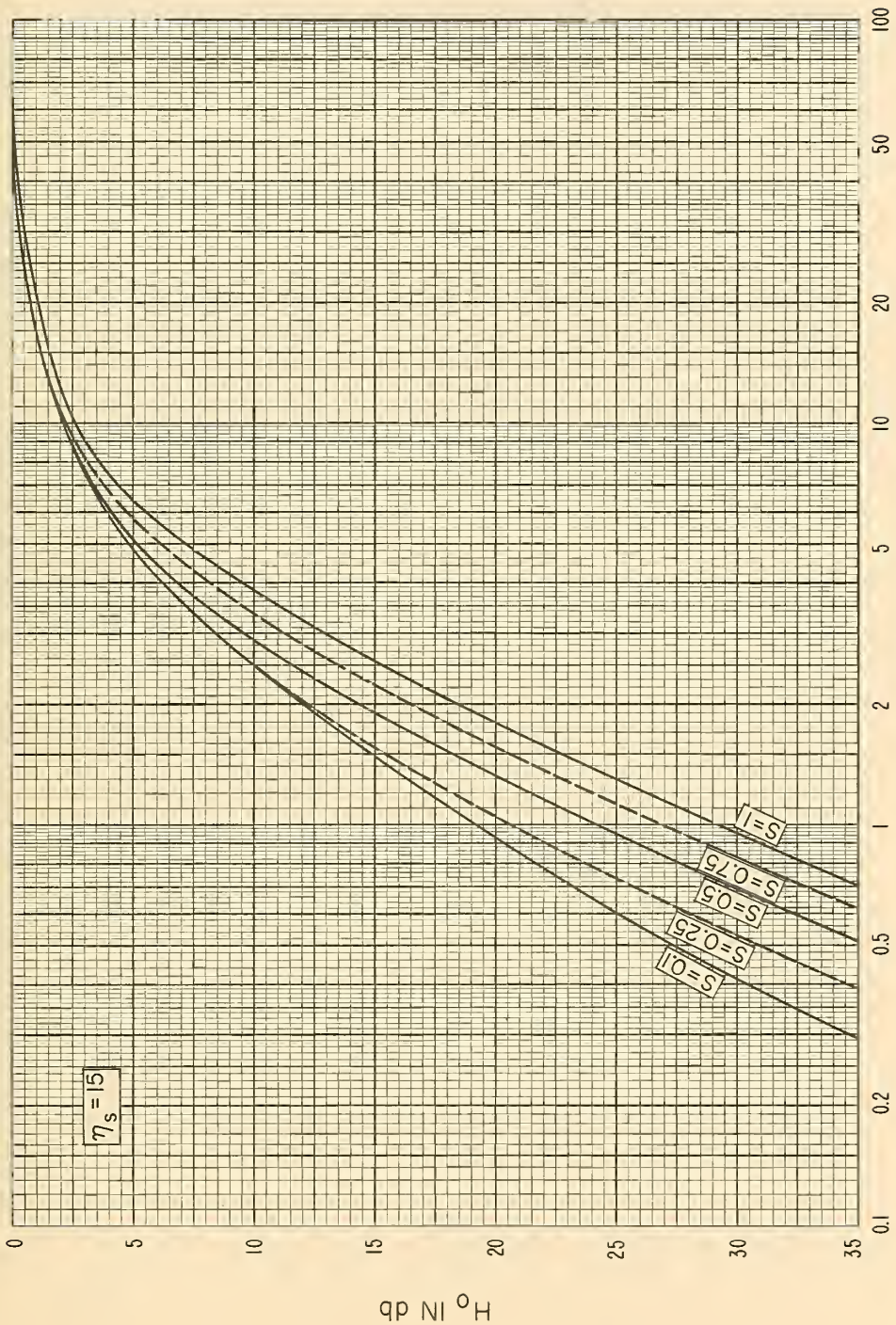
THE FREQUENCY GAIN FUNCTION H_o FOR $h_{te} = h_{re}$ (sq=1)
H_o IN db
V_f
$\eta_s = 15$
S=1
S=0.75
S=0.5
S=0.25
S=0.1
0
5
10
15
20
25
30
35
0.1
0.2
0.5
1
2
5
10
20
50
100

Figure 39f

THE FUNCTION h(r)

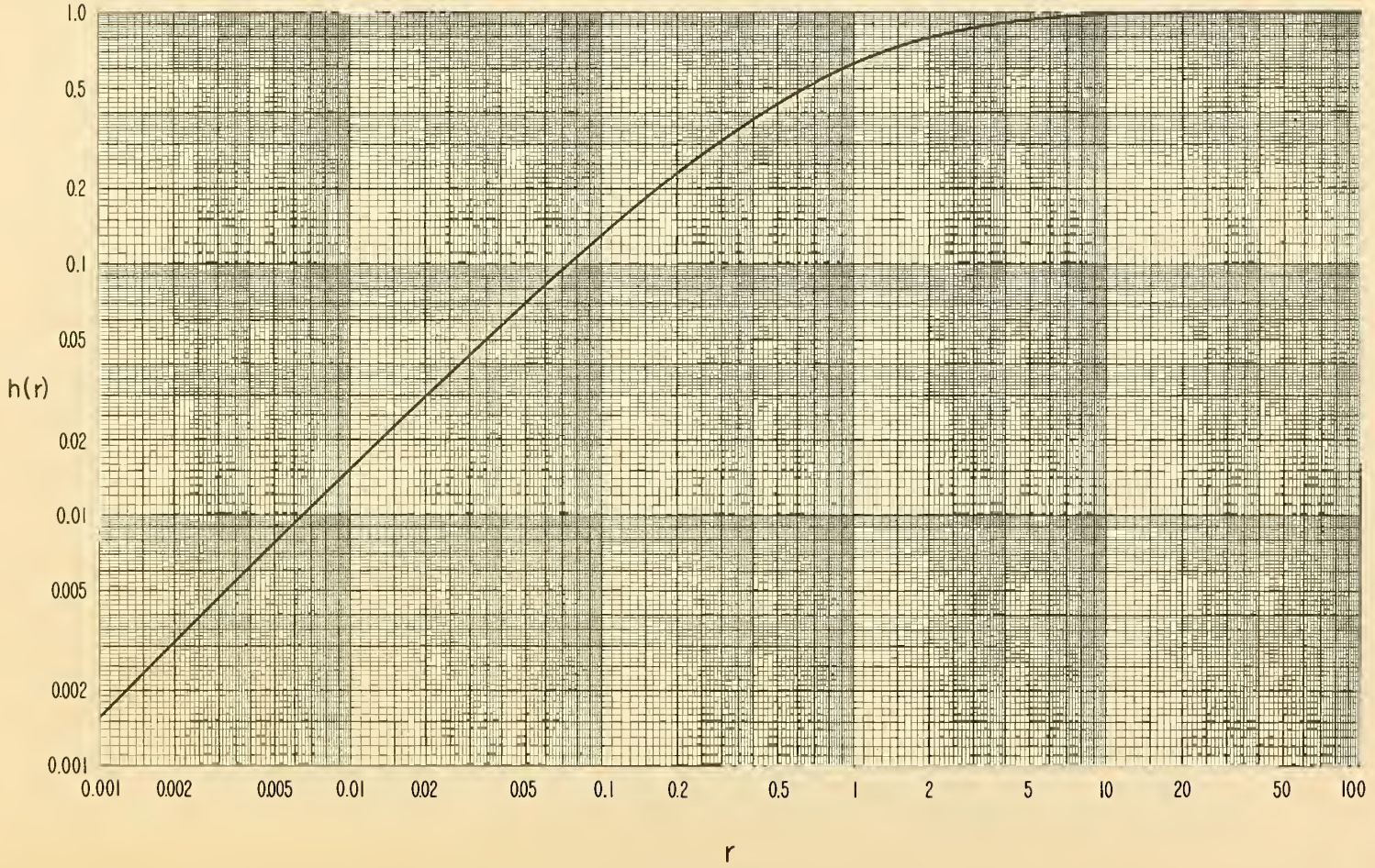

Figure 40

THE FUNCTION h(r)

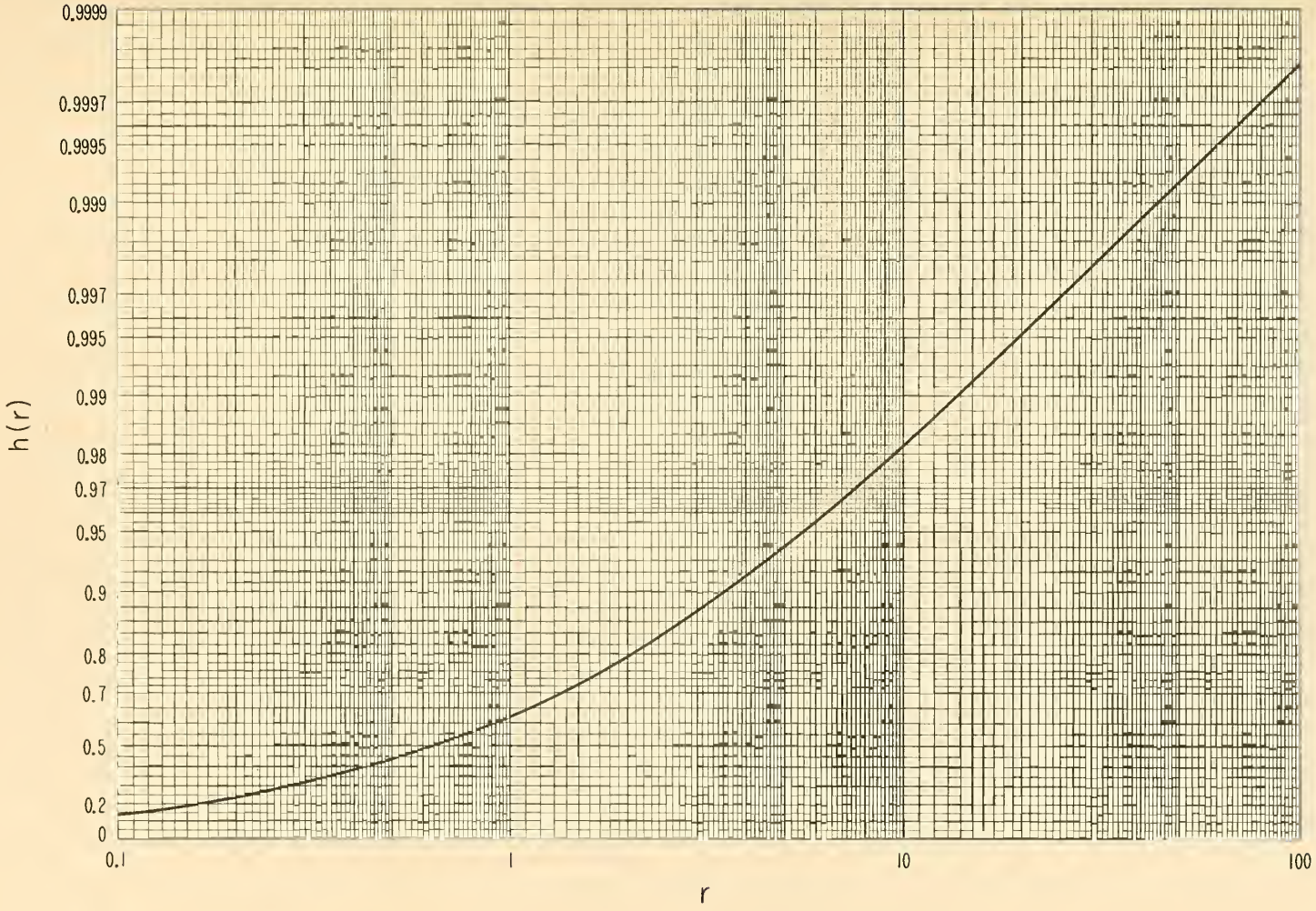

Figure 40 a

THE FREQUENCY GAIN FUNCTION H_o FOR $\eta_s = 0$ AND FOR $h_{te} = h_{re}$, (qs = 1)

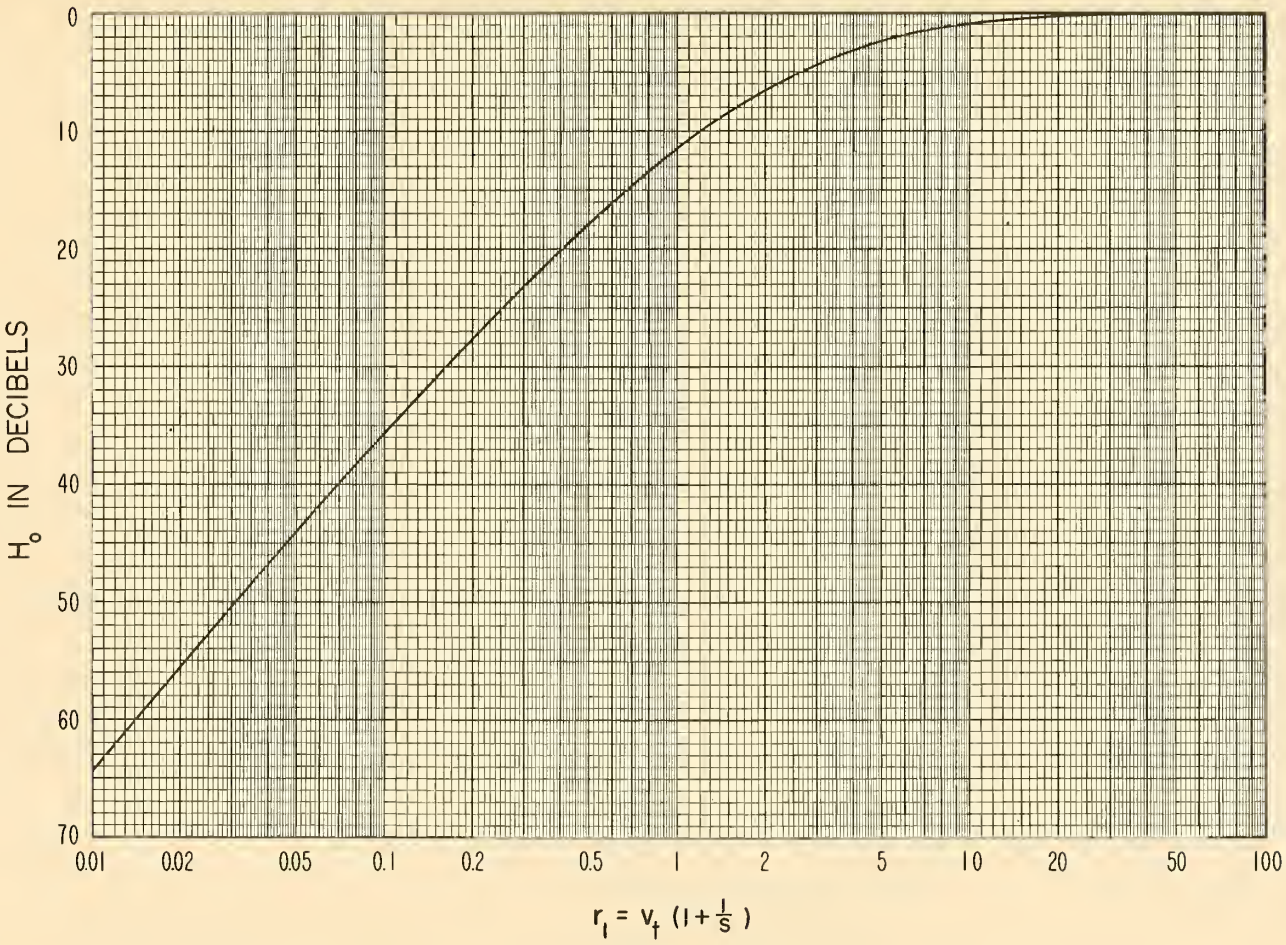

Figure 41

f. The Empirical Correction, $F(h_{cg}, N_s)$

This completes the discussion of terms in the prediction formula (3.1), except for the last term, $F(h_{cg}, N_s)$. This empirical correction, evaluated from radio transmission loss data, represents the variance of refractivity turbulence. [14] The origin of this term will be further discussed in Part III. $F(h_{cg}, N_s)$ is plotted as Fig. 42 for the reference atmospheres of Table II.

10. Atmospheric Absorption

For a recent study involving sixty-foot parabolic dishes at each end of propagation paths from 100 to 1000 miles long, the oxygen and water vapor absorption, A_a, exceeded 1% of the time was estimated, using methods described by B. R. Bean and R. Abbott in recent papers. [15] [16] Table III lists these values for frequencies from 100 Mc to 10,000 Mc. They are appropriate for the climate of Washington, D. C. in August, and take account of the decreasing rate of absorption as a ray is traced from an antenna to the high elevations corresponding to a "scattering volume." (See Fig. 14).

Table III

A_a in db

	Distance in Miles				
f_{mc}	100	200	500	700	1000
100	0.03	0.1	0.1	0.1	0.1
200	0.1	0.3	0.4	0.5	0.6
500	0.4	0.6	1.0	1.1	1.3
1000	0.6	1.2	1.6	1.8	2.0
2000	0.8	1.6	2.3	2.6	2.8
5000	1.2	2.4	3.3	3.7	4.1
10000	2.0	3.7	5.0	5.4	6.0

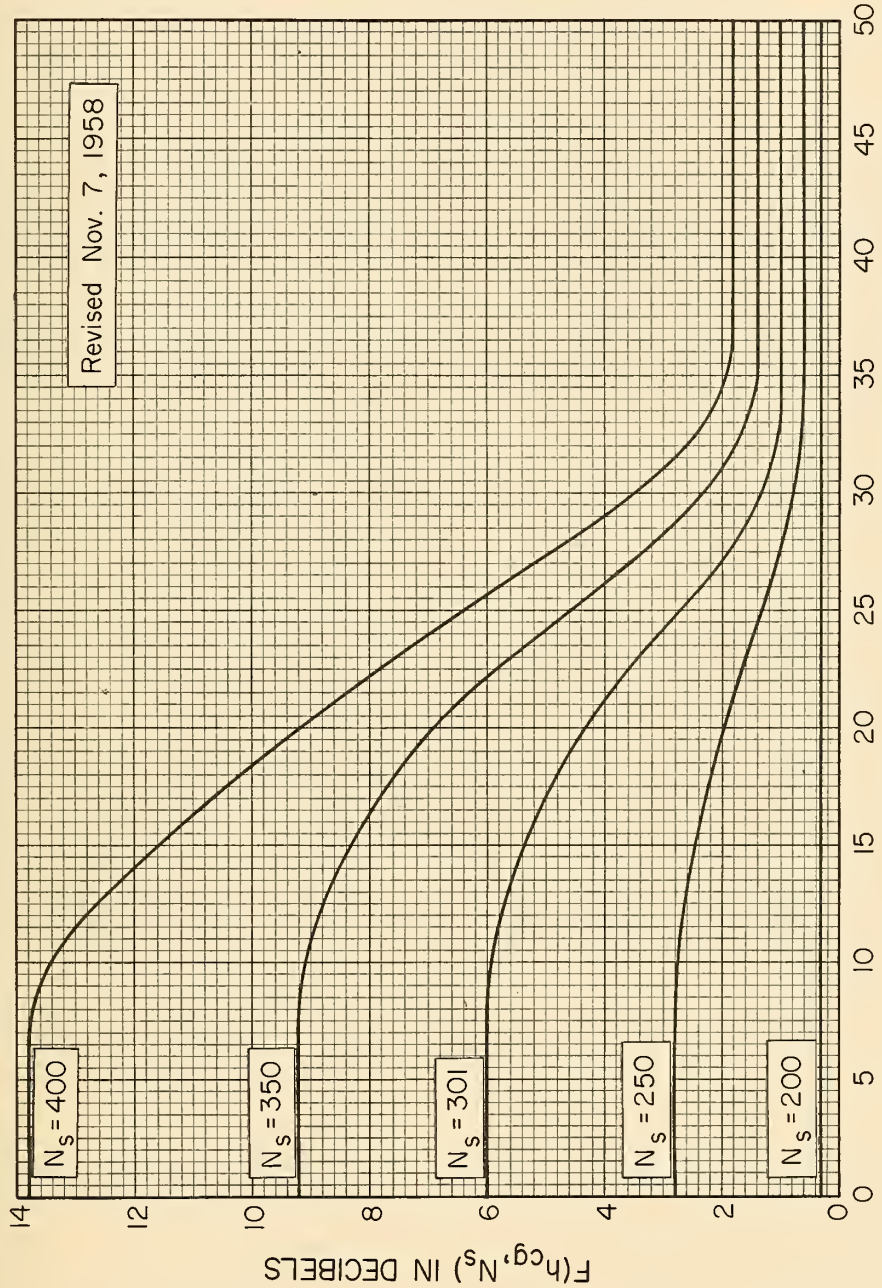
THE EMPIRICAL FUNCTION $F(h_{cg}, N_s)$
Revised Nov. 7, 1958
$N_s = 400$
$N_s = 350$
$N_s = 301$
$N_s = 250$
$N_s = 200$
$F(h_{cg}, N_s)$ IN DECIBELS
0
2
4
6
8
10
12
14
0
5
10
15
20
25
30
35
40
45
50
HEIGHT ABOVE GROUND, h_{cg}, OF SCATTERING CENTER
IN THOUSANDS OF FEET

Figure 42

11. Path Antenna Gain, G_p

The path antenna gain, G_p, may be determined from Fig. 43, which shows the loss in antenna gain, $G_L = G_t + G_r - G_p$, as a function of η_s and the ratio of angular distance, θ, to the half-power beamwidth, Ω, of each antenna. Note that θ and Ω are to be expressed in the same units.

The results shown in Fig. 43 correspond to the case $G_t = G_r$, $\Omega_t = \Omega_r = \Omega$, and $s = 1$; however, G_L is not very sensitive to changes in s. For more general results, the reader is referred to Reference 9.

A good engineering approximation relating half-power beamwidth, Ω_t, in milliradians to the free space gain G_t in decibels above an isotropic radiator is given by

$$G_t = 69.12 - 20 \log_{10} \Omega_t , \tag{11.1}$$

$$G_r = 69.12 - 20 \log_{10} \Omega_r , \tag{11.2}$$

from which it follows that

$$\theta/\Omega = [350\, \theta \times 10^{(G_t + G_r)/40}] \times 10^{-6} \tag{11.3}$$

where θ and Ω are in milliradians. The parameter η_s is defined by (8.4).

These formulas are derived for a parabolic dish of diameter D. At a frequency f_{mc} megacycles,

$$G_t \cong 20 \log_{10} D_{ft} + 20 \log_{10} f_{mc} - 52.43 \tag{11.4}$$

in decibels above an isotropic radiator, where the actual diameter of the dish, D_{ft}, is expressed in feet, and it has been assumed that the effective area of the dish is 56% of its actual area. The gain is that expected with a 10 db tapered illumination, where the feed illuminates the edge of the dish with 10 db less signal than its center.

LOSS IN ANTENNA GAIN, G_L
assuming equal free space gains G_t and G_r
at the terminals of a symmetrical path

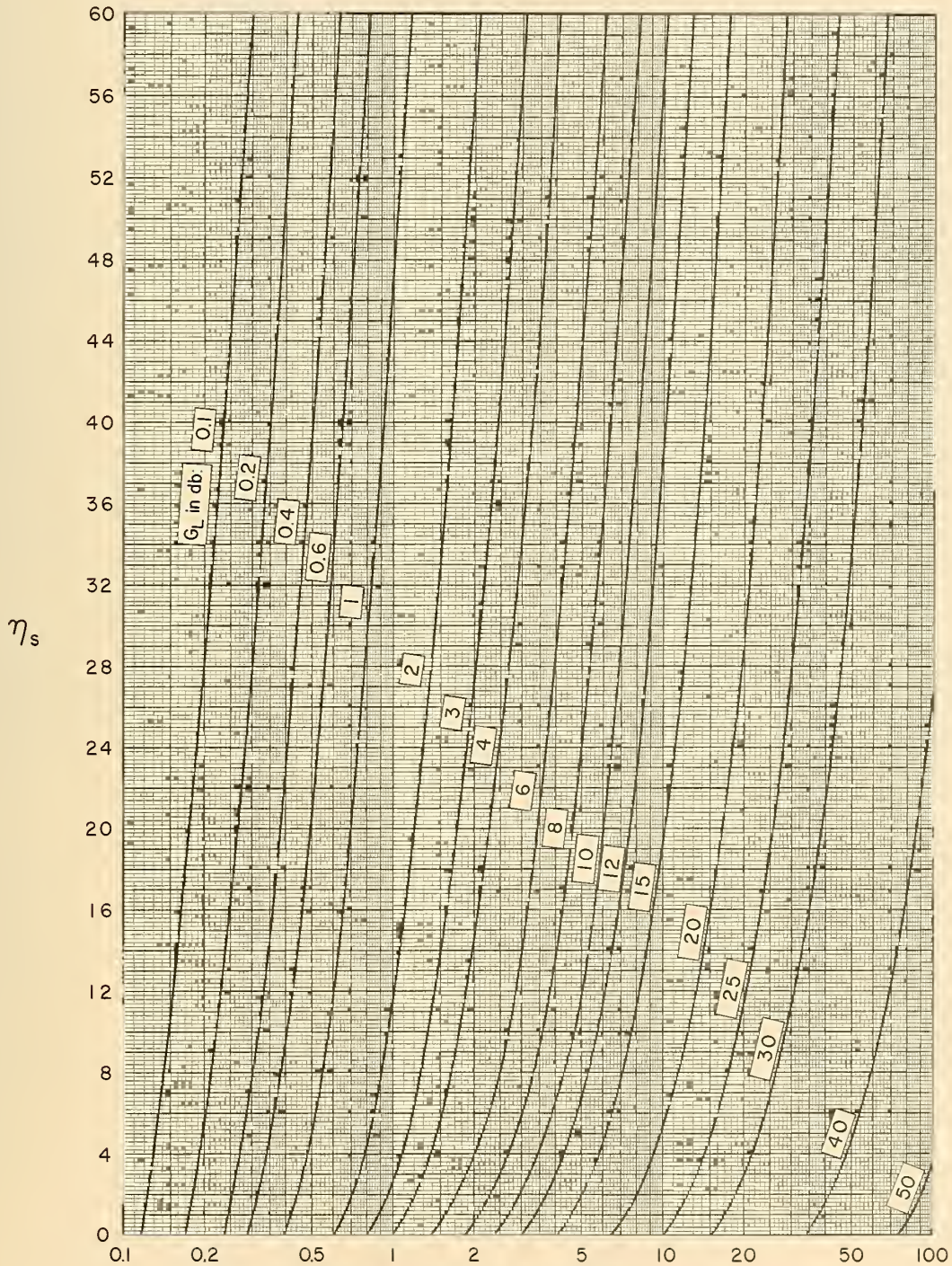

Figure 43

TERRAIN PROFILE FOR KIXL-FM, DALLAS, TEXAS TO AUSTIN, TEXAS

Distance = 175.9 miles. Profile shows straight lines drawn between high points of the terrain

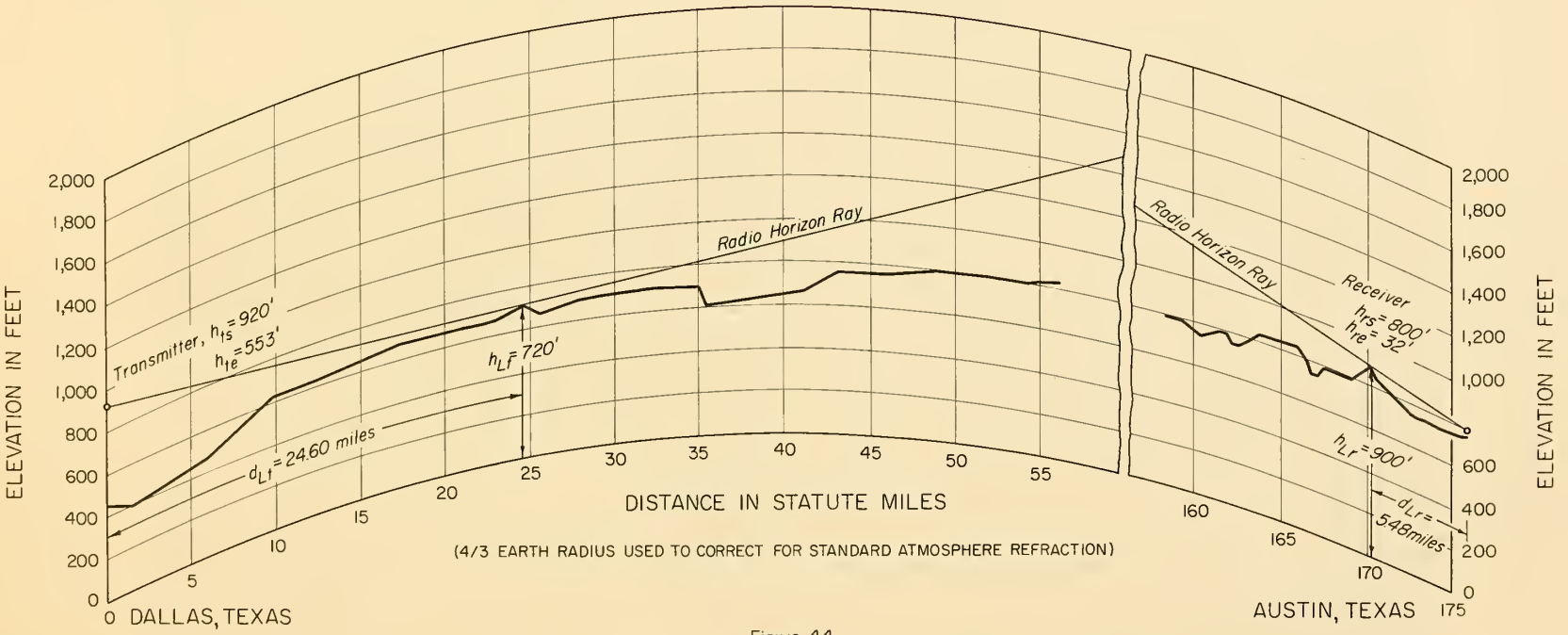

Figure 44

12. Calculations for Figure 13

The great circle path profile for the 176-mile KIXL-FM path is illustrated in Fig. 44 for the reference atmosphere corresponding to surface refractivity N_s = 301. For the first kilometer above the surface, this is the same as a "four-thirds earth" atmosphere, as may be seen from Table II. Only the parameters shown in Fig. 44 are needed from the terrain profile for each N_s value.

In this section are tabulated calculations of the theoretical curves of Fig. 13 for each time block and for all-day, all-year conditions. The reduced-to-sea level surface refractivity, N_o, for Time Block No. 2 is read from Fig. 34 at the location of each four-thirds earth radio horizon. These values, N_o = 313.0 and N_o = 316.3, correspond to heights above sea level h_{Lt} = 720' and h_{Lr} = 900', and to surface refractivity values N_s = 305.8 and N_s = 307.2, using (6.1) from Section 6. The average, N_s = 306.5, is taken to represent winter afternoon conditions along this path, and basic transmission less, $L_b(p)$ is calculated for p = 1, 10, 50, 90, and 99 per cent for N_s = 301 and for N_s = 350; the predicted values of $L_b(p)$ in Fig. 13 for N_s = 306.5 are then obtained by linear interpolation.

For KIXL-FM, d = 175.9 miles, f_{mc} = 104.5 megacycles, h_{te} = 553 feet, and h_{re} = 32 feet. See Section 7. Table IV shows calculations of L_{bms} for a = 5280 miles (N_s = 301) and a = 5896.66 miles (N_s = 350), using (3.1). An appropriate section, equation, or figure is referenced on each line of the table.

Table IV

Symbol	Value for N_s = 301	Value for N_s = 350	Reference
d_{Lt}	24.60 mi.	24.60 mi.	Fig. 44
d_{Lr}	5.48 mi.	5.48 mi.	Fig. 44
h_{Lt}	720'	720'	Fig. 44
h_{Lr}	900'	900'	Fig. 44
θ_{et}	-3.869 mr.	-3.626 mr.	Eq. (5.5)
θ_{er}	2.937 mr.	2.991 mr.	Eq. (5.6)
$(h_{ts}-h_{rs})/5.28d$	0.129 mr.	0.129 mr.	Eq. (5.7)
$d/2a$	16.657 mr.	14.916 mr.	Eq. (5.7)
α_{oo}	12.917 mr.	11.419 mr.	Eq. (5.7)
β_{oo}	19.465 mr.	17.778 mr.	Eq. (5.8)
θ_{ot}	0.789 mr.	0.546 mr.	Eq. (5.9)

Table IV (Continued)

Symbol	Value for N_s = 301	Value for N_s = 350	Reference
θ_{or}	3.975 mr.	3.921 mr.	Eq. (5.10)
D_s	145.82 mi.	145.82 mi.	Eq. (5.11)
$1000\, D_s/a$	27.617 mr.	24.730 mr.	Eq. (5.12)
θ_{oo}	32.382 mr.	29.197 mr.	Eq. (5.12)
d_{st}	81.1 mi.	82.5 mi.	Eq. (5.17)
d_{sr}	64.7 mi.	63.3 mi.	Eq. (5.18)
$\Delta\alpha_o$	0.060 mr.	0.001 mr.	Figs. 16 & 17
$\Delta\beta_o$	0.027 mr.	0.000 mr.	Figs. 16 & 17
α_o	12.977 mr.	11.420 mr.	Eq. (5.15)
β_o	19.492 mr.	17.777 mr.	Eq. (5.16)
θ	32.469 mr.	29.197 mr.	Section 5c
s	0.6658	0.6424	Eq. (8.1)
$s/(1+s)^2$	0.2399	0.2381	Eq. (8.2)
$d_{mi}\,\theta_{rad}$	5.7113 mi.	5.1358 mi.	Eq. (8.2)
h_o	1.3701 mi.	1.2228 mi.	Eq. (8.2)
h_1	1.1684 mi.	1.0456 mi.	Eq. (8.3)
h_{cg}	8,720 feet	7,840 feet	Eq. (4.4)
γ	0.1907/mi.	0.2102/mi.	Table II
η	1.0891	1.0796	Eq. (8.5)
η_s	1.0451	1.0282	Eq. (8.6)
$G_o(\eta)$	164.2 db	164.0 db	Fig. 36
ΔG	5.8 db	2.8 db	Table II
$G(\eta)$	170.0 db	166.8 db	Eq. (9.1)
$h_o - h_1$	0.2017 mi.	0.1772 mi.	Eq. (9.2)
F_o	0.17 db	0.16 db	Eq. (9.2)
$C(s)$	2.08	2.35	Fig. 37
$M(\eta)$	0.01	0.01	Fig. 38
F_s	0.02 db	0.02 db	Section 9c
v_t	9.58	8.43	Eq. (8.7)
v_r	0.833	0.760	Eq. (8.8)
q	0.0870	0.09015	Eq. (8.9)
ΔH_o	0.6 db	0.7 db	Eq. (9.4)
H_o	6.5 db	6.9 db	Eq. (9.3)
	$30 \log_{10} f_{mc} - 20 \log_{10} d = 15.7$ db		
$F(h_{cg}, N_s)$	6.0 db	9.2 db	Fig. 42
L_{bms}	186.0 db	180.0 db	Eq. (3.1)

At this point, L_{bd} is calculated by the methods of Reference 5. For such a long path, $L_{bd} >> L_{bms}$, so that $L_{bm} = L_{bms}$. [See (3.2)] Calculations of L_{bd} are listed in Table VII, however.

Because η_s is greater than 1, in Table IV it was not necessary to calculate $H_o(0)$. For $N_s = 301$, $r_1 = 23.97$ qs = 0.0579, and $r_2 = 1.388$ using (8.9). Then, $h(r_1) = 1$, $h(r_2) = 0.715$ from Fig. 40, and $H_o(0) = 5.6$ db, from (9.5). For $N_s = 350$, $H_o(0) = 6.2$ db.

Table V lists $V(p, \theta)$ as read from each time block (Table I) and for all hours, using Figs. 2 - 12.

Table V

$V(p, \theta)$ in decibels

$N_s = 301$, $\theta = 32.47$ milliradians:

	Time Blocks								
p	1	2	3	4	5	6	7	8	All hours
1%	15.5	12.0	14.9	21.8	12.3	18.3	22.1	18.1	19.1
10%	8.3	6.0	8.0	14.1	7.5	11.8	15.7	9.9	11.8
50%	1.0	0.0	1.1	6.7	2.7	5.1	9.5	1.5	3.5
90%	-4.5	-4.3	-4.3	0.5	-1.7	-0.6	1.8	-4.8	-3.0
99%	-8.8	-7.8	-8.6	-4.4	-5.4	-5.4	-4.5	-9.9	-7.7

$N_s = 350$, $\theta = 29.20$ milliradians:

1%	17.0	13.0	16.0	22.5	12.6	19.6	24.3	19.4	20.3
10%	9.2	6.5	8.5	14.4	7.6	12.5	16.8	10.7	12.2
50%	1.1	0.0	1.3	6.5	2.5	5.3	9.6	1.9	3.5
90%	-4.9	-4.9	-5.2	-0.1	-2.1	-1.0	1.5	-5.3	-3.4
99%	-9.5	-8.7	-10.4	-4.9	-5.9	-6.0	-5.1	-11.1	-8.8

Table VI lists $L_b(p)$ for each time block and all hours for $N_s = 301$, 350, and as obtained by linear db interpolation for $N_s = 306.5$. These values are plotted in Fig. 13.

Table VI

$L_b(p)$ in db

$N_s = 301$

Time Blocks

p	1	2	3	4	5	6	7	8	All hours
1%	170.5	174.0	171.1	164.2	173.7	167.7	163.9	167.9	166.9
10%	177.7	180.0	178.0	171.9	178.5	174.2	170.3	176.1	174.2
50%	185.0	186.0	184.9	179.3	183.3	180.9	176.5	184.5	182.5
90%	190.5	190.3	190.3	185.5	187.7	186.6	184.2	190.8	189.0
99%	194.8	193.8	194.6	190.4	191.4	191.4	190.5	195.9	193.7
$N_s = 350$									
1%	163.0	167.0	164.0	157.5	167.4	160.4	155.7	160.6	159.7
10%	170.8	173.5	171.5	165.6	172.4	167.5	163.2	169.3	167.8
50%	178.9	180.0	178.7	173.5	177.5	174.7	170.4	178.1	176.5
90%	184.9	184.9	185.2	180.1	182.1	181.0	178.5	185.3	183.4
99%	189.5	188.7	190.4	184.9	185.9	186.0	185.1	191.1	188.8
$N_s = 306.5$									
1%	169.7	173.2	170.3	163.4	173.0	166.9	163.0	167.1	166.1
10%	176.9	179.3	177.3	171.2	177.8	173.4	169.5	175.3	173.5
50%	184.3	185.3	184.2	178.6	182.6	180.2	175.8	183.8	181.8
90%	189.8	189.7	189.7	184.9	187.1	186.0	183.6	190.2	188.4
99%	194.2	193.2	194.1	189.8	190.8	190.8	189.9	195.4	193.1

In Table VII, calculations of L_{bd} from Section III and Appendix I of Reference 5 are summarized. There is an error at the top of page 1513 of this reference, where the formula $b^o = 2b'' - b'$ refers only to vertical polarization. The parameters in Table VII are for horizontal polarization, where $b^o = 180^o - b'$. References in this table are from Reference 5. Parameters also used in calculating L_{bms} are not repeated. L_{bd} is calculated from (43) of Appendix I, where $a' = 3960$ miles.

Table VII

Symbol	Value for $N_s = 301$	Value for $N_s = 350$	Reference
$k = a/3960$	4/3	1.48905	App. I, Ref. 5
α_1	0.014433 rad.	0.012679 rad.	Sect. III, (18) *
β_1	0.018035 rad.	0.016518 rad.	Sect. III, (19) *
k_t	1.4172	1.6433	Sect. III, (16) *
k_r	0.9076	0.9681	Sect. III, (17) *
k_{te}	0.7295	0.7295	Sect. III, (20) *
k_{re}	0.6256	0.6256	Sect. III, (21) *
$C_o(k_t)$	1.0205	1.0721	App. I, (37) *
$C_o(k_r)$	0.8797	0.8988	App. I, (37) *
$C_o(k_{te})$	0.8179	0.8179	App. I, (37) *
$C_o(k_{re})$	0.7771	0.7771	App. I, (37) *
$K(4/3)$	0.0010	0.0010	App. I, Fig. 30*

The figure heading for Fig. 30, Appendix I, on page 1512 of Reference 5 is misleading: The factor $[4/3k']^{1/3}$ should read $[4/(3k')]^{1/3}$ or $1/C_o(k')$.

$K(k_t)$	0.00098	0.00093	Fig. 30 *
$K(k_r)$	0.00114	0.00111	Fig. 30 *
$K(k_{te})$	0.00122	0.00122	Fig. 30 *
$K(k_{re})$	0.00129	0.00129	Fig. 30 *
$C[K(k_{te}), b^o]$	61.63 db	61.63 db	Fig. 33 *
$C[K(k_{re}), b^o]$	61.63 db	61.63 db	Fig. 33 *
$16.667 \log_{10} f_{mc}$	33.65 db	33.65 db	(43) *
$10 \log_{10} d_{mi}$	22.45 db	22.45 db	(43) *
$\beta_o(k_t)$	1.6061	1.6061	Fig. 32(a)*
$\beta_o(k_r)$	1.6060	1.6060	Fig. 32(a)*
$\beta_o(k_{te})$	1.6060	1.6060	Fig. 32(a)*
$\beta_o(k_{re})$	1.6059	1.6059	Fig. 32(a)*

Denote the last term in (43) by the symbol D:

$$D = 488.69\, f_{mc}^{1/3} \left\{ \beta_o(k_t)\, C_o(k_t)\, \alpha_1 + \beta_o(k_r)\, C_o(k_r)\, \beta_1 \right\} \qquad (12.1)$$

D	113.10 db	105.14 db	(43)*

* See Reference 5.

Table VII (Continued)

Symbol	Value for N_s = 301	Value for N_s = 350	Reference
$\beta_o^2(k_{te})/C_o(k_{te})$	3.153	3.153	(40) *
$\beta_o^2(k_{re})/C_o(k_{re})$	3.319	3.319	(40) *
$\overline{h}_{te}$	1.290	1.290	(40) *
$\overline{h}_{re}$	0.0786	0.0786	(40) *
$G(\overline{h}_{te})$	-8.2 db	-8.2 db	Fig. 35(c)*
$G(\overline{h}_{re})$	-16.7 db	-16.7 db	Fig. 35(c)*
$10 \log_{10} C_o(k_t)$	0.09 db	0.30 db	(43) *
$10 \log_{10} C_o(k_r)$	-0.56 db	-0.46 db	(43) *
L_{bd}	255.3 db	247.6 db	(43) *

For N_s = 306.5, L_{bd} = 254.4 db, as compared with $L_b(50)$ = 185.2 db in Time Block No. 2. (See Table VI).

ACKNOWLEDGMENT

Initial phases of the theoretical development and organization of data analysis for this paper were under the supervision of Mrs. Frances T. Daniel. Most of the detailed theoretical work was done by R. L. Abbott, A. P. Barsis, H. K. Hansen, W. J. Hartman, L. E. Vogler, and R. E. Wilkerson, under the direction of P. L. Rice. Terrain profile data were obtained at various times under the direction of W. V. Mansfield, P. H. Elder, A. M. Ozanich, and J. H. Longbotham. Most of the detailed calculation was supervised by Mrs. M. A. Schafer under the direction of Mrs. Longley. R. P. Baptist, V. D. Brand, S. A. Buckel, M. W. Clark, M. M. Coyle, C. S. Hays, R. V. Lisle, and V. H. Weitzel helped with calculations and graph plotting.

* See Reference 5

REFERENCES

1. B.R. Bean and G.D. Thayer, " On models of the atmospheric radio refractive index, " Proc. IRE, 47 (5) , 740 - 755 (1959) .

2. K.A. Norton, " Transmission loss in radio propagation , " Proc. IRE , 41, 146-152, (1953) . See also: K.A. Norton , "System loss in radio wave propagation," J. Research NBS, 63-D (Radio Propagation), 53, (1959) .

3. R.C. Kirby, "VHF propagation by ionospheric scattering - a survey of experimental results, " IRE Trans. Comm. Syst. CS-4 (1), 17-27, (1956).

4. K.A. Norton , " Point-to-point radio relaying via the scatter mode of tropospheric propagation, " IRE Trans. Comm. Syst. CS-4 (1), 39-49 , (1956) .

5. K.A. Norton, P.L. Rice, and L.E. Vogler, " The use of angular distance in estimating transmission loss and fading range for propagation through a turbulent atmosphere over irregular terrain, " Proc. IRE , 43, 1488-1526, (1955).

6. H.G. Booker and W.E. Gordon, "A theory of radio scattering in the troposphere," Proc. IRE, 38 , 401-412 , (1950).

7. H. T. Friis, A. B. Crawford, D. C. Hogg, "A reflection theory for propagation behind the horizon, " Bell Telephone System Technical Journal, 36, 627-644 , (1957) (Monograph No. 2823) .

8. B. Josephson and F. Eklund, "Some microwave propagation experiences from a just-below-horizon path," IRE Trans. Antenn. Prop. AP-6, 176-178, (1958) .

9. W. J. Hartman and R. E. Wilkerson, "Path antenna gain in an exponential atmosphere," to be published in J. Research NBS, 63-D, November, 1959.

10. K. A. Norton, L. E. Vogler, W. V. Mansfield and P. J. Short, "The probability distribution of the amplitude of a constant vector plus a Rayleigh distributed vector," Proc. IRE, 43(10), 1354, (1955) .

11. H. G. Booker and W. E. Gordon, "The role of stratospheric scattering in radio communication," Cornell University Research Report EE 308; September, 1956.

12. B. R. Bean and J. D. Horn, "On the climatology of the surface values of radio refractivity of the earth's atmosphere," to be published in J. Research NBS, 63-D, (Radio Propagation), September, 1959.

13. CCIR, "Atlas of ground-wave propagation curves for frequencies between 30 Mc/s and 300 Mc/s," published by l'Union internationale des Telecommunications in accordance with CCIR Resolution No. 11, Geneva, 1955.

14. Note added July 28, 1956, to Reference 4.

15. B. R. Bean and R. L. Abbott, "Oxygen and water vapor absorption of radio waves in the atmosphere," Geofis. Pura e Appl., 37 (2), 127-144, (1957).

16. Bradford R. Bean, "Some meteorological effects on scattered radio waves," IRE Trans., PGCS-4, 32-38, (1956).

Appendix

The Calculation of the Power Required for a Specified Grade of a Given Type of Service

The body of this report presents methods for predicting the basic transmission loss, $L_b(p)$, exceeded by p per cent of the hourly medians in a given time. Within each hour, signal variations may exhibit many different types of fading, depending on equipment and antenna characteristics and upon what propagation mechanisms are dominant during that hour. Various kinds of communication links (telegraph, teletype, voice, facsimile, data links), and broadcasting and navigation facilities are affected differently by various types of signal fading. For instance, an hourly median signal-to-noise ratio of 38 db is listed in a recent report by Norton [1] as desirable for good quality U.S. standard television reception of a severely fading Rayleigh distributed signal; service fields near a television broadcast station would not require such a large hourly median signal-to-noise ratio, since there would be little fading within an hour. Other types of service, such as FM voice, can get by with much smaller hourly median predetection signal-to-noise ratios, even where the same post-detection signal-to-noise ratio is desired.

Concepts represented by the following symbols are explained in other papers [2, 3, 4]. Capital letters refer to quantities expressed in decibels:

P_t = transmitter power in decibels above one watt, or dbw.

L_t = transmission line and matching network losses between transmitter and antenna. When the antennas are very near the surface, then radiation resistance changes and this results in an additional loss with vertical dipoles or gain with horizontal dipoles which may be included in L_t; a discussion of these additional transmission loss terms is given in Appendix III of Reference 3.

G_t = transmitting antenna gain in decibels above a theoretical isotropic radiator. (G_t or G_r for half-wave dipole is 2.15 db)

G_r = receiving antenna gain in db above an isotropic radiator.

L_r = transmission line and matching network losses between receiving antenna and receiver input terminals. (See also Appendix III of Reference 3.)

v = volts available across receiver input.

r = receiver input impedance in ohms.

P_a = power available at the terminals of a loss-free receiving antenna, dbw. $P_a = 20 \log_{10} v - 10 \log_{10} r + L_r$.

P_m = minimum acceptable value of P_a. For example: assuming a minimum useful signal of 5 microvolts, $r = 51$ ohms and $L_r = 1$ db, the minimum acceptable power at the terminals of the receiving antenna will be $P_m = -106.02 - 17.08 + 1.0 = -122.1$ dbw.

P_r = $P_t - L_t$ = total radiated power in dbw.

E.R.P. = effective radiated power = $P_t - L_t + G_t - 2.15$ in dbw.

L = $P_r - P_a$ = transmission loss.

A = attenuation relative to free space.

L_f = $L - A$ = transmission loss in free space.

$G_p \leq G_t + G_r$ = path antenna gain.

$L_b = L + G_p$ = transmission loss with isotropic radiators, called "basic transmission loss". *

L_{bf} = basic transmission loss in free space
= $36.58 + 20 \log_{10} f_{mc} + 20 \log_{10} d_{mi}$, where f_{mc} is the radio wave frequency in megacycles per second and d_{mi} is the distance in statute miles between transmitting and receiving antenna terminals.

E = field strength in decibels above one microvolt per meter (dbu) for one kilowatt E.R.P.

E_b = free space field strength between half-wave dipoles.

R = predetection hourly median signal-to-noise ratio required to provide a specified grade of service within the hour for which the median signal level is given. The factor R is best determined experimentally, but it may also be calculated with reasonable accuracy for some types of service by assuming that the received signal is Rayleigh distributed about its hourly median level. As an example, the calculated value of R is 16.9 db to provide a 60-word-per-minute frequency shift telegraph service with not more than one-per-cent binary error rate for a period of time of the order of one hour during which the transmission conditions may be

---

* This definition differs from that used in Reference 2.

considered relatively constant, except for the rapid, Rayleigh type, of fading [5]. The factor R may be reduced substantially by the use of diversity reception, this reduction being larger, the larger the reliability required. For discussions of the expected diversity gain, reference may be made to papers by Montgomery [6, 7], Mack [8], Brennan [9], and Staras [10].

b = effective bandwidth of the receiver in cycles per second, including allowance for differences between transmitter and receiver oscillator frequencies and including the component of the baseband required to accommodate the received modulation.

B = $10 \log_{10} b$ (An absolute lower limit for the noise level is the "Johnson noise" or "ktb noise". At 60° Fahrenheit, the ktb noise level is equal to B-204 db).

F = effective noise figure, referred to the receiving antenna terminals. This noise figure is the difference, or decibel ratio, between the actual noise level (P_m-R) decibels and the ktb noise level. Where external noise picked up by the receiving system is negligible, F is simply the decibel sum of the receiver noise figure F_r and the transmission line and matching network losses L_r. For carefully designed receivers at 100 Mc or at 1000 Mc, F_r equals about 5 db or 10 db, respectively. F = ($10 \log_{10} f_{mc}$ - 5) decibels, approximately.

Noises originating within and external to the receiving system add directly when expressed in watts, so in this case it is not permissible to add decibels. F includes the effects of the antenna noise (cosmic and man-made noise, for example) as well as the receiver noise, together with the receiving antenna circuit and transmission line loss. The proper method for estimating the expected value of F is discussed in detail in a recent National Bureau of Standards circular [11]. It is assumed that the receiver incorporates gain adequate to ensure that the first circuit noise is detectable. As a practical matter, F is within 3 db equal to whichever is greater, $F_r + L_r$ or P_n - (B-204), where P_n is the external noise picked up by the system, expressed in dbw.

Having once determined a value for P_m either from information about a minimum useful signal or from information about R, F, and B, it is a simple matter to compute the maximum allowable transmission

loss, L, the maximum allowable attenuation relative to free space, A, or the minimum allowable field strength, E. The following relationships are useful:

$$P_a = P_m = R + F + B - 204 \text{ dbw.} \tag{I-1}$$

$$P_r = P_t - L_t \text{ dbw.} \tag{I-2}$$

$$L = P_r - P_a , \tag{I-3}$$

where this is interpreted as a maximum allowable transmission loss if $P_a = P_m$. Definitions of P_a and P_m assume a matched load.

The difference (decibel ratio) between transmission loss L and basic transmission loss L_b is the path antenna gain G_p, which is equal to or less than the sum of free space gains G_t and G_r. In free space, the difference between L_f and L_{bf} is $G_t + G_r$:

$$L = L_b - G_p \tag{I-4}$$

$$L_f = L_{bf} - (G_t + G_r) \tag{I-5}$$

Attenuation relative to free space is defined in terms of the measured transmission loss L and the loss L_f expected in free space. Thus, this quantity, A, includes any effects of path antenna gain degradation (antenna-to-medium coupling loss), and is in general greater than the theoretical attenuation relative to free space for isotropic antennas. Subtracting (I-5) from (I-4):

$$A = L - L_f = L_b - L_{bf} + G_L , \tag{I-6}$$

where

$$G_L = G_t + G_r - G_p \geq 0. \tag{I-7}$$

Basic transmission loss in free space is known when frequency and distance are given:

$$L_{bf} = 36.58 + 20 \log_{10} f_{mc} + 20 \log_{10} d_{mi} \tag{I-8}$$

Similarly, the free space field strength E_{bf} dbu for one kw E.R.P. using half-wave dipoles at both ends of a path is known:

$$E_{bf} = 102.79 - 20 \log_{10} d_{mi} . \qquad \text{(I-9)}$$

Assuming $G_L = 0$ for transmission between dipoles, the correlatives of (I-4) through (I-7) may be written:

$$E = E_b - G_L \qquad \text{(I-10)}$$

Here is seen a major advantage of the concept of transmission loss, which is a measurable quantity, while field strength is not, except where a coherent wave front exists at the antenna and $G_L = 0$. Both E and E_b are plane wave field strengths that would have to exist at the receiving antenna to produce the voltages measured at its terminals, assuming antenna gains realized. E corresponds to the case where antenna gains are not realized and E_b to the case where gains are realized; other things being equal, antenna terminal voltages are less in the one case than in the other, so E is less than E_b by G_L decibels.

The correlative to (I-5) is

$$E_f = E_{bf} , \qquad \text{(I-11)}$$

which says simply that in free space, free space gains are realized. Attenuation relative to free space is obtained by subtracting (I-10) from (I-11):

$$A = E_f - E = E_{bf} - E_b + G_L . \qquad \text{(I-12)}$$

Compare (I-12) with (I-6). Equating these expressions and making use of (I-8), (I-9), and (I-10), a relationship emerges between L_b and E:

$$L_b = 139.37 + 20 \log_{10} f_{mc} - E_b$$

$$= 139.37 + 20 \log_{10} f_{mc} - (E + G_L) , \qquad \text{(I-13)}$$

The meaning of (I-13) is the same as that of (5) in Reference 4, where G_L is set equal to zero and in effect the statement is made that E underestimates E_b by the amount G_L.

APPENDIX
REFERENCES

1. K. A. Norton, "Point-to-point radio relaying via the scatter mode of tropospheric propagation," IRE Trans. Comm. Syst., CS-4 (1), 39-49, (1956).

2. K. A. Norton, "Transmission loss in radio wave propagation," Proc. IRE, 41, 146-152, (1953).

3. K. A. Norton, "Transmission loss in radio wave propagation: II," NBS Technical Note No. 12, June, 1959. See also K. A. Norton, "System loss in radio wave propagation," J. Research NBS, 63-D (Radio Propagation), 53, (1959).

4. K. A. Norton, P. L. Rice, and L. E. Vogler, "The use of angular distance in estimating transmission loss and fading range for propagation through a turbulent atmosphere over irregular terrain," Proc. IRE, 43, (10), 1488-1526, (1955).

5. G. Franklin Montgomery, "A comparison of amplitude and angle modulation for narrow-band communication of binary-coded messages in fluctuation noise," Proc. IRE, 42, 447-454, (1954).

6. G. Franklin Montgomery, "Message error in diversity frequency-shift reception," Proc. IRE, 42, 1184-1187, (1954).

7. G. Franklin Montgomery, "Ultrasonic switch aids diversity reception," Electronics, 28, 169, (1955).

8. C. L. Mack, "Diversity reception in UHF long-range communications," Proc. IRE, 43, 1281-1289, (1955).

9. D. G. Brennan, "On the maximum signal-to-noise ratio realizable from several noise signals," Proc. IRE, 43, 1530, (1955).

10. H. Staras, "The statistics of combiner diversity," Proc. IRE, 44, (8), 1057-1058, (1956).

11. W. Q. Crichlow, D. F. Smith, R. N. Morton and W. R. Corliss, "World-wide radio noise levels expected in the frequency band from 10 kilocycles to 100 megacycles," NBS Circular 557, August 25, 1955; available from the Superintendent of Documents, U. S. Government Printing Office, Washington 25, D. C., at 30 cents.


NBS